Distribution Agreement

In presenting this thesis or dissertation as a partial fulfillment of the requirements for an advanced degree from Emory University, I hereby grant to Emory University and its agents the non-exclusive license to archive, make accessible, and display my thesis or dissertation in whole or in part in all forms of media, now or hereafter known, including display on the world wide web. I understand that I may select some access restrictions as part of the online submission of this thesis or dissertation. I retain all ownership rights to the copyright of the thesis or dissertation. I also retain the right to use in future works (such as articles or books) all or part of this thesis or dissertation.

Signature:

_____ _____

Sherod E Haynes Date

When Stress Becomes Instructive: Paradoxical CRF Neuronal Activity Promotes Resiliency via Stress-History-Dependent Modulation in the BNST

By

Sherod Edward Haynes
Degree of Philosophy (Ph.D.)

Neuroscience

Larry Young, Ph.D.
Advisor

Helen Mayberg, M.D.
Advisor

Peter Wenner, Ph.D.
Committee Member

Ming-Hu Han, Ph.D.
Committee Member

Accepted:

Kimberly Jacob Arriola, Ph.D., MPH
Dean of the James T. Laney School of Graduate Studies

Date

When Stress Becomes Instructive: Paradoxical CRF Neuronal Activity Promotes Resiliency via Stress-History-Dependent Modulation in the BNST

by

Sherod Edward Haynes

B.A., Carleton College, 2008

Advisor(s): Helen S Mayberg, M.D.
Larry J Young, Ph.D.

An abstract of
A dissertation submitted to the Faculty of the
James T. Laney School of Graduate Studies of Emory University
in partial fulfillment of the requirements for the degree of
Doctor of Philosophy
in Neuroscience
2022

Abstract

When Stress Becomes Instructive: Paradoxical CRF Neuronal Activity Promotes Resiliency via Stress-History-Dependent Modulation in the BNST

By: Sherod Edward Haynes

While most individuals have the capacity to handle stress for a short time, cumulative stressors can emotionally overwhelm and precipitate neuropsychiatric conditions such as Major Depressive Disorder (MDD). Despite extensive research examining the relationship between stress and MDD, the substrates responsible for setting psychological tipping points remain elusive. Using repeated social defeat stress in tandem with electrophysiology, we uncovered a discrete stress window during which neuroadaptation in Corticotropin-Releasing Factor (CRF) neurons of the Bed Nucleus of the Stria Terminalis (BNST) demarcated the divergence of susceptible and resilient mice. In chapter one, I survey the literature surrounding the BNST and its role in adaptive responses to stress, with particular emphasis on mechanisms underlying resiliency. Chapter two details the research methods used to conduct the work herein described. Chapter three explores how CRF's paradoxical role as a resiliency modulator depends heavily on the stress-history context where resiliency is established between 7 and 10 episodes of social defeat. Much of the stress literature has shown CRF in the BNST to serve as a potent transducer of pro-stress and anxiety responses (via HPA axis regulation). Therefore, it was unexpected to find that CRF neuronal activation was necessary and sufficient for mice to develop resiliency. I used combinatorial cell-type selective chemogenetics with fiber photometry to simultaneously track and bidirectionally manipulate CRF neural dynamics essential to establishing resiliency. Further, I employed opsin-expressing transgenic CRF mice for cell-type selective optogenetics combined with RNAScope to correlate neural activity with genetic changes in critical targets of CRF transmission with behavior. Chapter four investigates whether developing resiliency to cumulative stress impacts the affective experience of stressful stimuli. Using a suite of behavioral assays, we uncover that resilience has state and trait dimensions associated with a blunting of aversion. Specifically, we observed that CRF activation positively biases social motivation, switches contexts of negative valence from aversive to appetitive, and promotes persistence in the face of ongoing stress. Chapter five offers concluding remarks and future directions. This work highlights an overlooked dimension to stress regulation in which resiliency processes are dynamically fine-tuned to one's stress history.

When Stress Becomes Instructive: Paradoxical CRF Neuronal Activity Promotes Resiliency via Stress-History-Dependent Modulation in the BNST

by

Sherod Edward Haynes

B.A., Carleton College, 2008

Advisor(s): Helen S Mayberg, M.D.
Larry J Young, Ph.D.

A dissertation submitted to the Faculty of the
James T. Laney School of Graduate Studies of Emory University
in partial fulfillment of the requirements for the degree of
Doctor of Philosophy
in Neuroscience
2022

Dedication

This dissertation is dedicated to my father, Gregory Haynes, Sr.

Acknowledgements

The decision to pursue graduate studies in the midst of completing a medical degree was, to date, one of the best decisions I could have made. While unconventional at the time, it was the loving support of friends, family, colleagues, and my faith in God that made it possible. I would first like to thank one of my best friends, Dr. Daniel Joh, M.D., Ph.D., who galvanized me to pursue graduate studies and dedicated hours and resources toward helping me plan and execute this endeavor. Dan continues to inspire me to this day. I would also like to acknowledge my family who continues to motivate me to inspire me to accomplish all that I have the audacity to dream. In particular, I owe my ability to dream from my paternal grandfather, Mr. John Haynes II. Papa, your legacy continues to live on through me. I thank my mother for her patience as she has listened to me describe the woes of laboratory science and working with mice. Despite her not having an idea of what my day-to-day looked like, she always showed genuine curiosity and a desire to learn about my experience in graduate school that made me feel supported and empowered.

To my father, whose battle with cancer ended less than a year ago, thank you for all of the wisdom that you have bestowed upon me. As I carry the torch to the race's final leg toward my doctorate, I feel your presence alongside me. There were many times during the construction of this thesis that I reflected on science-related conversations that we have had. In fact, you provided direct input on some of the figures presented in this text. In this way, your legacy lives on through the science I have undertaken and will continue to conduct.

I am grateful for the lab members, friends, family, and colleagues I have met along the way. This would not have been done without you. I credit all of these relationships as the greatest teacher during graduate school, for much of the experiments discussed in this dissertation came

after coffee-fueled conversations with the brilliant friends, colleagues, and communities of which I am lucky to be a part.

I am grateful throughout this process to have assembled a dream team of thesis advisors: Drs. Ming-Hu Han, Helen Mayberg, and Larry Young. I appreciate the patience, diligence, and confidence you have bestowed in me to pursue experiments that spark my curiosity and elevate the impact and scope of the overall body of work. Because of your mentorship, I feel empowered to continue developing into the physician-scientists I aspire to be.

List of Figures

List of Abbreviations

BDNF	Brain Derived Neurotrophic Factor
BNST	Bed Nucleus of the Stria Terminals
BNSTov	oval nucleus of the Bed Nucleus of the Stria Terminalis
ChR2	Channelrhodopsin
CNO	Clozapine-N-Oxide
CRF/CRFR1	Corticotropin-Releasing Factor/Corticotropin-Releasing Factor 1
DBS	Deep Brain Stimulation
DIO	Double-floxed inverted open-reading frame (cre-dependent construct)
GluN2D	Subunit of NMDA receptor
hM3Dq	Human M3 Muscarinic receptor
hM4Di	Human M4 Muscarinic receptor
HPA	Hypothalamic-pituitary-adrenal axis
MDD	Major depressive disorder
NAcc	Nucleus Accumbens
o-RTPP	Optical-Real-Time Place Preference
PVN	Paraventricular Nucleus of the Hypothalamus
RSDS	Repeated Social Defeat Stress
SDE	Social Defeat Episodes
SSRI/SNRI	Selective-Serotonin-Reuptake Inhibitor/Serotonin-Norepinephrine-Reuptake Inhibitor
TST	Tail-Suspension Test

Table of Contents

Chapter 1

Literature Review

Major Depressive Disorder

Major Depressive Disorder (MDD) is projected to be the leading cause of global disability around the globe by 2050, with a current lifetime prevalence of 25% in the U.S.(Heo et al. 2008) and expected to rise in response to the ongoing coronavirus pandemic (Veer et al. 2021). MDD is a debilitating condition characterized by episodes of emotional dysregulation, low mood, and a cluster of associated symptoms (American Psychiatric Association 2013). While much of the research on MDD (and associated treatments) targets the phases of the disorder marked by low mood, as these periods are most linked to morbidity (Kendler et al. 1999), this has come at the expense of examining MDD's episodic nature. For instance, the probability of recurrence increases by 16% with each successive episode (Solomon et al. 2000), and the total number of episodes is associated with treatment resistance and morbidity (Hayes et al. 2015)(Gold 2013). There is a need for treatment approaches that reflect this dynamic disease etiology, which may require targeting distinct mechanisms at specific time points over the longitudinal course of disease progression, similar to strategies employed in neurodegenerative diseases such as Parkinson's (Bowerman 2020). In order to explore novel drug mechanisms, I first survey the currently available antidepressant treatments.

Aside from improvements in formulations, treatments for MDD have remained essentially unchanged, some notable exceptions being psychedelics and Ketamine (Thase 2019). Treatments for MDD consist of antidepressants that include selective-serotonin/norepinephrine reuptake inhibitors (SSRI/SNRIs), tricyclic, and monoamine oxidase inhibitors (Shelton 1999; Stahl 1998). Recently, Ketamine has been proven efficacious as a rapidly acting antidepressant and has recently received FDA approval. While antidepressants have had variable degrees of efficacy in the short term, the long-term treatment outlook remains poor (Singh et al. 2020). Many patients suffer a relapse in MDD after a short course of antidepressant treatment. The likelihood of a failed course of therapy increases with the number of relapses (Solomon et al.

2000). As of this writing, there are no approved pharmacological treatment targeting mechanisms implicated in the prevention of MDD. Thus, there is a dire need to identify mechanisms involved in the development of pathological mood states that underlie the onset of a depressive episode, given that the occurrence of a first-time episode serves as a prognosis of further morbidity (Post 1992).

Structural changes implicated in the development of MDD

At present, the substrates that subserve the development of MDD are not well understood. Genetic (Mariani et al. 2021), cellular (Galvão et al. 2021; Ruiz et al. 2018), molecular(Galvão et al. 2021; Ivanets et al. 2021), structural(Schmaal et al. 2020; Liu et al. 2021), and circuit-level alterations (Eggart et al. 2019; Long et al. 2020; Wu et al. 2016; Neumann et al. 2014; Tahmasian et al. 2013; Liu et al. 2017) may catalyze the development of MDD are currently under investigation. Neuroprogression, defined by neurodegenerative loss, intracellular signaling changes, neuronal-immune uncoupling, apoptosis leading to decreased plasticity and neurotransmission, describes the progressive brain changes that promote the development of MDD (Ruiz et al. 2018). Areas of the prefrontal cortex, hippocampus, and amygdala are reduced in MDD patients (Tahmasian et al. 2013)(Ruiz et al. 2018). Decreased insula volume (Schmaal et al. 2020)(Liu et al. 2021), right para-hippocampus, and right fusiform gyrus is associated with MDD development (Kennis et al. 2020). Another study reported higher anterior cingulate cortical gray matter associated with the development of MDD. In response to sad faces, the amygdala, hippocampus, and insula volumes were smaller in patients for whom a first-time depression episode or recurrence was imminent (Treadway et al. 2009). Neuronal disorganization, loss of glial-neuronal interaction, atrophy, and cell death have been observed, thereby impacting neurotransmission and the function of these regions, which are involved in emotional regulation (Ruiz et al. 2018). Decreased myelination in the ventromedial prefrontal cortex (an area involved in depression) has been observed in depression, particularly in suicide

completers who suffered childhood abuse (Lutz et al. 2017). Mice exposed to chronic psychosocial stress revealed the genetic contribution of myelin plasticity, correlating with susceptible and resilient subgroupings. C57/Bl6J stress susceptible mice showed myelin thinning in the medial prefrontal cortex ventral hippocampus, and interestingly in the Bed Nucleus of Stria Terminalis, resilient not susceptible mice had reduced myelin thickness (Laine et al. 2018).

Molecular biomarkers implicated in the development of MDD

Molecular biomarkers of MDD are consistent across studies, due in part to the heterogeneous nature of the disorder. Serum mature Brain-derived-neurotrophin-factor (BDNF), serum cortisol, cortisol awakening response, and the Pittsburgh sleep quality inventory have been shown to predict chronicity of the longitudinal course with MDD in a regression model. The multi-biomarker panel was able to discriminate first-time episode MDD patients from those suffering from treatment-resistant depression with 96% sensitivity and 93% specificity, indicating that changes in these substrates may play a role in disease progression (Galvão et al. 2021). BDNF is necessary for cell proliferation, survival, and plasticity (Krishnan et al. 2007; Walsh et al. 2014; Wook Koo et al. 2016). Postmortem BDNF levels in the hippocampus are higher in depressed suicide completers than matched treated depressed and healthy controls. Conversely, antidepressant treatment and electroconvulsive therapy produce an upregulation in BDNF (Belmaker and Agam 2008). Stress and its associated HPA axis markers such as cortisol and CRF are important molecular substrates involved in the development of MDD that will be discussed later in this review (*see 'stress as a causative agent in MDD'*).

Genetic/Epigenetic factors in MDD development

Large-scale gene-wide associated studies (GWAS) have shed light on the genetic contribution to MDD onset. In one of the largest of such studies to date, a genetic analysis of more than 1.2

million individuals identified 178 genetic risk loci and 223 single-nucleotide polymorphisms (SNPs) associated with MDD (Levey et al. 2021). Of those, lead SNP, rs7531118, most closely identified with *negr1* (neuronal growth regulator 1), was strongly identified. NEGR1 is most enriched in the hypothalamus and associated with social and anxiety-like behavior. DRDR2 (D_2 dopamine receptor) is another top candidate to emerge from this study, with decreased expression being correlated with depressed individuals (Levey et al. 2021). DRD2 expression is markedly decreased in the NAcc and has implications for mesolimbic dopaminergic reward system dysfunction in the neuropathophysiology of MDD (Nestler and Carlezon 2006). However, the above studies were not designed to explore the genetic/epigenetic mechanisms specifically involved in the development of MDD. Immune-related genes, tumor necrosis factor (TNF), TNFR1, and interleukin-1b (IL-1b), have been implicated in the development of MDD garnered from a study of children and adolescents with MDD. They were significantly lower in the MDD group, suggesting that they may play a role in the early development of the disorder (Mariani et al. 2021).

Genomic analyses have revealed pathogenetic expression associated with MDD on the basis of differential gene expression, thought to be caused in part by epigenetic changes (Nestler et al. 2016). Histone methyltransferases G9 and G9a-like protein, which catalyzes H3K9me2 (a repressive mark) in the NAcc (Nestler et al. 2016). In depressed individuals, histone modifications to H3K4me3 or H3K27m3 (mark of gene activation) in promoter regions of *BDNF, TRKB* (tyrosine receptor kinase B, cognate receptor of *BDNF*) were observed in postmortem prefrontal cortex (Nestler et al. 2016). Chromatin remodeling via stress-related gene repression led to a lower level of histone marks H3M4me3 and H4K16ac (Nestler et al. 2016). Methylation of the corticotropin-releasing factor (*Crf*) promoter led to depressive-like behavior in chronically-stressed mice and was reversed with chronic antidepressant treatment (Elliott et al. 2010). In a rodent model of early-life stress involving maternal separation, which produces depression-like

behavior in adulthood, DNA methylation and expression of *nr3c1* and *bdnf* in prefrontal cortex and hippocampus were observed (Kundakovic et al. 2013). Methylation in the promoter region of SLC6A4 leading to reduced gene expression in the serotonin transporter was positively correlated with depression and is reversed by antidepressant treatment. Importantly, SLC6A4 methylation is linked with anterior cingulate cortical-frontal pole and medial-prefrontal resting-state functional connectivity (Ismaylova et al. 2017). While the above studies provide a genetic/epigenetic basis of MDD etiology, there is a dearth of studies that identify mechanisms of MDD onset distinct from those involved in the setting of established MDD pathology.

Neural Circuits implicated in the development of MDD

Maladaptive changes in structural, genetic, molecular, and physiological substrates give rise to neural circuit dysfunction underlying MDD development. A recently identified lateral-habenula (LHb)-lateral hypothalamus (LH) (LHb-LH) circuit was identified in driving depression onset via a 40 Hz firing frequency increase. This neuroadaptation occurred concomitantly with the progression of depressive behavior upon continuous stress exposure in mice (Zheng et al. 2022). In fact, mimicking the 40 Hz firing frequency in stress naïve mice brought about Long-Term Potentiation (LTP) and a persistent depressive state suggesting the need for stable circuit changes for MDD development (Zheng et al. 2022). Human functional MRI resting-state connectivity (rs-fMRI) imaging (where the participant is at rest and connectivity is inferred through local changes in blood flow and neuroanatomical landmarks) (Lv et al. 2018) uncovers potential neural circuits involved in MDD development (Long et al. 2020)(Tu et al. 2018). In a study of Parkinson's Disease, patients with subclinical neuropsychiatric symptoms showed reduced functional connectivity between striatal/thalamus and frontal and limbic cortical regions (Tinaz et al. 2021). Since anxiety and depression consistently predate motor symptoms in Parkinson’s disease by years, these functional resting-state findings shed light on mechanisms involved in the development of MDD. In one of the more comprehensive rsFMRI studies used

to validate subtypes of depression, two broad clusters or nodes of connectivity were identified: (1) One cluster consisted of frontostriatal and orbitofrontal connectivity associated with dysthymic depression (persistently low mood) containing large anhedonia and psychomotor retardation components; (2) a cluster defined by the amygdala, ventral hippocampus, ventral striatum, subgenual cingulate, and lateral prefrontal areas that comprised a depression with predominant anxiety features (Drysdale et al. 2017). Of these two broad clusters, four depression biotypes were identified. Out of the patients who experienced a depressive episode during the study, 90% received the same depression biotype between rs-fMRI scans (Drysdale et al. 2017; Kumar et al. 2014). As a basic science corollary, in a study by Hultman et al., mice were implanted with multi-channel electrodes in seven MDD-related areas, in-vivo recordings were conducted in conjunction with machine learning to uncover network-level spatiotemporal dynamic signatures that mapped on to distinct depression subtypes. Moreover, using rodent models of depression, the authors could predict depression vulnerability and onset by identifying circuits more critical for the development of depression in maintaining the depressed state or antidepressant efficacy (Hultman et al. 2018). Many of the circuits that underlie depression formation are regions implicated in stress response.

Stress is a causative agent in MDD development.

Stress plays a critical role in the development of depression. The association between major stressful life events and MDD is 75% (Kendler et al. 1999). The likelihood of a significant life stressor to provoke MDD is strongest with the first episode, with less severe stressors required to prompt subsequent episodes (Kendler et al. 1999; van de Leemput et al. 2014; Cramer et al. 2016). This suggests that stress effects on underlying mechanisms that cause depression may differ from those that cause recurrent episodes or maintain the depressed state. Notably, the temporal relationship between the major life stressor and subsequent MDD occurs in the order of several weeks – to months (Kendler et al. 1999). This suggests a stress incubation period

and the distinct time scale over which changes precipitate MDD (van de Leemput et al. 2014). Stress acuity plays a role, chronic, not acute, stress is a greater predictor of depressive symptoms. Interestingly, the relationship of stress on MDD is weakest in individuals with endogenous (strong familial/genetic/metabolic cause) depression (Hammen 2005). Most animal models of MDD heavily rely on stress exposure to produce depressive-like behaviors in rodents.

Rodent models of MDD

Animal models of MDD have provided experimentalists avenues to circumspect the mechanisms in hopes of discovering and testing novel therapeutics. The forced swim and tail suspension test mimic "depression-like behavior" in which a rodent is placed in a cylinder of water or suspended by their tail following a period of struggling (by way of swimming or climbing attempts)(Krishnan and Nestler 2011). The display of immobility is tracked and interpreted as "despair-like" behavior. Both FST and TST have been reversed by acute administration of most antidepressants (Wang et al. 2017). Similarly, learned helplessness models that typically involve uncontrollable and inescapable stress, usually in the form of electric shocks, over time produce despair-like behavior as animals seize escape behaviors (Wang et al. 2017). In learned helplessness models, mice display weight loss, sleep alterations, and HPA axis dysregulation that lasts 2-3 days (Yao et al. 2019)(Bougarel et al. 2011)(Landgraf et al. 2015)(Wang et al. 2017). Acute stressors offer ease of use and rapid screening purposes, yet a downside is the relatively simplistic interpretations offered as behavioral readouts. Chronic stressors tend to give rise to a broader behavior repertoire of adaptive behaviors that permit better clinical translatability and more dynamic mechanistic insights into MDD pathogenesis. Chronic mild stress (CMS) involves intermittent and prolonged stressors (2-5 weeks on average) ranging from electric shocks, stressful environmental exposures (freezing or very hot temperatures, damp bedding), mechanical (vibrating, rattling, air puffs), or positional stressors (cage tilted past 45 degrees, restrained in small enclosures) (Wang et al. 2017). CMS reliably

generates anhedonic-like mice/rats that display decreased exploration and social deficits. Notably, these phenotypes are reversed after chronic, not acute, antidepressant treatment. The drawbacks with CUS are mainly due to its lack of reliability and variability in the use of stressors, replicating studies across laboratories is a considerable challenge (Kudryavtseva et al. 1991; Gururajan et al. 2021; Wang et al. 2017).

MDD invariably involves a psychosocial component that CUS does not incorporate through its use of primarily physical stressors. In contrast, repeated social defeat stress (RSDS) capitalizes on naturalistic stressors as it leverages intermale territorial aggression endemic to rodents in the wild (Kudryavtseva et al. 1991; Golden et al. 2011; Krishnan et al. 2007; Martinez et al. 1998; Berton et al. 2006). RSDS involves two components: (1) physical stress via a predetermined amount of exposure to physical antagonistic interactions with a larger, more aggressive mouse and (2) psychosocial stressor by way of sensory contact with the aggressor in a separate compartment that obviates social contact but enables visual and olfactory cues (Golden et al. 2011; Krishnan et al. 2007; Challis et al. 2014; Challis et al. 2013). RSDS has been conducted with rats, mice, tree shrews, and Syrian hamsters, with several established variations around this same theme (Krishnan and Nestler 2011). Notable for RSDS is the segregation of resilient and susceptible groups on various genetic, molecular, neurophysiological, endocrine, and behavioral measures. In the context of depressive-related behavior, social interaction and sucrose-preference tests are most typically employed as an index to explore other underlying differences between the susceptible and resilient groups (Gururajan et al. 2021; Golden et al. 2011; Krishnan et al. 2007; Matsuda et al. 1996). RSDS has been employed in mice of various strains adding to its validity (Gururajan et al. 2021). Animals of depression have enabled investigators to identify critical substrates important for regulating stress responses, are candidate was shown consistently is Corticotropin-Releasing Factor (also referred to as 'hormone') (CRF or CRH).

Treatment failures of CRF antagonists

CRF is a 41-amino acid peptide released as serves as a master stress regulator via activating corticotrophs of the pituitary gland, thereby instantiating the HPA axis to mobilize an adaptive endocrine response to stress (Behan et al. 1995)(Heinrichs et al. 1995)(Turnbull and Rivier 1997). CRF is found throughout the brain and is evolutionarily conserved, but is densely concentrated in the paraventricular nucleus of the hypothalamus (PVN), Bed Nucleus of the Stria Terminalis (BNST), Central nucleus of the amygdala, dorsal raphe, locus coeruleus, external cuneate nucleus, and the medullary reticular formation (Cummings et al. 1983)(Rodaros et al. 2007; Dabrowska et al. 2016; Chen et al. 2015; Imaki et al. 1993)(Swanson et al. 1983). CRF has been administered in many animal models of depression, revealing its role in anxiety and despair-like behaviors, and is reversed by CRF-receptor antagonists.

Despite 30 years of scientific investigation, no CRF receptor antagonist has successfully completed a phase III trial. CP-316,311 was tested in a double-blind, placebo-controlled trial and was seized due to negative efficacy. Verucefront (GSK561679) also was shown to lack efficacy, while R121919 and PF-00572778 showed promising efficacy in trials but had to be halted due to elevated liver enzymes in participants. Small-molecule CRF antagonists have not consistently shown animal models of depression. Indeed, most of the tests of depression in which CRF receptor antagonists were used were in response to an acute stressor instead of the chronic undulating, non-habituating stressors that mimic the natural conditions giving rise to clinical depression.

Moreover, piloting potential antidepressants in more static depression models prevents uncovering mechanisms that become engaged as depressive behaviors emerge as an adaptation to ineffective chronic stress coping (Koob and Zorrilla 2012). Regions with dense

populations of CRF neurons that respond dynamically to chronic stress regulation would make better candidates for future exploration of CRFR-antagonists. One such region under intensive study for involvement in neuropsychiatric conditions is the BNST (Neumann et al. 2014).

Bed Nucleus of the Stria Terminalis (BNST)

The BNST is part of the extended amygdala, so named, due to its embryologic origins where tissue migrated along with the rostral-caudal extent between the anterior olfactory area toward the ventral striatopallidal. The extended amygdala consists of the central and medial amygdala at the caudal extent and runs rostralmedially through the Interstitial Nucleus of the Posterior aspect of the Anterior Commissure (IPAC), ending at the BNST at the most rostral extent. The embryologic origins provide a basis for the critical role of the extended amygdala generally, and BNST specifically in its role in integrating sensory, autonomic, interoceptive, and internal state to enact adaptive and anticipatory responses (Waraczynski 2016). The BNST has been implicated in diverse functions ranging from fear, anxiety, drugs of abuse, aggression, reward learning, salt appetite, urinary function, and sexual reproduction (Waraczynski 2016). Perhaps, the most extensively studied function of the BNST is coordinating stress responses, as its dysfunction has been implicated in numerous psychiatric disorders.

The BNST has over 16 individual sub-nuclei spanning its rostral-caudal extent (Fig 1). To provide adequate background on the studies contained within this dissertation, I focus specifically on the oval nucleus (BNSTov). The oval nucleus is located in the anterior-lateral aspect of the BNST is bound inferiorly by the anterior commissure, laterally by the dorsal striatum, superiorly by the lateral ventricle, and anteriorly by the NAcc. The oval nucleus consists primarily of GABAergic neurons, with a small percentage of Glutamatergic neurons. The BNSTov consists of a heterogeneous milieu of neuropeptides, including neuropeptide Y, enkephalin, somatostatin, CRF, neurotensin, and dynorphin (Daniel and Rainnie 2016; Daniel et

al. 2019; Dabrowska et al. 2013; Kash et al. 2015). Tracing studies reveal that BNSTov^{CRF} neurons project heavily to the Ventral Tegmental Area (VTA) (Silberman et al. 2013; Takahashi et al. 2019; Rodaros et al. 2007), Dorsal Raphe (DR) (Matthews et al. 2016; Dabrowska et al. 2016; Daniel and Rainnie 2016; Garcia-Garcia et al. 2018; Dong et al. 2001)(Marcinkiewcz et al. 2016), Lateral Hypothalamus (LH) (Giardino et al. 2018), Parabrachial Nucleus (PB) (Dong et al. 2001; Kim et al. 2013), Retrorubral Nucleus (RR) (Dong et al. 2001), Periaquectual Gray (PAG) (Dong et al. 2001; Johnson et al. 2016; Daniel and Rainnie 2016; Kaouane et al. 2021), and the Nucleus Tractus Solitarius (NTS) (Dong et al. 2001) (Fig 1a). As BNSTov^{CRF} neurons project from the rostral-caudal extent, several themes emerge: (1) BNSTov^{CRF} neurons do not project to any areas rostral to the BNST such as prefrontal cortical, with the NAcc being a notable exception. (2) BNSTov neuronal projections are densest in brainstem areas such as the NTS that coordinate somatomotor, autonomic, visceromotor, and neuroendocrine functions. (3) While the BNST contains several nuclei of enriched CRF neurons (oval, fusiform, and ventral nuclei), they have vastly different projection profiles. Together, this indicates remarkable segregation and organization of the BNST, with respective functions that may contribute to a diverse array of, and even opposing, adaptive behavioral strategies in response to relevant internal and external stimuli. The BNST is anatomically conserved, though the naming conventions differ among rodents and humans (Avery et al. 2016; Lebow and Chen 2016)(Fig 1b). There have been notable differences in projection targets in BNSTov^{CRF} neurons of mice compared to the rat, possibly indicating inter-species variability in the BNSTov. Notably, tracing experiments relied heavily upon transgenic *Crf*-cre mice and ratlines, which have variability in CRF expression.

Stress in the BNST

Electrophysiological profiles have been established based on three distinct cell types in the anterolateral BNST (named type I -III), of which type III neurons are considered the putative

CRF-expressing neurons. Chronic stress causes neuroadaptive changes such as decreased input resistance and time constant and increased action potential rise time and half-width selectively in Type III cells. As opposed to repeated restraint stress, chronic shock stress caused an increase in LTP in non-type III cells, suggesting that different stressors have distinct effects on BNST neuronal activity. Concomitantly, using single-cell quantitative-polymerase-chain-reaction (qPCR), the type III BNSTov neurons showed an increase in *Crf* and decreased in striatal-enriched-protein-tyrosine-phosphatase *(STEP)* mRNA (Daniel et al. 2019). STEP dephosphorylates tyrosines within the regulatory domain of kinases such as extracellular signal-regulated kinase 1 and 2 (ERK1/2) or stress-activated protein kinase p38. STEP has been shown to inhibit downstream activity in stress-responsive brain regions such as the amygdala or dorsal hippocampus. Notably, STEP acts on NMDA receptor subunits GluN2B, thereby abolishing the development of synaptic plasticity (Dabrowska et al. 2013). Thus, if CRF plays the putative role in the BNSTov as stress actuator, then STEP serves an attenuating role in stress responding. The GluN2D sub-unit selectively contributes to depression-like behavior in BNST CRF neurons, as GluN2D$^{-/-}$ knockout mice abolished LTD and decreased action potential rise time-correlated with depressive behavior on forced-swim and novelty-suppressed feeding tests, suggesting different circuit mechanisms for anxiety and depression. Concomitant with the expression of increased immobility in the forced swim test and novelty-suppressed feeding tests. While anxiety-like behavior was unaffected (Salimando et al. 2020), different circuit mechanisms may underlie anxiety and depression. Chronic variable stress has been shown to over-activate BNSTov^{CRF} neurons via a CRFR1 dependent activation of a PKA mechanism, resulting in increased membrane trafficking of AMPA-R GluR1 subunits and durable neuroadaptive changes (Hu et al. 2020). BNSTov^{CRF} neurons are nearly exclusively GABAergic (Salimando et al. 2020; Dedic et al. 2018; Dabrowska et al. 2016; Lebow and Chen 2016), selection deletion of the α1 subunit of the GABA(A) receptor in BNST CRF neurons led to increased anxiety-like, but not depressive behavior. Upon induction of short-term plasticity of

inhibitory transmission, only the CRF GABA(A)α1 knockout mice failed to exhibit short-term synaptic depression when stimulated at 20 Hz, suggesting a role in modulating high-frequency inputs. Of note, there were no significant differences among the groups with 10 Hz short stimulation, nor the intrinsic physiological properties of CRF neurons (Gafford et al. 2012). Indeed, high-frequency stimulation from ventral subiculum/CA1 into the BNST produces LTP and angiogenesis, whereas infralimbic cortical inputs lead to LTD and anxiolysis, suggesting that BNST gates responses based on input frequency (Glangetas et al. 2017).

The relationship between intra- and extra-hypothalamic CRF neuronal regulation remains under investigation. When discussing stress in the BNST, the link between CRF of the HPA axis and that released in the oval nucleus comes into question. FKBP51, a co-chaperone of a heat shock protein 90 kDa (Hsp90), is expressed in the BNSTov and found in neurons that co-express CRF. A knockout of *Fkbp5* in the BNST led to an increase in anxiety-like behavior on the elevated plus-maze and light-dark box and increased blood corticosterone concentration in acute restraint stress. Interestingly, the *fkbp5* knockout was associated with decreased *Crf* mRNA in the BNSTov (Engelhardt et al. 2021). This is particularly interesting because $BNSTov^{CRF}$ neurons have not been observed to send direct projections to the paraventricular nucleus of the hypothalamus, whose CRF cells regulate HPA axis activity. However, it is plausible that an indirect connection may exist whereby $BNSTov^{CRF}$ neurons project to neurons of the anteroventral BNST (Dong et al. 2001) which then sends direct projections to the PVN in a trisynaptic BNSTov-BNSTam-PVN circuit.

Optogenetic inhibition of BNSTav projecting PVN neurons during a 10-minute tail suspension stress led to an increase in serum adrenocorticotropic hormone (ACTH), a pituitary hormonal mediator of the HPA axis and corticosterone up to 60 minutes after the stress. Optogenetic activation led to an elevation of ACTH and corticosterone levels; this bidirectional modulation of

the HPA axis suggests that the BNSTav-PVN circuit is essential in stress activation and recovery. The functional consequences of BNSTov input into this circuit have yet to be described (Johnson et al. 2016). PVN^{CRF} neurons differ from $BNSTov^{CRF}$ neurons in a variety of important ways. $BNSTov^{CRF}$ neurons are almost exclusively GABAergic with a high degree of GAD67 mRNA expression, whereas the majority of PVN^{CRF} are glutamatergic and highly express VGLUT2. $BNSTov^{CRF}$ and PVN^{CRF} neurons differ in their electrophysiological profiles, with $BNSTov^{CRF}$ neurons having a more hyperpolarized resting potential, lower input resistance, and lower action potential spike threshold on average (Dabrowska et al. 2013). However, these profiles may differ under conditions of acute or chronic stress. For instance, repeated social defeat stress (RSDS) led to increased *Crf* mRNA expression in susceptible mice secondary to demethylation of CpG sites in the *Crf* promoter region (Elliott et al. 2010), suggesting that CRF is under epigenetic regulation. Future studies are needed to determine better why distinct stressor types and duration provoke vastly different responses among CRF neurons. A potent transducer of CRF and transmission and a key target for stress regulation are CRF receptors.

Corticotropin-Releasing Factor Receptor-1 (CRFR1)

Corticotropin-releasing factor receptors are members of the 7 transmembrane G-protein-coupled receptor (GPCR) family. CRFR1 and CRFR2 are observed widely throughout the vertebrate brain with the highest densities in areas that respond to stress such as the BNST, PVN, and hippocampus and are evolutionarily conserved (Hillhouse and Grammatopoulos 2006). Despite the shared genetic structure, CRFR1 has a greater binding affinity for CRF than CRFR2 (Chen et al. 2015; Dabrowska et al. 2013; Behan et al. 1995; Turnbull and Rivier 1997). Following agonist binding, CRFR1, Gs activation sets off a cascade, leading to increased cAMP-PKA activity (Konishi et al. 2003; Turnbull and Rivier, 1997). Regulation of CRFR1 is varied, including genetic splicing, glucocorticoid regulation, G-protein Related Kinase (GRK) regulation, and **β**-integrin clathrin-mediated receptor internalization (Turnbull and Rivier 1997).

The genetic mechanisms underlying *Crf* and *Crfr1* gene regulation are dynamic and poorly understood. *Crf* overexpression using lentiviral viral vector over four weeks led to a CRFR1 downregulation selectively in the BNST (Regev et al. 2011; Sink et al. 2013). Interestingly, in primary culture of hypothalamic neurons, CRF directly induces *Crfr1* mRNA expression in an apparent autocrine signaling mechanism (Konishi et al. 2003). *Crfr1* knockout mice have a decreased anxiety profile, whereas CRFR1 overexpression produces anxiety-like behavior in transgenic mice (Reul 2002). Repeated water stress (forced swim stress) for 60 minutes daily for 7 days led to an increase in *Crf, Crfr1, Crfr2*, and the pronounced ratio of *Crfr1/2* mRNA expression in the dorsolateral BNST (region containing the oval nucleus). CRFR1 antagonist did not affect baseline stress responding, but significant time in open arm and internal-pain perception on an intestinal distention assay (Tran et al. 2014). The CRFR1 antagonist, CP-154,526, dose-dependently reversed inescapable shock-stress deficit in a rodent depression model of learned helplessness (Mansbach et al. 1997). In summary, these findings implicated aberrant CRF/CRF1 signaling in the BNST as playing a role in maladaptive stress responding, which may precipitate mood disorders, such as MDD.

The Role of the BNST in Major Depressive Disorder

As of this writing, a PubMed search on the BNST in MDD yielded only four studies; suffice to say, this area is immensely understudied. Mice that overexpress CRF in the dorsolateral BNST using a lentiviral construct exhibited depressive-like behaviors upon a four-month post-injection assessment, suggesting an incubation effect. Additionally, *Crfr1* mRNA in these mice is markedly downregulated, hinting that CRF-CRFR1 interactions may play a role in developing depressive behavior (Regev et al. 2011). Selective genetic deletion of GluN2 -NMDARs (a subunit of the heteromeric N-Methyl-D-Aspartate Receptor) of the BNST produced a depressive-like phenotype in mice by increased immobility time on forced swim test (Salimando et al. 2020). GluN2D-NMDAR deletion increased BNSTov^{CRF} neuronal excitability with

increased spontaneous excitatory postsynaptic current (eEPSC) frequency and amplitude, decreased spontaneous inhibitory postsynaptic current frequency and amplitude (IPSC), as well as a decreased action potential decay time(Salimando et al. 2020). Together, suggesting a role in increased excitability of BNSTov^{CRF} neurons in depressive behavior. Despite these findings, most of the work investigating negative aversive states coordinated by the BNST have been related to animal models of anxiety and post-traumatic stress disorder (PTSD)(Clauss et al. 2019; Sink et al. 2013; Lee et al. 2008; Mazzone et al. 2018; Engelhardt et al. 2021; Gafford et al. 2012; Avery et al. 2016; Rodríguez-Sierra et al. 2016; Kim et al. 2013; Garcia-Garcia et al. 2018; Waddell et al. 2006; Duvarci et al. 2009; Dedic et al. 2018; Tran et al. 2014; Walker et al. 2003; Walker et al. 2009; Ago et al. 2014). While there are overarching neurological correlations that stretch across neuropsychiatric disorders as evidenced by NIMH's DOC, the dearth of research on depression makes drawing inferences on shared underlying etiology elusive. Still, much of the work involving depression focus on the oval nucleus of the BNST (BNSTov).

The BNSTov serves as a key integrator of intero- and exteroceptive information has important implications for playing a causative role in the development of depression that may be distinct from that which is involved in recurrent or sustained disease states. The subjective experience of an external stimulus is influenced by one's internal state, called alliesthesia. Internal states are governed by the milieu of interoceptive, viscerosensory, motivational, and homeostatic cues and inputs. The BNST is well-positioned to serve as the hub of this integration, and dysregulation of this region may lead to vulnerability or resiliency to developing MDD (Paulus and Stein 2010). The interoceptive deficit hypothesis posits that MDD stems from a deficit in the accurate perception and representation of external signals (i.e., social or environmental contexts) as informed by internal states and awareness. In other words, the inability to regulate mood based on the attribution of internal awareness. Interoception is encoded by the anterior

cingulate cortex, ventral hippocampus, insular cortex, and infralimbic prefrontal cortex – all areas that innervate the BNST. Particularly, the anterior insula, which subserves the role of a unified representation of bodily sensations at any given moment, sends dense projections onto BNSTov^{CRF} neurons (Harshaw 2015). Social contexts require both the assessment of environment (i.e., aggression, motivation of social target, prediction of danger or aggression, presence of sexual receptivity) and integration of internal state (i.e., anxiety/fear state, the necessity for interaction to achieve homeostatic needs such as feeding or sex), and thus provide a readout of deficits in interoception. There is a decrease in insula activity with the change in social interest. Depression could also be thought of as an imbalance in interoceptive-exteroceptive processing, such that hypersensitivity to internal stimuli (such as fear/anxiety due as a chronic stress response) drives hyporesponsive to external stimuli such as misattribution of typically rewarding activities as less so (anhedonia, decreased social motivation) or cognitive flexibility style becoming rigid (giving apathy, pessimism, guilt) and other core features of MDD (Harshaw 2015). Chronic stress plays a distinct role in altering interoception by altering frontostriatal regions and their downstream projectors (Dias-Ferreira et al. 2009).

The BNSTov projects directly to hedonic and motivational processing areas, such as the VTA (Takahashi et al. 2019). An inhibitory input from the dorsolateral BNST (an area that includes the oval nucleus) to the VTA increases in conditions of chronic pain, thereby leading to tonic suppression of VTA dopamine neurons. Blockade of BNST CRFR1 in chronic pain rats led to increased extracellular dopamine levels in the NAcc and increased conditioned place preference, suggesting a role in hedonic-like behavior and mood dysregulation under chronic pain conditions (Takahashi et al. 2019). Chronic unpredictable stress in rats gradually produces anhedonic-like behavior as indicated by decreased VTA self-stimulation and associated with increased CRF immunoreactivity in the BNST concomitant with the display of depressive-like

behavior (Stout et al. 2000). Taken together, despite extensive studies on the matter, there is reason to examine further the role the BNST plays in the development of MDD.

BNST CRF involvement in social behavior

Social behavior in the BNST is understudied, as the first review on this subject has only recently been published in 2021 (Flanigan and Kash 2020). Still, the BNST organized social behavior, particularly in settings where social interactions are highly salient such as in social conflict (Jasnow et al. 2004). D-Phe CRF(12-41), a CRF receptor antagonist, prevented submissive/defensive behavior and increased the duration of nonsocial investigatory behavior of the intruder in a model of social defeat stress involving Syrian hamsters (Jasnow et al. 2004). Repeated daily subanxiogenic doses of Urocortin1 (UCN1, a CRF receptor agonist) infusions into the BNST for five days led to persistent (lasting up to 4 weeks) social deficits leading to decrease social interaction time without affecting anxiety on elevated plus-maze. The social interaction effect was blocked by the daily pretreatment of Astressin (non-selective CRF receptor antagonist) prior to the daily Ucn1 infusion. Importantly, the decreased social interaction effect was apparent only after five injections, as a separate experiment involving three infusions had no effect. This finding suggests that urocortin sensitization occurs in a dose-dependent manner, and the long-lasting effects of these manipulations suggest a likely mechanism involving CRFR1-mediated LTP. Importantly, unlike in the basolateral amygdala, rats receiving repeated urocortin1 priming failed to exhibit increased heart rate and blood pressure following lactate infusion (a chemical manipulation that provokes panic-like behavior in rodents)(Lee et al. 2008). This finding suggests that the BNST may be uniquely wired to integrate the deleterious effects of stress on socially motivated behavior. Similarly, a CRF-Binding Protein (CRF-BP) antagonist, $CRF_{(6-33)}$, infused into the BNST after intermittent social defeat stress prevented social avoidance (Vasconcelos et al. 2019).

Deep brain stimulation of the BNST for the MDD

Several small trials have targeted deep brain stimulation (DBS) for treatment-resistant depression (TRD) targeting the BNST. In one such study, of five participants, two achieved total remission at 18-24 months, with partial benefit in two others (Fitzgerald et al. 2018). In another case report, DBS of the BNST leads to a decrease in clinical improvement in the mood at 12 months, with a notable improvement in neurocognitive domains (Cassimjee et al. 2018). Local field potential (LFP) recordings of implanted DBS electrodes revealed significantly higher alpha-power in MDD compared to matched patients who received DBS in the BNST for Obsessive-Compulsive Disorder (OCD). The alpha-power was correlated with depression severity on the Beck Depression Inventory. However, this study design did not include follow-up, nor use of baseline depression scores, thus not designed nor powered to answer the question of BNST DBS treatment efficacy for MDD (Neumann et al. 2014). Altogether, DBS for BNST holds promise as a therapeutic approach for individuals with severe depression, but small sample sizes have not yielded enough statistical power to confer effectiveness as a treatment modality at this time.

Neural Circuits Underlying Resiliency

Resiliency is an active process involving changes in genetic, molecular, circuit, structural, and behavioral changes that are independent of processes giving rise to pathological mood states (Franklin et al. 2012; Cathomas et al. 2019; Russo et al. 2012)(Feder et al. 2009). Circuits are just now being identified that play a role in resiliency. In a study by Roeckner et al., increased functional connectivity among amygdala and prefrontal cortex, amygdala-insular, and ventrolateral periaqueductal grey-prefrontal cortical regions were upregulated conferred resistance to developing depression for some and not others (Roeckner et al. 2021). Recent studies have identified that neuroadaptation in a dopaminergic VTA-NAcc circuit involving KCNQ voltage-gated potassium (K+) channels promotes stress resilience (Costi et al. 2022). In

fact, KCNQ2/3 channel openers targeting this mechanism have been piloted in a clinical trial as a novel antidepressant, ezogabine. Participants treated with 10 weeks of the KCNQ channel opener ezogabine (or retigabine) led to changes in rs-fMRI wherein decreased functional connectivity between the ventral caudate and clusters within the mid-and posterior-cingulate cortex was associated with symptom improvement of depression and anhedonia symptoms (Tan et al. 2020). The clinical data correlated with basic science studies showing that ezogabine normalized neuronal hyperactivity in ventral striatal dopaminergic neurons in mice (Friedman et al. 2016; Friedman et al. 2014; Ku and Han 2017). Together, these data reveal translational promise in exploiting circuit mechanisms implicated in resiliency, which may or may not overlap with those that produce pathological behavioral states, as has been the tradition of antidepressant rational drug design.

McEwin's theory of Allostasis references an inverted U curve of stress diathesis, wherein a small amount of stress is activating, and a positive physiological response is required for healthy adaptation. However, as stress accumulates, the changes overwhelm the ability for endogenous homeostatic and allostatic controls to adjust, and systems begin to decompensate (allostatic load). Areas sensitive to stress adaptation, which may also be important for resiliency, appear to subscribe to the same “goldilocks” of conditions (Roeckner et al. 2021). Nodes initially investigated for their involvement in MDD are also pivotal points of integration in developing resiliency. DBS of the subcallosal cingulate for MDD guided by personalized tractography-guided implantation showed a 45.6% decrease in depression scores after a week based on brief intraoperative stimulation (Sendi et al. 2021). The early antidepression treatment effect was characterized by a decrease in beta (13-30 Hz) rhythm observed by the stimulating/recording electrode local field potential, suggesting that distinct electrophysiological biomarkers can be used to classify circuits of resiliency with relevance to treatment efficacy (Sendi et al. 2021). Infralimbic cortex, prelimbic cortex, and ventral hippocampus were

observed to be part of a circuit or “electome” selectively involved in the development of MDD, which were separate from circuits involved in the maintenance of MDD or antidepressant response (Hultman et al. 2018). Interestingly, anatomically, the BNST receives direct inputs from infralimbic and ventral hippocampal inputs (Lebow and Chen 2016).

In this dissertation, I will explore the dynamic manner in which stress in the BNST serves as a dynamic modulator and critical substrate for the development of resiliency using a variety of neuroscience methods (chapter 2). I will explore the stress-history-dependent modulation that BNSTov^{CRF} undergoes to establish resiliency (chapter 3), investigate the contributory role of internal motivation of the contribution to resiliency (chapter 4), and lastly conclude with implications and future directions (chapter 5).

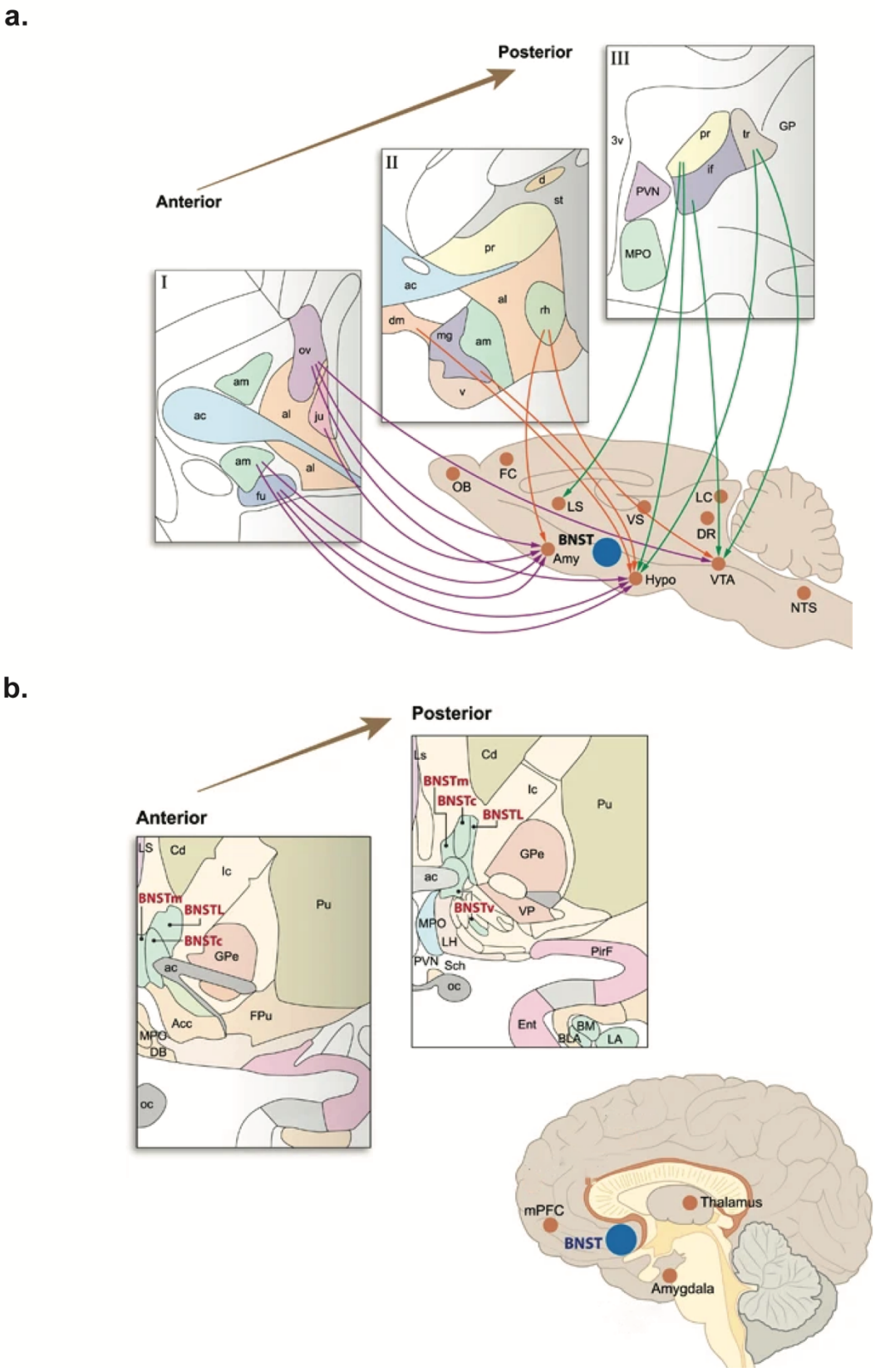

Figure 1: Anatomical location of the Bed Nucleus of the Stria Terminalis (BNST) in rodents and humans. Adapted from *(Lebow and Chen 2016)*

Figure 1: Anatomical location of the Bed Nucleus of the Stria Terminalis (BNST) in rodents and humans.

a, The Bed Nucleus of the Stria Terminalis (BNST) consists of 16 subnuclei. The purple, orange, and green arrows signify the efferent projections from the anterolateral, anteromedial, and ventral BNST areas respectively. the principle (pr), the interfascicular (if) and the transverse (tr). 3v, third ventricle; ac, anterior commissure; al, anterolateral BNST; am, anteromedial BNST; Amy, amygdala; BNST, bed nucleus stria terminalis; d, dorsal nucleus; dm, dorsomedial nucleus; DR, dorsal raphe; FC, frontal cortex; fu, fusiform nucleus; GP, globus pallidus; hypo, hypothalamus; if, interfascicular nucleus; ju, juxtacapsular nucleus; LC, locus coeruleus; LS, lateral septum; mg, magnocellular nucleus; MPO, medial preoptic area; NTS, nucleus solitary tract; OB, olfactory bulb; ov, oval nucleus; pr, principle nucleus; PVN, paraventricular nucleus; rh, rhomboid nucleus; st, striatum; tr, transverse nucleus; VS, ventral subiculum; VTA, ventral tegmental area. **b,** The BNST is anatomically conserved from rodents to humans, with equivalent subregions also identified. ac, anterior commissure; Acc, nucleus accumbens; BLA, basal lateral nucleus of the amygdala; BM, basal medial nucleus of the amygdala; BNST, bed nucleus of the stria terminalis; BNSTc, bed nucleus of the stria terminalis central subdivision; BNSTL, bed nucleus of the stria terminalis lateral subdivision; BNSTm, bed nucleus of the stria terminalis medial subdivision; BNSTv, bed nucleus of the stria terminalis ventral subdivision; Cd, caudate; DB, diagonal band; Ent, entorhinal cortex; FPu, putaminal fundus region; GPe, globus pallidus external; Ic, internal capsule; LA, lateral nucleus of the anygdala; LH, lateral hypothalamus; LS, lateral septum; mPFC, medial prefrontal cortex; MPO, medial preoptic nucleus; oc, optic chiasm; PirF, piriform cortex; Pu, putamen; PVN, paraverntricular nucleus; Sch, suprachiasmatic nucleus; VP, ventral pallidum; vPFC, ventral prefrontal cortex.

Chapter 2

Experimental Methods

Mice

The study used wild-type, Crf-ires-cre (Jackson labs: 011087), ai14 (cre-responsive tdTomato reporter mouse; Jackson labs: 007915), ai32 (cre-responsive channelrhodopsin-2/fused with eYFP; Jackson labs: 012569) mice on c57bl/6J background that were bred at Icahn School of Medicine at Mount Sinai and used were between 6-7 weeks at the start of experimental manipulations. Upon receipt from Jackson Laboratories, mice were acclimated to the housing facility for 1-2 weeks prior to the start of experiments. As reported in prior work (cite), all mice were group-housed and maintained on a 12/12 light-dark cycle with ad libitum access to food and water. Following social defeat stress, mice were singly housed and maintained on a 12/12 light-dark cycle with ad libitum access to food and water. All experiments were approved by the Institutional Animal Care and Use Committee and comply with institutional guidelines for the Animal Care and Use Committee set forth by Icahn School of Medicine at Mount Sinai.

Repeated social defeat stress paradigm

The repeated social defeat stress paradigm was performed according to published protocols (cite). Briefly, CD1 aggressors were singly housed in cages (26.7 cm width x 48.3 cm depth x 15.2 cm height; Allentown Inc) at least 24 hours before the start of the experiment on one side with a clear perforated Plexiglas divider. Social stress consists of physical and sensory stress components. During the period which marks the physical stress, C57BL/6J mice are placed on the ipsilateral side of the cage as the CD1 aggressor for 10 minutes. Following this, the intruder mouse is placed in the contralateral side of the perforated Plexiglas divider for the remainder of the 24-hour period, marking the sensory-stress period. Every 24 hours, the intruder mouse is paired with a new aggressor for 10 episodes. Control mice were housed two mice per cage divided by a perforated Plexiglas divider and rotated and handled daily like the socially defeated mice.

Social interaction test

Social interaction testing was performed as described (Golden et al. 2011; Cao et al. 2010; Krishnan et al. 2007; Kumar et al. 2014; Koo et al. 2019; Laine et al. 2017; Riga et al. 2017; Barthas et al. 2020). Briefly, a novel conspecific of CD1 strain is placed in an interaction zone of a standard open-field arena, and the time the intruder spends in the interaction zone is measured. The mice spend a total of 5 minutes in the open arena (2.5 min with and without the novel CD1). Ethovision (Noldus Information Technology) video-tracking software is used to track interaction time. All social interaction testing takes place 24 hours after the last defeat. Social interaction (SI) is measured by time spent in the interaction zone during first (CD1 absent) over second (CD1 present) trials. Mice are categorized according to SI ratios; an SI ratio >1 defines resilient, whereas an SI ratio <1 is susceptible as described previously ([5,18,19,21]).

Sucrose preference test

For sucrose preference testing, a solution of 1% sucrose or diluent alone (drinking water) is filled in 50 ml tubes with ball-pointed sipper nozzles (Ancare). Animals are acclimatized to two-bottle choice conditions prior to testing. The bottles are weighed, and positions interchanged daily. Sucrose preference is calculated as a percentage [100 x volume of sucrose consumed (in bottle A)/total volume consumed (bottles A and B)] and averaged over 2 days of testing.

Cell-attached electrophysiology

Acute coronal brain slices of the BNSTov were prepared according to previously published protocols ([63,64,89,90]). All recordings were carried out blind to stress history, behavioral phenotype, or drug treatment. Male 8-12 weeks old mice were perfused with cold artificial cerebrospinal fluid (aCSF) containing (in mM): 128 NaCl, 3 KCl, 1.25 NaH_2PO_4, 10 D-glucose, 24 $NaHCO_3$, 2 $CaCl_2$, and 2 $MgCl_2$ (oxygenated with 95% O_2 and 5% CO_2, pH 7.35, 295-305 mOsm). Acute brain slices containing BNSTov were cut using a microslicer (DTK-1000, Ted

Bella) in sucrose-ACSF, derived by replacing NaCl with 254 mM sucrose, and saturated by 95% O_2 and 5% CO_2 (2.5 ml/min) and 35ºC. Glass recording pipettes (2-4 MΩ) were filled with an internal solution containing (mM): 115 potassium gluconate, 20 KCl, 1.5 $MgCl_2$, 10 phosphocreatine, 10 HEPES, 2 magnesium ATP and 0.5 GTP (pH 7.2, 285 mOSm). BNSTov CRF neurons were identified by location, and infrared differential interference contrast microscopy and recordings were made from CRF-positive neurons as indicated by the presence of tdTomato (in crf::tdTomato mice) or eYFP in the case of (crf::ChR2) mice. Spontaneous firing rates were recorded in cell-attach mode, and data acquisition and online analysis of firing rates were collected using a Digidata 1440 digitizer and pClamp 10.2 (Axon Instruments). The timing of recordings was made consistent throughout treatment groups. A burst was defined as containing at least three spikes, with interspike intervals <15 ms. Neuronal firing rates were considered bursting or non-bursting if they had undergone a statistically significant change with a $P<0.05$ on the rank-sum test.

Qualitative defeat assessment

Social defeat encounters were recorded, and BORIS (Behavioral Observation Research Interactive Software) was used to code behaviors. Five behaviors (cage exploration, aggressor grooming, flight, motionless, rearing/defensive posturing) were scored per published reports on typical social defeat behaviors[20,91–93]. The total time engaging in each behavior was tallied to a blinded observer, and scores were aggregated.

Viral constructs

For DREADD experiments in CRF neuronal populations, CRF-ires-Cre animals were injected with AAV5-hSyn-DIO-hM4D(Gi)-mCherry (Addgene: 44362-AAV5) (≥7x10^12), AAV5-hSyn-DIO-hM3D(Gq)-mCherry (Addgene: 44361-AAV5) (≥7x10^12), and AAV5-hSyn-DIO-mCherry

(Addgene: 50459). For fiber photometric recordings, CRF-ires-Cre animals were injected with AAV9-syn-FLEX-jGCaMP7f-WPRE (addgene: 104492-AAV9) (>1x10^12). All viruses were purchased from Addgene.

Stereotaxic virus and optic fiber implantation

Under ketamine (80 mg/kg)/xylazine (10 mg/kg) anesthesia, mice were placed in a stereotaxic frame (Kopf Instruments) and the BNSTov was targeted (coordinates: anterior/posterior +0.20, media/lateral: +/- 2.15, dorsal/ventral, –4.0 mm; 15-degree angle). Hair was shaved around the crown of the head, alcohol, and betadine were applied to the scalp. Ophthalmic ointment was applied to the eyes to prevent dryness, a midline incision was made down the scalp, and a craniotomy was made using a dental drill. A 10 ul Nanofil Hamilton syringe (WPI, Sarasota, Fl) with a 34-gauge beveled metal needle was used to infuse 0.5 ul virus at a rate of 85 nl/minute. Following infusion, the needle was kept at the injection site for 10 minutes and slowly withdrawn. For the optogenetic experiments, chronically implantable optic fibers constructed with 1.25 mm diameter, 200 um core, 0.39 numeral aperture (NA) were used (RWD). For the fiber photometry experiments, chronically implantable optic fibers constructed with 1.25 mm diameter, 400 um core 0.48 numerical aperture (NA) optic fiber and unilaterally implanted into the BNSTov (coordinates: anterior/posterior +0.20, media/lateral: +/- 2.15, dorsal/ventral, –3.9 mm; 15* angle) (thor labs). Fiber optical ferrules were cemented to the skull using dental acrylic (Parkell C&B Metabond). All optical stimulation and fiber photometric recording experiments were conducted a minimum of 3-4 weeks post-implantation.

CNO-drinking water construct

Clozapine-N-Oxide (CNO) was obtained from (Hello Bio, catalog no HB6149). The dry chemical was dissolved in drinking water obtained from the vivarium and diluted such that each mouse received 5 mg/kg/day based on previous studies. CNO was made fresh each day for the three

days it was administered. CNO solutions were protected from light throughout the experimental procedure. On average, mice consumed ~4-5 mL of water per day. Water bottles and mice were weighed daily. CNO water bottles were exchanged for normal drinking water after the social interaction test 1 and 8-12 hours before social defeat stress to ensure neuronal modulation during stress exposure.

Elevated plus-maze

Mice began testing by being placed in the center of the maze (Model ENV-560A, Med Associated, Fairfax, VT, USA), where movement was tracked using Ethovision behavioral tracking software (Noldus). The test lasted 5 minutes.

Open field test

Mice were placed in an arena (42 cm (w) x 42 cm (d) x 42 cm (h); Nationwide Plastics, custom order). Mice were tracked using behavioral tracking software (Ethovision, Noldus), and time spent in the designated center and surround zone, as well as locomotor activity, were measured.

Optogenetic manipulation of BNSTov^{CRF} neurons

Optical fibers were implanted on Ai32 (transgenic mouse line expressing light-gated cation channel channelrhodopsin-2 (ChR2). Optical fiber Optogenetic stimulation was conducted via the use of a diode-pumped solid-state (DPSS) 473-nm blue laser (Crystal Laser, BCL-473-050-M), using a patch cord with an FC/PC adaptor (Doric Lenses, MFP_200/240/900-0.22_4m_FC-MF2.5). A functional generator (Agilent Technologies; 33220A) was used to generate a 5 Hz frequency, pulse width of 10 ms for 15 minutes[94,95], and power density between 7-9 mW mm$^{-2.}$ Experimenters were blinded to the stimulation group.

Fiber photometry calcium imaging

Optical recordings of GCaMP7f fluorescence were acquired using two LEDs at 490 and 405 (Thor Labs), reflected off dichroic mirrors (Semrock, FF495) and coupled into a 400 micro 0.48 NA optical fiber (Thorlabs BFH48-600) using a 40 x 0.48 NA microscope objective and fiber launch with the pat chord linked to an implanted 400 um optical fiber with zirconia sheath. Signals in both 470 and 405 nm channels are monitored throughout the recordings, whereas the 405 nm is used as an isosbestic control for ambient fluorescents and motion artifacts caused by movement or torque about the fiber optic implant. Wavelengths were modulated at frequencies of 210-220 and 330 Hz, respectively, with power output maintained at 20 mA and a DC offset of 3 mA for both light sources. All signalers were acquired at 1 kHz and lowpass filtered at 3 Hz. Prior to social interaction testing, mice were handled for and connected via a patch cable and placed in the home cage for 5-7 minutes for basal BNSTov recording and habituation prior to the start of the no-target trial.

Fiber photometry analysis

A custom-written MATLAB code was used to analyze the GCaMP7f signal. Firstly, the bulk fluorescent signal from both the 470 nm and 405 nm channels were normalized. A linear regression (slope of the 405 nm fitted against the 470 nm signal) was applied over the data to correct for bleaching of signal of the duration at each recording. The Initial 3 seconds for the signals were discarded because of the photoreceiver/LED rise time artifact. Detection of GCaMP7f signal is calculated as a change in the 470 nm/fitted 405 nm signal over the fitted 405 signal ($\Delta F/F$). For the calculation of intensity values around events of interest (PC2), a 6-second window was used. We used 3 seconds before and after the PC2 event onset and computed z-scores for all such event windows. These z-scored intensity values were then averaged within and between animals in particular groups, and 95% confidence intervals for the averaged intensities were computed.

RNAScope *in-situ* hybridization

To prepare frozen sections, mice were placed in an air-tight chamber with 2.5 ml of isoflurane-infused cotton balls. After 45-60 seconds (after respiratory depression and loss of consciousness as evidenced by the negative tail and paw pinch), brains were acutely harvested and placed in a -80°**C** storage chamber until RNAScope *in-situ* hybridization protocol commenced.

16-µm coronal sections were collected on a cryostat (Leica Biosystems) at -20°C and mounted directly onto ColorFrost Plus microscope slides (Fischer Scientific). Slides were stored at -80°C until *in situ* hybridization (ISH) processing. ISH was performed using the RNAscope multiplex fluorescent kit (Advanced Cell Diagnostics, ACD) according to the manufacturer's instructions. The tissue was fixed in 4% paraformaldehyde (PFA) in PBS chilled to 4°C for 15 minutes, washed twice briefly in 1x PBS, then dehydrated in 50% ethanol, 70% ethanol, and twice in 100% ethanol for 5 minutes each at room temperature (RT). A hydrophobic barrier was traced around sections of interest using an ImmEdge pen (Fischer Scientific), and once the barrier dried, sections were incubated in Protease IV reagent for 30 minutes at RT, then rinsed twice in 1x PBS for 5 minutes. Probes for CRH and either CRHR1 or CRHR2 (ACD) were warmed, mixed, and placed onto sections for hybridization at 40°C for 2 hours in a HybEZ II oven (ACD), which was used for all subsequent incubations. Sections were washed twice in 1x wash buffer (ACD) for 2 minutes each, then incubated with a series of amplification reagents at 40°C, Amp 1-FL for 30 minutes, Amp 2-FL for 15 minutes, Amp 3-FL for 30 minutes, and Amp 4-FL Alt A or C for 15 minutes, washing twice in 1x wash buffer for 2 minutes each between steps. DAPI was applied to the sections for 30 s, then immediately coverslipped with ProLong Gold mounting medium (Invitrogen).

Images were collected on a Zeiss LSM 780 confocal microscope at 20x, 40x, or 63x magnification. mRNA puncta were quantified manually using FIJI 1.0 software (Image J), all experimental conditions were blinded to the imager, and all cell analysis and quantification.

Social Optical Real-Time Place Preference

In this test of sociability, mice were placed in a 3-chamber rectangular apparatus (61 cm x 40.5 cm x 23.5 cm) with clear acrylic walls and a white matte flooring. Initially, mice are habituated by being placed inside the center chamber for 5 minutes after being tethered to fiber optic cables. The second phase of 5 minutes of the experiment, occurs with the placement with the placement of 2 CD-1 male mice that were placed in target enclosures with grid-iron opening on one side to enable social interaction. The CD-1 mice were used only if they consistently failed screening criteria for being use in social defeat stress, and in a separate social interaction test mice display social interest and zero antagonistic behaviors. During the 5 minutes of phase 2 mice are tracked using Ethovision 10 (Noldus) and separate time spent in chamber side and interaction time were collected. Data from phase 2 were assessed “on-line” directly afterward and a side preference was identified. All mice showed a preference for one CD-1 compared to the other. On the third phase of the experiment (5 minutes), 5 Hz stimulation was assigned to the chamber opposite of that which the mouse preferred in phase 2. During the stimulation session, optical stimulate was delivered whenever the mouse enters into the stimulation chamber and was stopped once the mouse left.

Salient Urine Odorant Exposure

Odorants were placed in a 3-chamber rectangular apparatus (61 cm x 40.5 cm x 23.5 cm) and water, female, male, or fox urine was placed on 1 cm x 1 cm pieces of cotton (Nestlet). and contained in 2 cm diameter miniature petri dishes. Mouse urine and water volumbers were 500 µl, fox urine was 5 µl. Mice were tested over 3 trials over 3 days, each trial consisted of 2

minutes. Trial 1 was water vs male urine, trial 2 was male urine vs female urine, trial 3 was male urine vs predator urine and time spent interacting between the odorants were tracked with ethovision (Nodus). Odorants were counter-balanced on sides across mice and conditions (control vs ChR2 mice). Sniffing was described as nose to nestlet.

Immunohistochemistry

Mice were quickly anesthetized with urethane and perfused with cold 1x-PBS (OmniPure, Bio-Rad) followed by cold 4% PFA (Fisher Hamilton Scientific). Brains were placed in PFA at 4ºC for at least 24 hours, followed by being replaced with a 15% sucrose/PBS solution at 4ºC for 24 hours and brain sinking. The next day, brains were placed in a 30% sucrose/PBS solution at 4ºC for 24 hours. Once the brains sunk, it was washed in 1xPBS three times and mounted on a freezing microtome for sectioning at 35 micrometers.

Sections were washed three times for 10 minutes in 1x PBS, then blocked in 5% bovine serum albumin (Sigma-Aldrich) in 1x PBS with 0.3% Triton-X (Sigma-Aldrich) for 1 hour. Tissues were incubated with primary antibodies for rabbit anti-mCherry ((1:1000), Invitrogen) and goat anti-GFP (1:500, abcams) overnight at 4ºC. Sections were washed three times with 1xPBS and blocked with 0.3% Triton-X for one hour. Tissue was blocked with secondary antibodies anti-rabbit/568 (1:1000, Abcams) and anti-goat Alexa-488 (1:500) at room temperature for 1 hour. Sections were washed three times with 1x PBS for 10 minutes and mounted on slides with ProLong Gold antipode reagent with DAPI (invitrogen, P36931). Z-stacked images were acquired with a Zeiss LSM780 multi photon confocal system and z-stacks were collated using ImageJ (Fiji). Cell counters were obtained using the Cell Counter feature on ImageJ.

Statistical analysis

Animals were randomly assigned to control and experimental groups and all experimenters were blinded. Mice were excluded if viral infection was off-target. No data was excluded for other reasons. Student's two-tailed t-tests were used for comparisons of two experimental groups. For parametric data sets, comparisons among three or more groups were performed using one or two-way ANOVA tests followed by Tukey's or Bonferroni posthoc tests. For all tests, $p<0.05$ was determined to be significant. Statistical analyses were performed using Graph Pad Prism 9 .3.1 software (La Jolla, CA, USA). For data not normally distributed, non-parametric analyses were performed.

Code availability

MATLAB code used to analyze photometry data is available upon request.

Chapter 3

CRF Neurons Establish Resilience via Stress-History Dependent Modulation

Introduction to chapter 3

Cumulative stress is a major risk factor for developing major depressive disorder (MDD), yet not everyone experiencing chronic stress develops MDD. In those who do not, it is unclear at what point, or by what mechanism, a trajectory of stable resiliency emerges. Utilizing a 10-day repeated social defeat stress model (RSDS) for MDD, we observed that a critical period between 7 and 10 daily defeats marks the phenotypical divergence of resilient from susceptible mice. In response to ongoing stress, corticotropin-releasing factor (CRF) neurons of the oval nucleus of the bed nucleus of the stria terminalis (BNSTov) display a sustained increase in firing rate in resilient but not susceptible mice. This neurophysiological adaptation generated resiliency, but only after 7 critical stress exposures, indicating that this process is dependent on stress history. Our study reveals the role of stress accumulation-dependent activation of the CRF system in the establishment of resiliency to psychosocial stressors.

Major depressive disorder (MDD) is a crippling heterogeneous neuropsychiatric condition with high morbidity and lifetime prevalence, exacerbated by the ongoing global pandemic (Veer et al. 2021). MDD is episodic in nature, with treatment success diminishing with each subsequent depressive episode (Post 1992). Major life stressors are key risk factors for precipitating the onset of an episode (Gold 2013; Kendler et al. 1999). While most people report at least one major life stressor at some point in their lives, not everyone goes on to develop MDD. It is also known that depression can emerge after repeated significant stressor exposure, suggesting that cumulative exposure to stress is associated with increased depression risk in vulnerable individuals (Barthas et al. 2020; Golden et al. 2011; Martinez et al. 1998; Zheng et al. 2022). Cumulative stress causes numerous psychological insults that predispose neuropsychiatric conditions (Kudryavtseva et al. 1991; Laine et al. 2017; Barthas et al. 2020). Many studies have explored the individual differences in stress susceptibility or resiliency, and investigations in rodents have begun to identify the potential underlying neural mechanisms. Recent studies suggest mechanisms involved in the emergence of depression may be distinct from those that maintain the depressive state (Hultman et al. 2018; Drysdale et al. 2017). With the odds of treatment failure increasing with subsequent depressive episodes[2,9] and increased depression risk of cumulative stress, a potentially more effective strategy would be to target the mechanisms mediating resilience, enhancing the ability to cope with cumulative stress.

The ability to engage in social and hedonic-like behaviors in the face of psychosocial stress is an adaptive behavioral strategy, and failing to do so is associated with high morbidity (Franklin et al. 2012; Russo et al. 2012; Karatsoreos and McEwen 2011). Resiliency is defined as the "process of adapting well in the face of adversity… [to] threats, or significant sources of stress[14]." Resiliency is unlikely to emerge from the absence of a pathological stress response but instead is an active process involving a myriad of cellular and circuit-level changes in the brain. Repeated social defeat stress (RSDS) induces robust depression-like behavioral

phenotypes in roughly 2/3 of mice (Golden et al. 2011; Laine et al. 2017). The standard 10-day RSDS protocol has been employed widely to identify and study neurobiological features of susceptible and resilient subpopulations (Laine et al. 2018; Markham et al. 2009; Gururajan et al. 2021; Walsh et al. 2014; Golden et al. 2011; Krishnan et al. 2007; Martinez et al. 1998; Matsuda et al. 1996; Berton et al. 2006). However, temporal dynamics of the divergence of susceptible and resilient phenotypes following repeated stress and the underlying mechanisms driving the divergence in isogenic mice are not well understood.

The bed nucleus of the stria terminalis (BNST) is an important node for integrating sensory cues, interoception, cognition, and motivational states to enact adaptive responses (Waraczynski 2016; Flanigan and Kash 2020). The BNST is well-positioned in the social salience network to integrate external cues with internal states to influence the outcome and context of social interactions (Lebow and Chen 2016; Waraczynski 2016; Daniel and Rainnie 2016; Flanigan and Kash 2020). The oval nucleus of the BNST (BNSTov) is a stress-sensitive subregion that is a key candidate region for encoding stress modulation of social behavior through its projections to areas such as the ventral tegmental area (VTA) (Jennings et al. 2013; Dedic et al. 2018; Chen et al. 2015; Dabrowska et al. 2016) and dorsal raphe(Matthews et al. 2016; Marcinkiewcz et al. 2016). Corticotrophin-releasing factor (CRF) neurons of the BNSTov ($BNSTov^{CRF}$) are a major output of this region and can influence affective states(Regev et al. 2011; Sink et al. 2013; Konishi et al. 2003;Jasnow et al. 2004). Since $BNSTov^{CRF}$ neurons are thought to promote arousal and adaptive responding according to stress-related changes in internal state(Avery et al. 2016; Kim et al. 2013; Rodríguez-Sierra et al. 2016; Ventura-Silva et al. 2012; Giardino et al. 2018; Duvarci et al. 2009; Waraczynski 2016; Duque-Wilckens et al. 2020; Flanigan and Kash 2020; Daniel and Rainnie 2016), we hypothesized they might play a role in establishing resiliency to repeated social stress.

Using the 10-day RSDS paradigm, we used cell-type selective *ex vivo* electrophysiology, chemogenetics, optogenetics, and *in vivo* fiber photometry to interrogate the BNSTov^{CRF} system to explore its role in the divergence of susceptible and resilient phenotypes. We observed that BNSTov^{CRF} neurons encode repetitive social stress and undergo adaptation that coincides with the divergence of resilient and susceptible phenotypes. Unexpectedly, we observed that resiliency entails cumulative stress-dependent neuroadaptive changes, whereas susceptibility emerges in the absence of similar adaptations. Inhibition of BNSTov^{CRF} neurons using designer receptors exclusively activated by designer drugs (DREADDs) during social defeat led to a susceptible phenotype while activating those neurons promoted resiliency. Finally, using RNAscope and optogenetics, we provide intriguing evidence for a potential role of *Crfr1* in BNSTov^{CRF} neurons in mediating resilience.

Results:

Susceptible versus resilient phenotypes emerge between 7 and 10 daily episodes of social defeat stress.

RSDS produces divergent and enduring resilient/susceptible phenotypes following 10 episodes of social defeat stress (Golden et al. 2011; Krishnan et al. 2007; Berton et al. 2006), has high ethological validity, and enables the investigation of the consequences of stress accumulation (Barthas et al. 2020; Martinez et al. 1998). To examine the temporal divergences of resilient and susceptible phenotypes in mice, a modified RSDS stress protocol was employed in which mice were subjected to discrete numbers of social defeat episodes (SDEs) interspersed with social interaction (SI), and sucrose preference (SP) tests administered after 1, 4, 7, and 10 SDEs (Fig. 2a-d). Social Interaction (SI) Ratio is a behavioral score of the SI test and measures the time spent in the area proximal to the enclosure of a novel social target (social interaction

zone). To generate the SI ratio, interaction zone time was calculated both in the absence and presence of the social target, such that SI ratio > 1 is resilient and <1 is susceptible. Surprisingly, we found that the susceptible phenotype emerged between 7 and 10 SDEs, reflected by a robust decrease in social interaction on day 10 compared to day 7 (Fig. 2e) (SI ratio: 2.062 +/- 0.226 after 7 SDEs to 0.559 +/- 0.093, $p<0.0001$, n = 11 for susceptible and 1.967 +/- 0.188 (7 SDEs) to 1.554 +/- 0.163 (10 SDEs), $p=0.2929$, n=11 for resilient). There were no significant differences in SI ratios after 7 SDEs between mice that went on to become susceptible vs resilient after 10 SDEs (mean: 2.062 +/- 0.226 vs 1.967 +/- 0.188, two-tailed t-test, $p=0.7483$, n= 11/group) (Extended Data Fig. 3a). To test whether this was a result of repeated SI tests, in a separate experiment, we subjected independent groups of mice to either 1, 4, 7, or 10 SDEs, conducting the SI and SP tests only once, and observed a similar effect of susceptible/resilient subgroups emerging after the seventh episode of social defeat (Extended Data Fig. 3b-d). Resilient (10 SDEs) mice had an indistinguishable SI ratio from all mice after 7 SDEs, while susceptible (10 SDEs) mice had an SI ratio significantly lower than both groups (Fig. 2f). In the SP test, resilient 10 SDE mice showed a similar preference for sucrose to all 7 SDE and stress-naïve control mice. Susceptible mice, by contrast, exhibited a decreased SP relative to 7 SDE and resilient groups (Fig. 2g). Previous studies reported that RSDS produces susceptible and resilient phenotypes after 10 SDEs in a bimodal distribution (Krishnan et al. 2007). Here, we observed a unimodal distribution of social interaction toward a novel conspecific in 7 SDE mice but a bimodal distribution in 10 SDE mice, consistent with the emergence of distinct resilience and susceptible phenotypes (Fig. 2h,i). The susceptible population of mice represents a statistically distinct group compared to 7 SDE and 10 SDE resilient mice (Kolmogorov-Smirnov, $p<0.0001$; Fig. 2j). The time spent interacting with a novel conspecific is significantly less in susceptible 10 SDE mice than the 7 SDE and 10 SDE resilient mice, which were indistinguishable from each other (Fig. 2k). The divergence into susceptible and resilient phenotypes depended on the number of SDEs, rather than the passage of time.

Mice subjected to 7 consecutive days of social defeat stress displayed social approach behavior when tested on day 11 and day 30, yet social avoidance emerged when subjected to three additional defeat episodes (Extended Data Fig. 3g). Thus, the number of episodes (8-10 SDEs), not the duration of time after the 7th SDE, is responsible for the emergence of the susceptible phenotype. To gain insight into potential neural mechanisms involved in the phenotypic divergence, we used c-Fos immunohistochemistry as a proxy of neural activation in mice subjected to 10 SDEs following a 30-minute social interaction with a non-aggressive novel conspecific (Extended Data Fig. 4a). While several brain regions implicated in social behavior and motivation were assessed, only the anterior dorsal BNST showed significant differences in c-Fos immunoreactivity (FOS-ir) between the stress-naïve, susceptible 10 SDE and resilient 10 SDE mice (Extended Data Fig. 4b). Given its role in responding to chronic stress, valence, and motivational processes, we more specifically examined the BNSTov (Waraczynski 2016). While no difference in FOS-ir was detected between stress-naïve and 7 SDE mice, there was a significant decrease in FOS-or in susceptible (10 SDEs) and a significant increase in resilient (10 SDEs) mice, respectively (Extended Data Fig. 4c-e). Thus, the FOS-ir data suggests a neural divergence in BNSTov in response to a social threat that paralleled the divergence in SI defining resilient and susceptible phenotypes.

Divergence in BNSTov^{CRF} neuronal firing rates tracks the emergence of resilient and susceptible phenotypes.

CRF neurons are a major output source of the oval BNST and are sensitive to chronic stressors (Dabrowska et al. 2013; Hu et al. 2020; Daniel et al. 2019; Daniel and Rainnie 2016). Thus, we hypothesized that chronic stress would alter BNSTov^{CRF} neuronal activity in a manner coinciding with the divergence in resilient and susceptible behavioral phenotypes. To test this hypothesis, *Crf*-ires-*Cre;*ai14 (tdTomato) mice(Chen et al. 2015; Wanat et al. 2013; Salimando et al. 2020;

Hartley et al. 2019; Sanford et al. 2017) were subjected to either 7 or 10 daily SDEs, and cell-attached *ex vivo* electrophysiological recordings were conducted in the BNSTov (Fig. 5a-b). CRF^+, but not CRF^-, BNSTov neurons significantly increased firing rate in 7 SDE mice compared to stress-naïve control mice. By contrast, CRF^+ firing rates in susceptible 10 SDE mice were indistinguishable from that of controls and were lower than that of 7 SDE and resilient 10 SDE mice. CRF^- neuron firing did not differ between any groups (Fig. 5c-d). Moreover, there was a strong correlation between firing rate and social interaction ratio in CRF^+ but not CRF^- neurons in 10 SDE mice (CRF^+, R^2=0.5725, *p=0.0113; CRF- R^2=0.06096, p=0.5219, Fig. 5e). CRF neurons display both burst and non-burst firing patterns (Rodríguez-Sierra et al. 2016; Rodríguez-Sierra et al. 2013; Gungor and Paré 2016). Burst firing patterns were prominent in resilient and 7 SDE mice, but few were seen in susceptible and control mice (Fig. 5f-h). Additionally, percentage spikes within burst were higher in 7 SDE and resilient compared to susceptible 10 SDE mice (***p=0.0004, one-way ANOVA, Fig. 5i), but not susceptible or control mice. The number of spikes per burst and number of bursts per cell was not significantly different amongst the groups (Fig. 5j,k). These data and correlation analysis suggest the possibility that there is a causal link between the neuronal activity of $BNSTov^{CRF}$ neurons and the divergence of behavioral phenotypes.

$BNSTov^{CRF}$ neurons bidirectionally modulate the emergence of resiliency.

To test the hypothesis that $BNSTov^{CRF}$ neurons are regulating the maintained resiliency over the last 3 episodes of RSDS, during which susceptible and resilient phenotypes emerge, we injected *Crf*-ires-*Cre* mice with adeno-associated viruses (AAVs) encoding Cre-dependent excitatory (DIO-hM3Dq), inhibitory (DIO-hM4Di) DREADDs, or a control mCherry construct into the BNSTov, and administered clozapine N-oxide (CNO) via drinking water (Zhan et al. 2019; Schalbetter et al. 2021; Wess et al. 2013) (Fig 6a-b). We speculated that this experimental

design allowed modulating neurons over a longer time span than intraperitoneal (IP) injections would allow with minimal invasiveness, particularly because it was not clear over when neuroadaptation occurs within the 3-day window. mCherry control mice exhibited both susceptible and resilient phenotypes (SI ratio <1.0 and >1.0, respectively) in roughly the 60/40 ratio as expected (Krishnan et al. 2007; Golden et al. 2011). Interestingly, mice injected with inhibitory DIO-hM4Di displayed a robust susceptible phenotype, while DIO-hM3Dq mice displayed resilient phenotypes following CNO drinking water administration (Fig. 6c). Moreover, none of the DIO-hM4Di + CNO mice went on to develop resilience (0/10, SI >1.0) while 89% (8/9, SI >1.0) of the DIO-hM3Dq were resilient (Fig 6f). Notably, the social defeat experience was not affected by the DREADDs manipulations (Extended Data Fig. 7a, b). The SP test — a test of hedonic behavior — revealed differences between mCherry susceptible (mCherry (S)) and resilient (mCherry (R)) mice that were mirrored in DIO-hM4Di and hM3Dq mice, respectively. mCherry (S) and hM4Di mice displayed a significant decrease in SP relative to mCherry (R) and hM3Dq-injected mice (Fig. 6d). There were no significant differences in locomotion (Fig. 3e). The chemogenetic manipulation also produced bidirectional effects on anxiety-like behavior in elevated plus maze (EPM) and open-field tests (Extended Data Fig. 8a-g). Surprisingly, mice injected with hM3Dq-DREADDs went on to become resilient (Fig 6c) even though activation of *Crf* neurons of the BNST have previously been shown to produce depressive- and anxiogenic-like responses (Salimando et al. 2020; Kim et al. 2013; Walker et al. 2009; Daniel and Rainnie 2016; Hu et al. 2020; Regev et al. 2011). Interestingly, the resiliency only occurred as a result of BNSTov^{CRF} chemogenetic activation between 8-10 episodes of social defeat; excitatory hM3Dq-DREADDs activation during episodes 4-7 or 10-13 failed to display resiliency (Fig. 6g-i). Modulating *Crf* neurons with inhibitory hM4Di- or excitatory hM3Dq- DREADDs between 8 and 10 SDEs led to enduring susceptible or resilient phenotypes, respectively, up to 6 weeks after CNO manipulation (Extended Data Fig. 9a-c). These

observations strongly support that the behavioral outcomes induced by the activation of BNSTov^{CRF} neurons are stress history-dependent.

Calcium dynamics underlying stress adaptation

We combined fiber photometry with excitatory or inhibitory DREADDs to determine whether SD-induced neuroadaptation in BNSTov^{CRF} neurons, *in vivo*, reflects the behavioral response to a novel conspecific consistent with resilient and susceptible phenotypes. Mice were co-injected with CRE-dependent GCaMP7f and either DIO-hM4Di, -hM3Dq DREADDs, or -mCherry viral vectors (Fig. 10a,b). CNO was administered via drinking water over the last 3 episodes of RSDS, commensurate with the observed divergence of susceptible and resilient phenotypes. We observed that mCherry (S) mice experienced a decrease in neuronal activity upon initiation of social interaction with a novel conspecific in contrast to an increase in activity observed in mCherry (R) mice (Fig. 10c-e). Mice injected with DIO-hM4Di significantly decreased calcium-related neuronal activity during social interaction. In contrast, social interaction initiation led to increased activity in DIO-hM3Dq injected mice (Fig. 10f-h). There were no significant differences in SI of mice subjected to 7 SDEs, yet differences emerged following 3 additional SDEs, with subsets of mice becoming susceptible or resilient (mCherry(R)/(S)). Chemogentically activating or inhibiting BNSTov^{CRF} neurons during this period promoted resiliency or susceptibility, respectively (Fig. 10i). We observed a strong correlation between SI ratio and calcium activity only after 10 SDEs (Fig. 10j). No significant differences were observed in calcium-based neuronal activity upon social interaction with a novel conspecific in mice subjected to 7 SDEs (Extended Data Fig. 11a,b) or in the absence of social interaction (Extended Data Fig. 11c). In contrast, after 10 SDEs, mCherry (R) and DIO-hM3Dq injected mice displayed significantly greater neuronal activation upon social contact relative to mCherry (S) and DIO-hM4Di injected mice (Extended Data Fig. 11d). Despite the difference in time spent interacting with a novel conspecific, the number of interaction zone entries or distance

traveled were not significantly different (Fig. 10k, Extended Data Fig. 11e). These data suggest that BNSTov^{CRF} neuronal dynamics are differentially altered by stress modulation in accordance with phenotypical displays of resiliency/susceptibility.

***Crfr1* expression in BNSTov^{CRF} neurons mirrors the behavioral emergence of resilience.** We observed a stress-induced enhancement in firing rates of BNSTov^{CRF} neurons in resilient mice. To explore the effect of this BNSTov^{CRF} stress modulation on CRF receptor transmission, we used RNAScope *in situ* hybridization to quantify *Crfr1* and *Crfr2* in accordance with stress history. Mice were subjected to either 7- or 10-daily episodes of social defeat, and *Crfr1* and *Crfr2* expression in the BNST were assessed (Fig. 12a-c) due to their reported role in mediating stress responses (Tran et al. 2014; Lee et al. 2008; Dedic et al. 2019; Chen et al. 2015). The percentage of CRFR1-expressing neurons among CRF-expressing neurons was higher in mice subjected to 7 SDEs than in susceptible mice but not significantly different than resilient mice (Fig. 12d). In contrast, there were no significant differences in BNSTov neurons co-expressing *Crfr2 and Crf mRNA* across groups of mice (Fig. 12e). The overlap between *Crfr1* and *Crf* in the BNST was significantly greater in the oval nucleus than in anterolateral, anteromedial, and ventral subregions of the anterior dorsal BNST (Fig. 12c,f).

To explore the role of firing rate changes on gene expression and the development of resiliency, we optogenetically stimulated BNSTov^{CRF} neurons using transgenic *Crf-Cre*::ai32 mice, which express channelrhodopsin-2 (ChR2) in *Crf*-containing neurons (Wang et al. 2021) (Fig. 12g). For control experiments, transgenic mice of a similar background were used, except instead of ai32, mice expressed the tdTomato fluorophore in Crf neurons (*Crf-tdTomato*). 5 Hz stimulation frequency was used in order to mirror the average firing rate observed in the spontaneous firing rate of resilient mice (Fig. 5d). Mice received 15-minute 5 Hz photostimulation of BNSTov^{CRF} neurons following physical stress on SDEs 8-10. Mice were placed in the adjacent

compartment separating the aggressor, preventing physical contact. The compartment divides the aggressor cage in half by a clear plexiglass that allows for continuous sensory cues (Fig. 12h,i). Photostimulation of *Crf*::ChR2 mice led to a significantly higher SI ratio and greater percentage resilient than control *Crf::tdTomato* mice (89% vs. 33%) when stimulated during 8-10 SDEs (Fig. 12j). Surprisingly, *Crf::ChR2* mice that received photostimulation but were not subjected to 8-10 SDEs showed a significant decrease in SI ratio, and 100% of the mice became susceptible (0/6, SI > 1.0) (Fig. 12j). Photostimulation paired with SDEs 8-10 increased *Crfr1* mRNA expression in CRF neurons relative to mice that experienced photostimulation in the absence of additional stress (Fig. 12k, l). In a cell-attached slice preparation, we applied a CRFR!-selective antagonist, NBI 27914, in the bath of the optogenetically-induced resilient mice and it significantly decreased firing rates (Extended Data Fig. 13a-c, e,f). Additionally. optical stimulation produced burst-firing, suggesting that in addition to producing resiliency, it also replicated the burst-firing pattern observed in this group (Extended Data Fig. 13, Fig 5f). In summary, these data show that maintenance of resiliency requires social defeat stress BNSTovCRF activation and is correlated with the upregulation of *Crfr1* expression in a stress-history dependent manner (Fig. 6g-i).

Discussion

The RSDS paradigm was modified to observe the effects of cumulative stress on neuroplasticity in regions critical for mood regulation. Many of the studies investigating mechanisms of susceptibility and resiliency have explored changes occurring after the 10 SDEs when stable susceptible/resilient phenotypes have already emerged. Indeed, our work has uncovered a discrete window of neuronal and behavioral plasticity between 7 and 10 SDEs during which susceptible and resiliency phenotypes are established. By capturing behavioral, electrophysiological, and *in vivo* fiber photometric measures during the intra-social defeat stress

period, we uncover the mechanisms underlying the establishment of susceptible and resiliency phenotypes, which may differ from those involved in its maintenance.

The BNST is a complex structure consisting of 16 different subnuclei and has been implicated in prosocial behaviors (Rodríguez-Sierra et al. 2013; Waraczynski 2016; Gungor and Paré 2016; Daniel and Rainnie 2016). While the oval nucleus has been investigated in stress responses, we hypothesized that the region would be instrumental in processing contexts associated with social stress. Indeed, we observed that BNSTovCRF neurons encode individual differences of stress effects on social behavior. Prior studies have implicated the overactivation of CRF in the BNST as being pro-depressive and anxiogenic (Salimando et al. 2020; Dabrowska et al. 2016; Kim et al. 2013; Daniel et al. 2019; Hu et al. 2020); therefore, we were surprised to observe that $BNSTov^{CRF}$ neurons exhibited increased activity in resilient mice. Moreover, cell-type-specific activation of this CRF neuronal population yielded resiliency in mice. Importantly, we were able to replicate the effects of $BNSTov^{CRF}$ activation, achieving a social avoidant response in line with previous studies in stress-naïve mice, suggesting that stress history may play a critical role. To our knowledge, this study is the first to target this neuronal population in a stress history-dependent manner in the context of social behavior, although CRF peptide or CRF neuronal involvement in stress responding has been known (Walsh et al. 2014; Chen et al. 2020; Elliott et al. 2010). Indeed, we observed that the activating hM3Dq manipulation only produced resilient mice after a certain duration of daily stressors (7 SDEs), suggesting that the BNSTov may be tightly modulated based on stress history resulting in adaptive responses in contexts where they may be most advantageous. Our findings support a view that resilience is a stress history-dependent state, which does not exist prior to stress. This is also consistent with previous demonstrations that resilience is a status achieved by active regulation of genes even more than that in susceptible animals (Zhang et al. 2019; Friedman et al. 2014; Krishnan et al. 2007).

CRF neurons have been observed to influence the salience of stressful contexts according to stress exposure (Dabrowska et al. 2013; Lemos et al. 2012; Dedic et al. 2019; Waraczynski 2016; Daniel and Rainnie 2016). One feasible mechanism by which this occurs is through CRF receptor dynamics. We hypothesized that the development of resiliency or susceptibility occurs via CRF-CRFR interactions in the BNST. We were surprised to observe *that Crfr1* mRNA expression in CRF neurons corresponded to establishing resilient/susceptible phenotypes. CRFR1 has been found largely on non-CRF neurons in the BNST (Justice et al. 2008; Dabrowska et al. 2013), but our finding suggests that stress promotes *Crfr1* mRNA expression on CRF neurons themselves in a stress history-dependent manner. This is evidenced by there being a higher overlap of *Crfr1/Crf* mRNA expression in mice subjected to 7 SDEs than in severely stressed mice that underwent 10 SDEs and became susceptible.

CRFR1 has been shown to be selectively activated in settings of stress following a chronic stressor, serving as a signaler of ongoing stress (Ramot et al. 2017). Several studies using viral constructs to overexpress CRF in the dorsolateral BNST led to a decrease in CRFR1, presumably as a compensatory response, yet the behavioral consequences of this were not explored in the context of susceptibility and resiliency to stress (Regev et al. 2011; Sink et al. 2013). CRFR1 is a G_s-coupled receptor that leads to strong depolarization promoting cell activation (Hu et al. 2020; Konishi et al. 2003; Ramot et al. 2017; McClard et al. 2018; Hillhouse and Grammatopoulos 2006). Therefore, these neurons establish resiliency by way of prolonged activation of CRF neurons, in part, by the maintenance of CRFR1 expression. This auto receptor-like ability has also been observed in terms of neuronal activation. Chronic stress was shown to shift connectivity of local CRF^+ neurons from CRF^+-CRF^- to a larger percentage of CRF^+-CRF^+ cells (Partridge et al. 2016). Studies using prolonged overactivation (over weeks to months) of CRF activity have yielded antidepressant and anxiolytic results (Regev et al. 2011; Sink et al. 2013; Dedic et al. 2018). Here we identify a more discrete timeline in the span of

days to capture the transition of when BNSTov^{CRF} activation becomes pro-resilient. By optogenetically activating BNSTov^{CRF} neurons, we observed an increase in CRFR1 expression. Though correlative, this exquisite regulation of CRFR1 according to stress history may underlie why clinical trials of CRFR1 antagonists for MDD have been met with variable success (Spierling and Zorrilla 2017; Waters et al. 2015; Reul 2002; Lee et al. 2008). Although beyond the scope of the current study, future experiments using siRNA or CRISPR knockdown approaches should be performed to determine whether upregulation of CRFR1 is a critical step of neuromodulation leading to resiliency.

Stress-sensitive regions such as the BNST have been found to be of critical importance in stress coping and reactivity (Johnson et al. 2016; Crestani et al. 2010; Fiedler et al. 2021). Stress resiliency has long been considered a response separate from or in the absence of stimuli that gives rise to stress susceptibility, mediated by parallel circuits or cell-types in a particular brain region (Cathomas et al. 2019; Franklin et al. 2012; Russo et al. 2012). Here, we observe that activity dynamics of CRF neurons can shape and influence resiliency to stress, potentially through (auto)regulation of *Crfr1* mRNA. Other substrates may be used to classify these neurons either on the basis of dual-neuropeptide or circuit-specific identities and should be the object of future exploration.

Previous work has shown that resiliency is influenced by dopaminergic VTA neurons in the nucleus accumbens (NAc) (Dedic et al. 2018), in part, through the actions of brain-derived-neurotrophic-factor (BDNF) (Krishnan et al. 2007; Koo et al. 2019; Wook Koo et al. 2016). CRF peptide has been important for BDNF release in the NAc as a stress-coincidence sensor (Walsh et al. 2014), yet the sources of CRF important for altering stress effect on social and hedonic behavior has not been extensively characterized. While long-range GABAergic BNST neurons projecting to the VTA have been shown to influence reward and anxiety-like behavior

(Takahashi et al. 2019; Caillé et al. 2009; Silberman et al. 2013; Wanat et al. 2013; Rodaros et al. 2007), it is unclear to what degree these cells comprise the oval nuclear BNST population. The BNST also sends projections to the dorsal raphe, lateral and paraventricular hypothalamus, and ventrolateral periaqueductal gray (Matthews et al. 2016; Dabrowska et al. 2016; Dong et al. 2001; Marcinkiewcz et al. 2016; Daniel and Rainnie 2016; Maita et al. 2021; Giardino et al. 2018; Johnson et al. 2016; Kaouane et al. 2021), among others, whose modulation have been linked to stress on affect and social motivation. In this way, the BNST acts as a node for integrating information regarding stress history and determining socio-affective outcomes according, possibly due to CRFR1 receptor dynamics occurring on CRF neurons of the oval nucleus, thereby shaping the long-lasting outcome of resiliency.

Our study highlights a previously unknown mechanism by which the BNST encodes cumulative social stress and effectuates susceptible or resilient outcomes. Importantly, there are currently no Food and Drug Administration-approved drugs aimed at preventing a depressive episode from occurring. By targeting mechanisms involved in establishing resiliency, the possibility may exist to therapeutically leverage windows of plasticity to effectuate resiliency and evade the development of MDD.

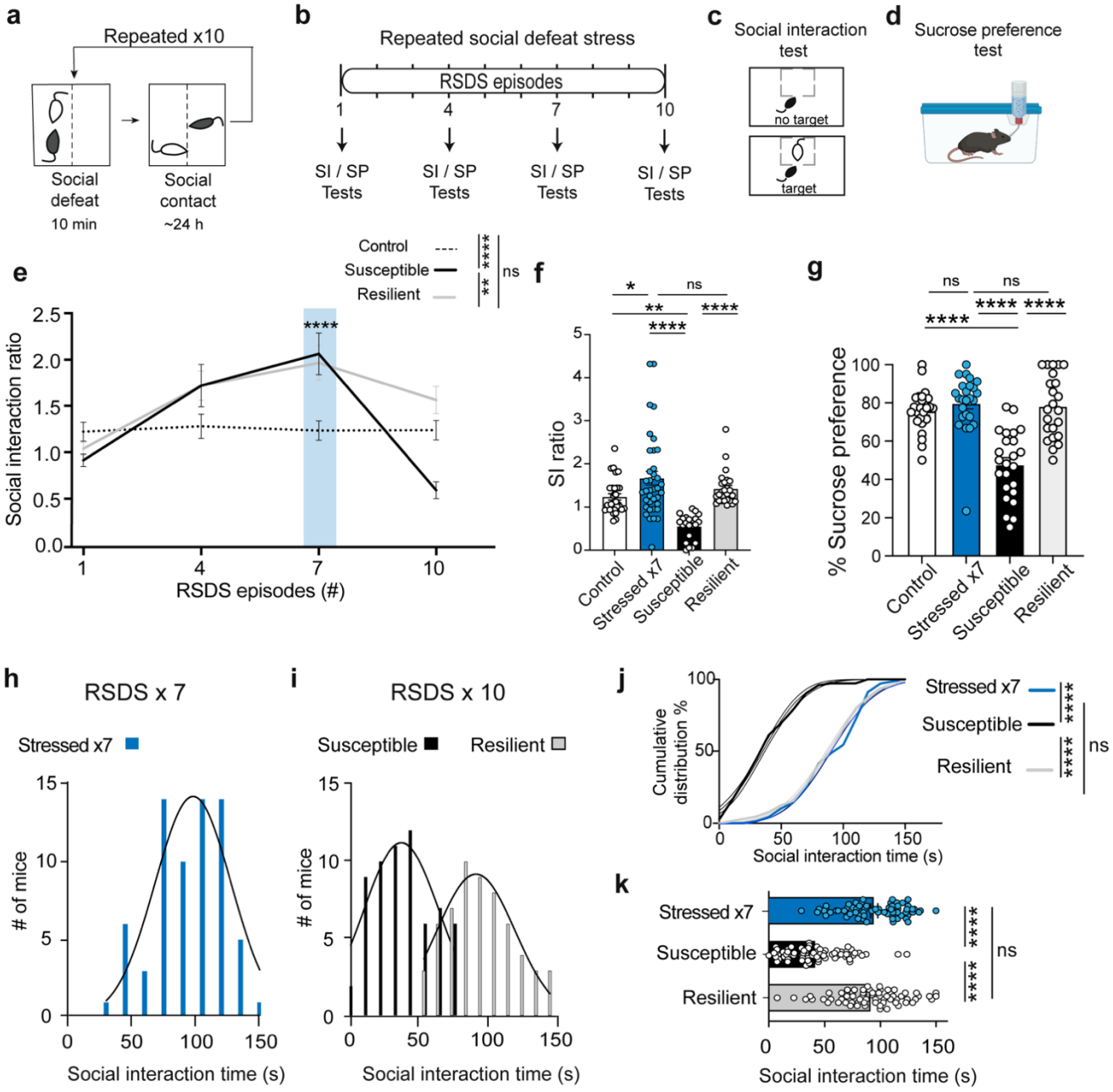

Figure 2. Susceptible and resilient subgroups emerge between 7 and 10 daily episodes of social defeat stress.

Figure 2. Susceptible and resilient subgroups emerge between 7 and 10 daily episodes of social defeat stress.

a, Experimental design for RSDS. **b,** Experimental timeline of social defeat stress and behavioral tests. **c,** Social interaction test schema involving target and no target trials. **d,** Sucrose Preference Test schematic. **e,** Effect of cumulative social defeat stress on social interaction. SI ratios after 1, 4, 7, and 10 defeat episodes (n=11-18 mice/group), two-way ANOVA interaction $F(6,134)=5.783$ ****$p<0.0001$, row factor $F(3,134)=12.11$ ****$p<0.0001$, $F(2,134)=4.086$ column factor *$p=0.0167$, Tukey's post-hoc test susceptible vs resilient ****$p<0.0001$, susceptible vs control **$p=0.0074$, resilient vs control $p=0.2751$. SI test susceptible (SI test 7 vs 10) ****$p<0.00001$. **f,** Aggregated data on social interaction test across experiments. One-way ANOVA treatment $F(3,109)=14.61$ ****$p<0.0001$. Tukey's post-hoc test control vs stressed x7 *$p=0.0309$, control vs susceptible **$p=0.0012$, stressed x7 vs susceptible ****$p<0.0001$, susceptible vs resilient ****$p<0.0001$ (n=25-37 mice) **g,** Sucrose preference test. One-way ANOVA treatment $F(3,93)=24.06$ $p<0.0001$). Tukey's post-hoc test control vs stressed x7 $p=0.77$, control vs susceptible ****$p<0.0001$, control vs resilient $p=0.9387$, stressed x7 vs susceptible ****$p<0.0001$, stressed x7 vs resilient $p=0.984$, susceptible vs resilient ****$p<0.0001$ (n=23-25 mice). **h,** Distribution of stressed mice who underwent 7 SDs. **i,** Distribution of mice who underwent 10 SDs and sorted into susceptible and resilient mice**. j,** Cumulative distribution of all stressed mice. Kolmogorov-Smirnov (distance) 0.2054, ****$p<0.0001$. **k,** Time spent interaction socially with a novel conspecific. One-Way ANOVA $F(2,201)=76.63$, ****$p<0.0001$. Tukey's post-hoc susceptible vs resilient ***$p<0.0001$, susceptible vs stressed x7 ****$p<0.0001$, stressed vs resilient $p=0.4984$ (n=72 susceptible, 64 resilient mice respectively).

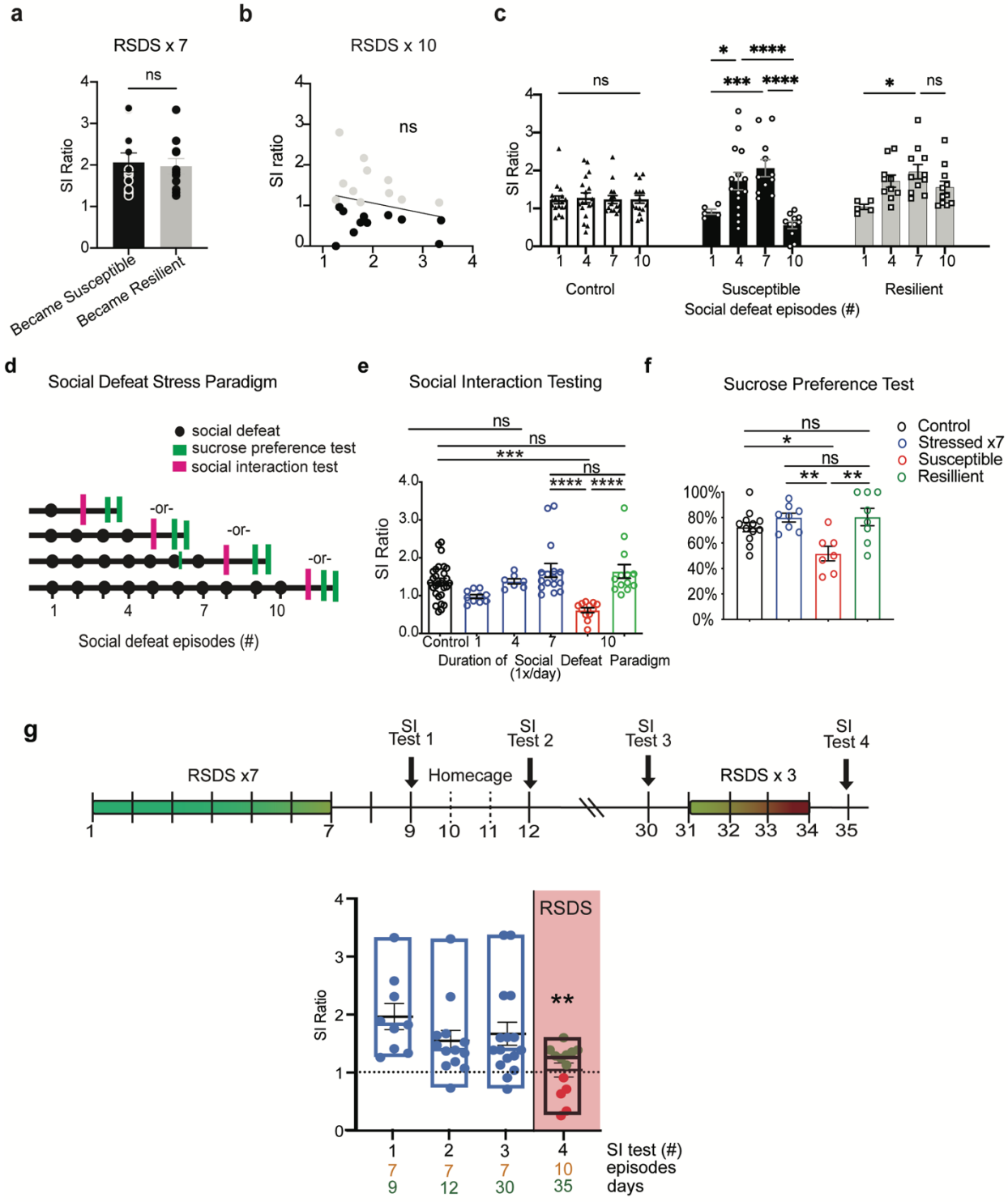

Figure 3. Social defeat episodes, not days, promulgate the divergence of susceptible/resilient phenotypes(Extended Data).

Figure 3. Social defeat episodes, not days, promulgate the divergence of susceptible/resilient phenotypes (Extended Data).

a, Social interaction (SI) test of mice subjected to 7 episodes of social defeat stress (SDEs). Became susceptible vs became resilient, 2.062+/-0.226 vs 1.967 +/- 0.188, n=11, unpaired t-test, two-tailed t=0.3253, df=20, n=11 mice/group, p=0.7483. Correlation of mice subjected to 10 SDEs (stressed x 10) and 7 SDEs (Stressed x7). R^2=0.06314, p=0.06314, n=22 mice. **c,** SI test of mice after 1, 4, 7, and 10 SDEs (n=5-18 mice/group). Two-way ANOVA, interaction F(6,132) = 5.741, p<0.0001, row factor (episode #) F(3,132) = 12.10, ****p<0.0001, column factor (phenotype) F (2, 132) = 3.958, *p=0.0214. Tukey's post-hoc test Susceptible (1 vs 2 SDEs: *p=0.0214, 1 vs 3 SDEs: ***p=0.0009, 2 vs 4 SDEs: ****p<0.0001, 1 vs 4 SDEs: p=0.6295, 2 vs 3 SDEs: p=0.3994). Resilient (1 vs 2 SDEs: p=0.1114, 1 vs 3 SDEs: *p=0.0111, 1 vs 4 SDEs: p=0.3072, 2 vs 3 SDEs, p=0.7298, 2 vs 4 SDEs: p=0.8999, 2 vs 4 SDEs: p=0.2929). Control (1 vs 2 SDEs: p=0.9899, 1 vs 3 SDEs: p>0.9999, 1 vs 4 SDEs: 0.9998, 2 vs 3 SDEs: 0.9954, 2 vs 4 SDEs: 0.9966, 3 vs 4 SDEs: >0.9999). **d,** Schematic of social defeat stress of 4 distinct cohorts as cross-sectional behavioral assessment of stress effect on SI. **e,** Social interaction test of cross-sectional behavioral assessment of 4 distinct cohorts of 1, 4, 7, 10 SDEs. Control=1.367+/-0.09087, n=28; SDE 1=0.9762+/-0.05049, n=10; SDE 4= 1.377+/-0.06854, n=7; SDE 7=1.669+/-0.1801, n=16; SDE 10(R)= 1.640+/-0.1811, n=13; SDE 10(S)= 0.6164+/-0.06406, n=12. One-Way ANOVA F(5,80)=8.341, P=<0.0001, Sidak's post-hoc test control vs 10: ***P=0.0006, SDE 1 vs 7: *P=0.0144, SDE 1 vs 10: *P=0.0341, SDE 4 vs 10: *P=0.0301; SDE 7 vs 10 (S): ****P<0.0001, SDE 10 (S) vs SDE 10 (R)=****P>0.0001. **f,** Sucrose preference test of independent cohorts of mice subjected to 1, 4, 7, or 10 SDEs. Control, n=12, 72.5160+/-3.6657%; Stressed x7, n=8, 80.0383+/-3.5376%; Susceptible, n=7, 51.7406+/-5.716%; Resilient, n=8, 80.4516+/-6.8360%. One-way ANOVA F(3,31)=6.337, P=0.0018. Tukey's post-hoc test control vs susceptible: *P=0.0243, stressed x7 vs susceptible: **P=0.0035, susceptible vs resilient: **P=0.003. **g,** Schematic of experimental design containing modified RSDS consisting of 10 episodes dispersed

over 33 days, with intervention SI testing at days 9, 12, 30, and 35. **h,** 7 SDEs, SI Test 1: 1.966+/-0.2245, n=9; 7 SDEs, SI Test 2: 1.549+/-0.179, n=13; 7 SDEs, SI Test 3: 1.67+/-0.1976, n=16; 10 SDEs (S), SI Test 4: 0.5712+/-0.121, n=5; 10 SDEs (R), SI Test 4: 0.5712+/-0.121, n=8. One-Way ANOVA F(4,46) = 4.320, **P=0.0047, Tukey's post-hoc test 7 SDEs/SI Test 2 vs 10 SDEs (S): **P=0.0023, 7 SDEs/SI Test 2 vs 10 SDEs (S): *P=0.0393, 7 SDEs/SI Test 3 vs 10 SDEs (S): *P=0.012

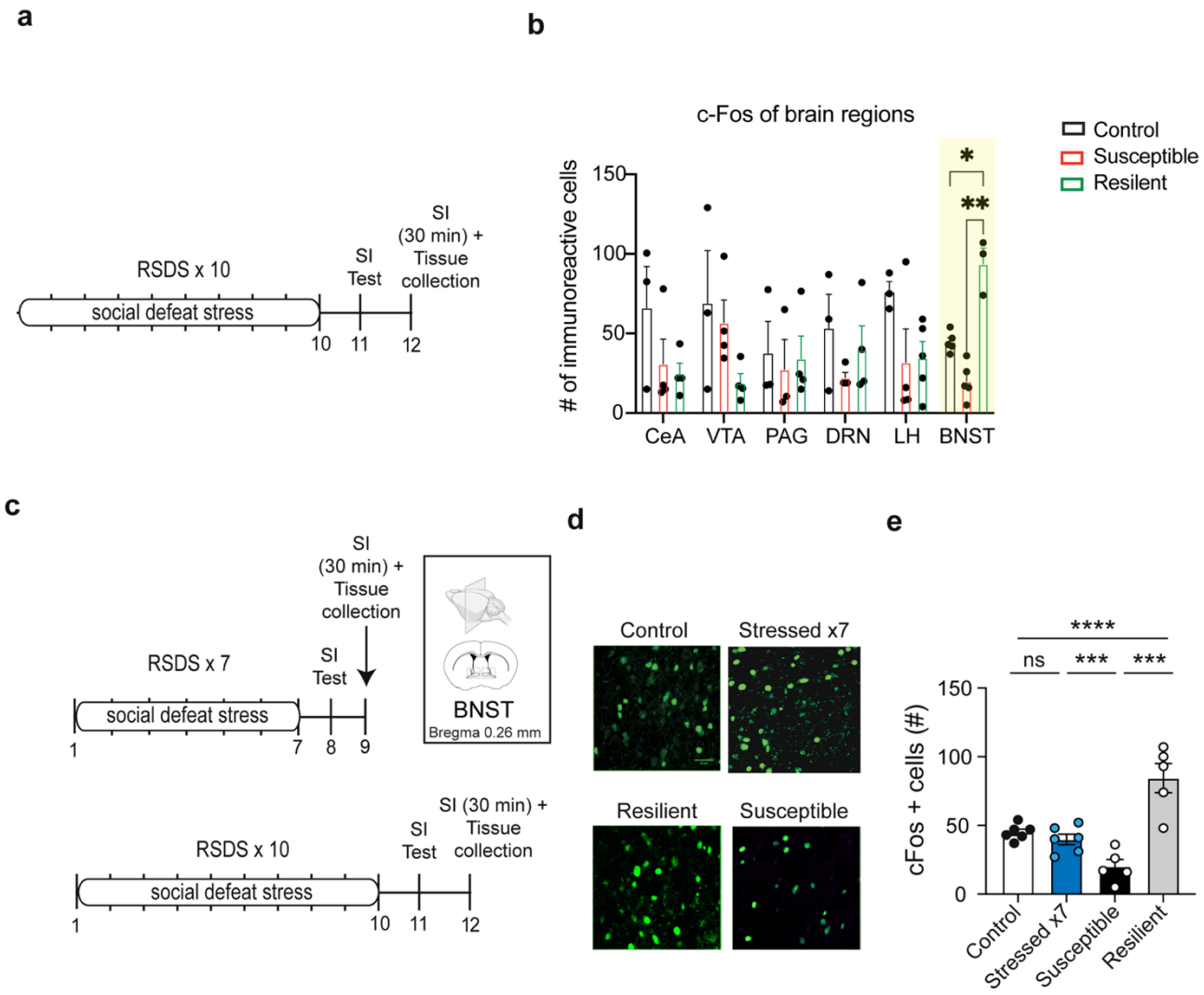

Figure 4: c-Fos immunohistochemistry of stress-sensitive regions reveals distinct patterns of activity to social interaction in the BNST (Extended Data).

Figure 4: c-Fos immunohistochemistry of stress-sensitive regions reveals distinct patterns of activity to social interaction in the BNST (Extended Data).

a, Experimental schematic, mice were subjected to 10 SDEs and a 15 minute non-physical social contact, 60 minutes after which brains were procured for c-Fos immunohistochemical analysis. **b,** Analysis of cFos immunoreactivity. Two-Way ANOVA brain interaction (region x phenotype) F(10,50) = 2.247, *P=0.0295, brain region F(5,50) = 0.7553, P=0.5862, phenotype: F(2,50) = 4.807, *P=0.012, Tukey's post-hoc test: BNST control vs resilient: *P=0.0489, susceptible vs resilient: **P=0.0018. **c,** Experimental schematic, mice were subjected to either 7 or 10 SDEs followed by a 15 minute non-physical social contact, 60 minutes after which brains were collected. **d,** Analysis of c-Fos immunoreactivity. Control: 45+/-2.352, n=6, stressed x7: 39.83+/-3.911, n=6, susceptible: 20+/-5.206, n=5, resilient: 84.4+/-10.63, n=5. One-Way ANOVA phenotype F(3,18) = 19.20, P=<0.0001. Tukey's post-hoc test: control vs susceptible *P=0.0359, control vs resilient ***P=0.0009, stressed x7 vs resilient ***P=0.0002, susceptible vs resilient P<0.0001. Central Amygdala (CeA), Ventral Tegmental Area (VTA), Periaquactual Gray (PAG), Dorsal Raphe Nucleus (DRN), Lateral Hypothalamus (LH).

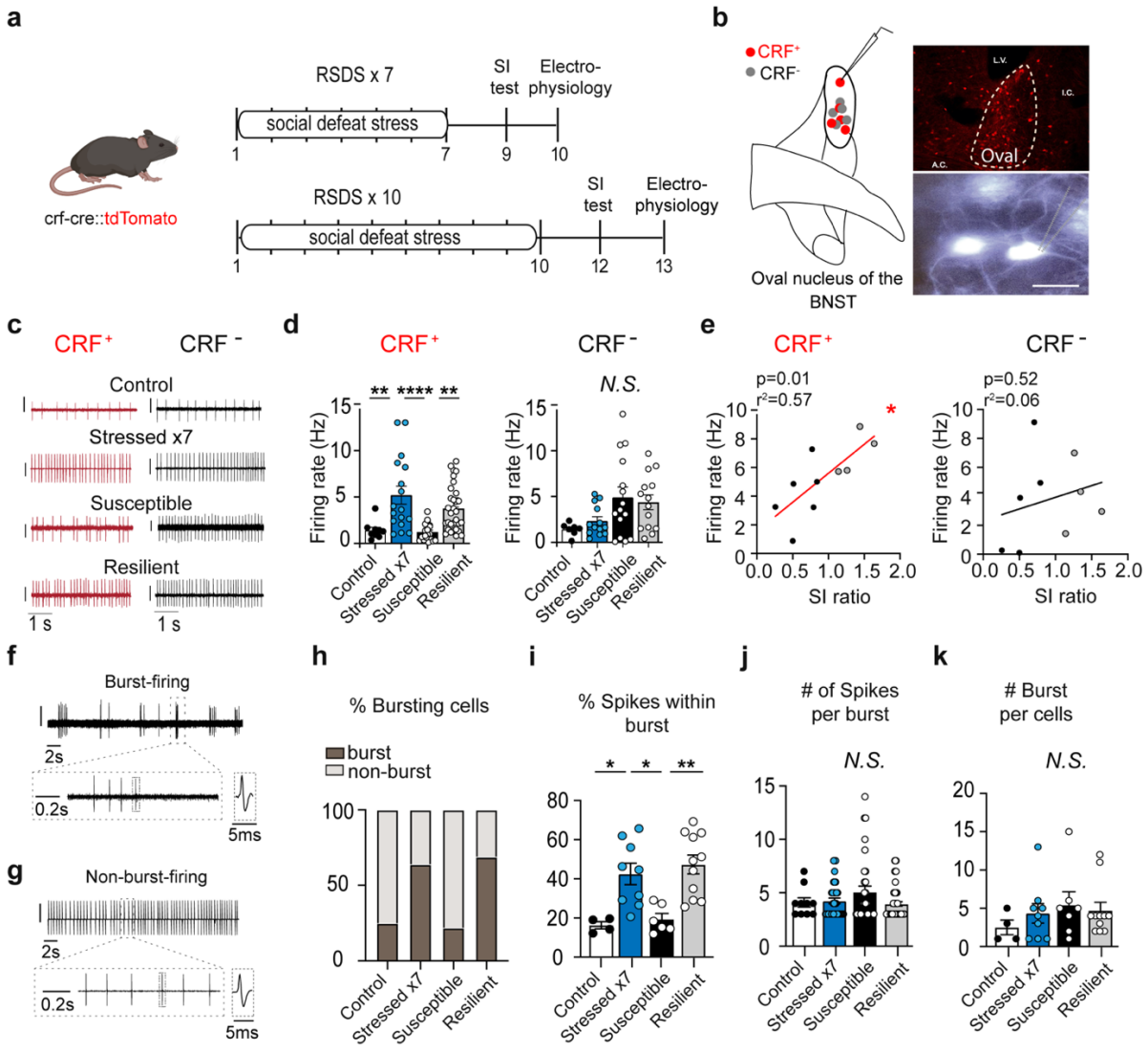

Figure 5. Firing rate alterations in BNSTov^{CRF} neurons occur as an adaptation to social stress that persists in resilient not susceptible mice.

Figure 2. Firing rate alterations in BNSTov^{CRF} neurons occur as an adaptation to social stress that persists in resilient not susceptible mice.

a, Mouse genotype and timeline of cell-attached electrophysiology experiments**. b,** Fluorescence-guided cell-attached electrophysiology setup, brain slice of the BNST (crf cells, tdTomato) x10x and DIC image of crf-neurons x20x, scale bar 0.63mm **c,** representative trace of BNSTov^{crf} positive and negative neurons of control, stressed (7 day duration), susceptible, and resilience mice. **d,** firing rate of CRF+ neurons (n=9-31 cells), p<0.0001 one-way ANOVA, tukey's multiple comparison's test, control vs stressed (7 days) **p<0.0028, susceptible vs resilient **p<0.0050, susceptible vs stressed (7 days), ****p<0.0001. Firing rate of CRF- neurons (n=7-15 cells per 4-6 mice/group), p<0.0355 one-way NOVA, F (3, 45) = 3.113, Tukey's multiple comparison's test, control vs stressed (7 days) p=0.9192, control vs susceptible p=0.0769, control vs resilient p=0.1742, stressed (7 days) vs susceptible p=0.1370, stressed (7 days) vs resilient p=0.3219, susceptible vs resilient p=9673; not significant. **e,** correlation of firing rate with social interaction ratio CRF+, R^2=0.5726, p=0.0113; CRF$^-$, R^2=0.0609, p=0.5219. **f,** Representative sample of burst and **g,** tonic firing. **h,** Percentage of bursting cells per animal group. **i**, Percentage of spikes within burst. **j,** Number of spikes per burst. **k,** Number of bursts per cell. (n=10-52 cells per 4-6 mice/group), and, N.S. = not significant, *p<0.05, **p<0.005, One-Way ANOVA.

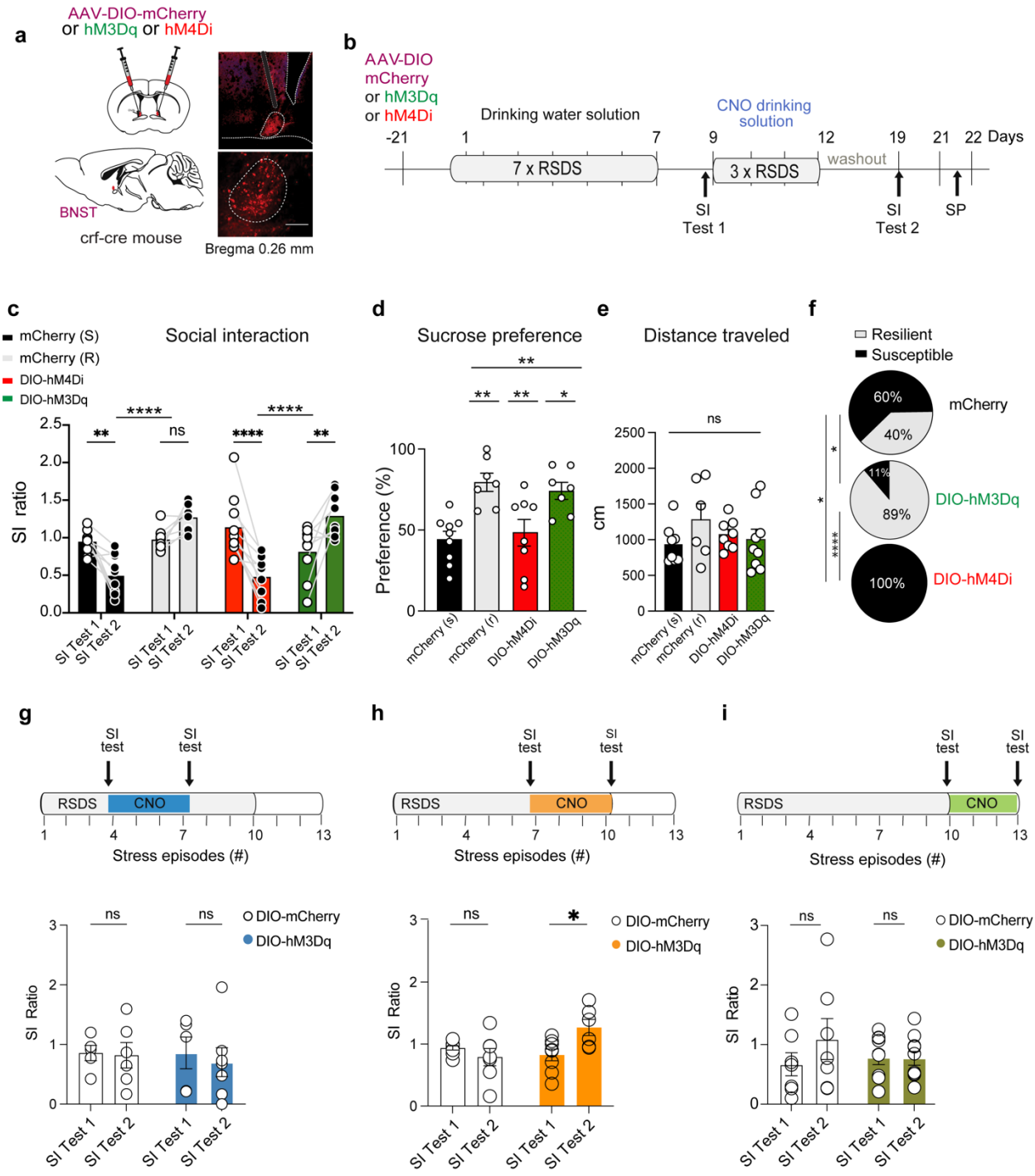

Figure 6. Chemogenetic modulation of BNSTov^{CRF} neurons bidirectional recapitulates behavioural tipping point.

Figure 6. Chemogenetic modulation of BNSTov^{CRF} neurons bidirectional recapitulates behavioural tipping point.

a, viral targeting of BNSTov. **b,** Experimental design of chemogenetic manipulation of BNSTov neurons with CNO-drinking water construct. **c,** social interaction test, two-way ANOVA F(3,68) = 18.01 row, P<0.0001 row factor, F(3, 68) = 9.965, p=0.2616 (time), row factor x time F(1,68) = 1.281, p<0.0001, Sidak's multiple comparisons test mCherry (s), **p=0.0047 (n=11 mice), mCherry (r) n.s. n= 9 mice, hM4Di, ****p<0.0001 n=10 mice, hM3Dq, **p<0.0022. **d,** sucrose preference test. one-way ANOVA treatment F(3,27) = 8.310 p=0.0004, Tukey's post-hoc testing susceptible vs hM4Di n.s., susceptible vs resilient **p=0.002, susceptible vs hM3Dq **p=0.0095, hM4Di vs resilient **p=0.0083, hM4Di vs hM3Dq *p=0.0347, resilient vs hM3Dq p=0.9368 (7-9 mice per group). **e,** distance traveled one-way ANOVA F(3,27) = 1.031, p=0.3944. **f,** percentage of susceptible or resilient mice DIO-hM4Di 100% susceptible, DIO-hM3Dq 89% resilient/11% susceptible, mCherry 40% resilient/60% susceptible. chi-square test=15.66, df = 2, ***p=0.0004 (n=21 mCherry, 10 hMDi, 9 mH3Dq); Fisher's post-hoc test mCherry vs hM4Di *p=.0317, mCherry vs hM3Dq *p=0.0169, hM4Di vs hM3Dq ****p=0.0001 . **g,** repeated social defeat DREADDs manipulation (4-7 episodes of stress), 2-way ANOVA treatment F(1,19) = 0.06175, pre vs post-CNO F(1,19) = 0.07055, interaction F(1,19) = 0.07055, n.s. (n=5-6 mice/group). **h,** RSDS DREADDs manipulation (7-10 episodes of stress), 2-way ANOVA treatment, F(1,25) = 1.871 **p=0.0094 pre vs post-CNO F(1,25) = 1.947, interaction F(1,25) = 7.907. Sidak's post-hoc test pre vs post CNO control p=0.4993, DIO-hM3Dq *p-0.0185 (n=6-8 mice/group). **i,** RSDS DREADDs manipulation (10-13 episodes of stress), 2-way ANOVA pre vs post-CNO, F(1,30) = 1.192 treatment F(1,30) = 0.3132, interaction F(1,30) = 0.2623.

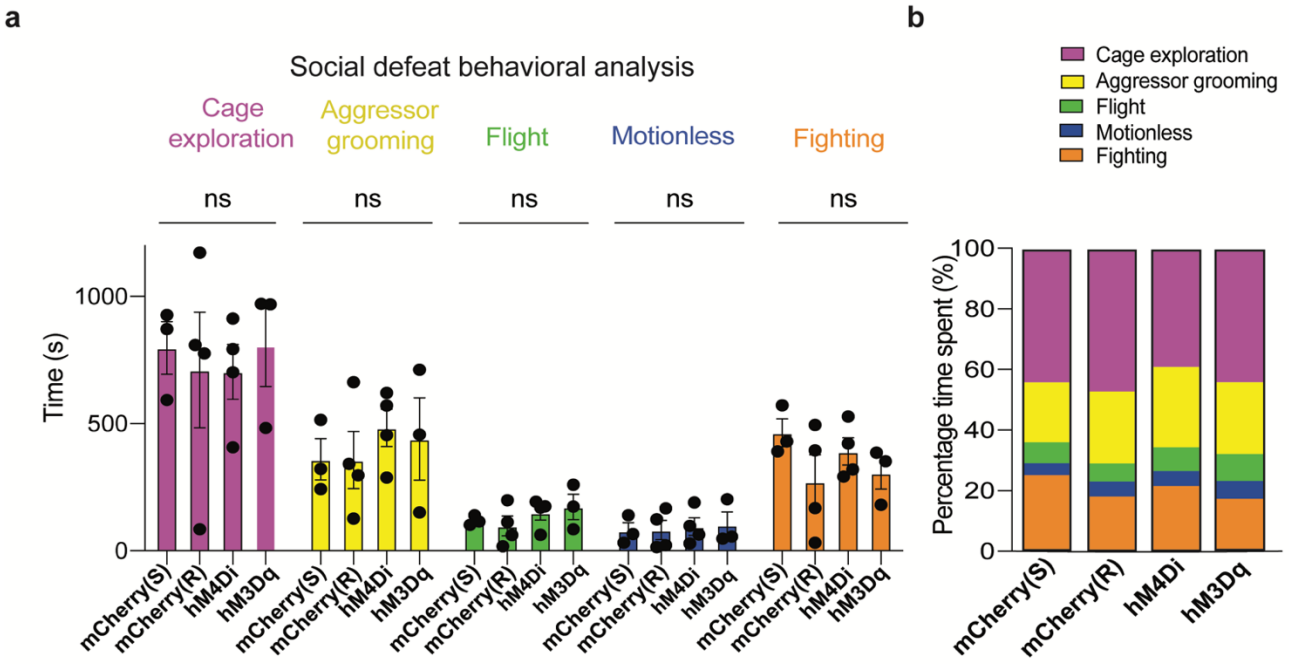

Figure 7: Chemogenetic manipulation of BNSTov^{CRF} neurons does not effect social defeat dynamics between aggressor CD-1 and C57/BL6J subordinate mice (Extended Data).

Figure 7: Chemogenetic manipulation of BNSTov^{CRF} neurons does not effect social defeat dynamics between aggressor CD-1 and C57/BL6J subordinate mice (Extended Data).

a, Analysis of physical confrontational phases of the social defeat stress paradigm over SDEs 8-10. Two-Way ANOVA treatment x behavior $F(12,50) = 0.2682$ $P=0.9917$, treatment $F(3,50) = 0.5199$, $P=0.6705$, behavior $F(4,50)=28.4$, $P<0.0001$. n=14 mice). **b,** percentage of time spent exhibiting defensive behaviors associated with social defeat stress. mCherry (S): 44% cage exploration. 20% excessive grooming, 7% flight, 4% motionless, 25% fighting. mCherry (R): 47% cage exploration. 24% excessive grooming, 6% flight, 5% motionless, 18% fighting. hM4Di: 39% cage exploration, 27% excessive grooming, 8% flight, 5% motionless, 21% fighting. hM3Dq: 44% cage exploration. 24% excessive grooming, 9% flight, 6% motionless, 17% fighting.

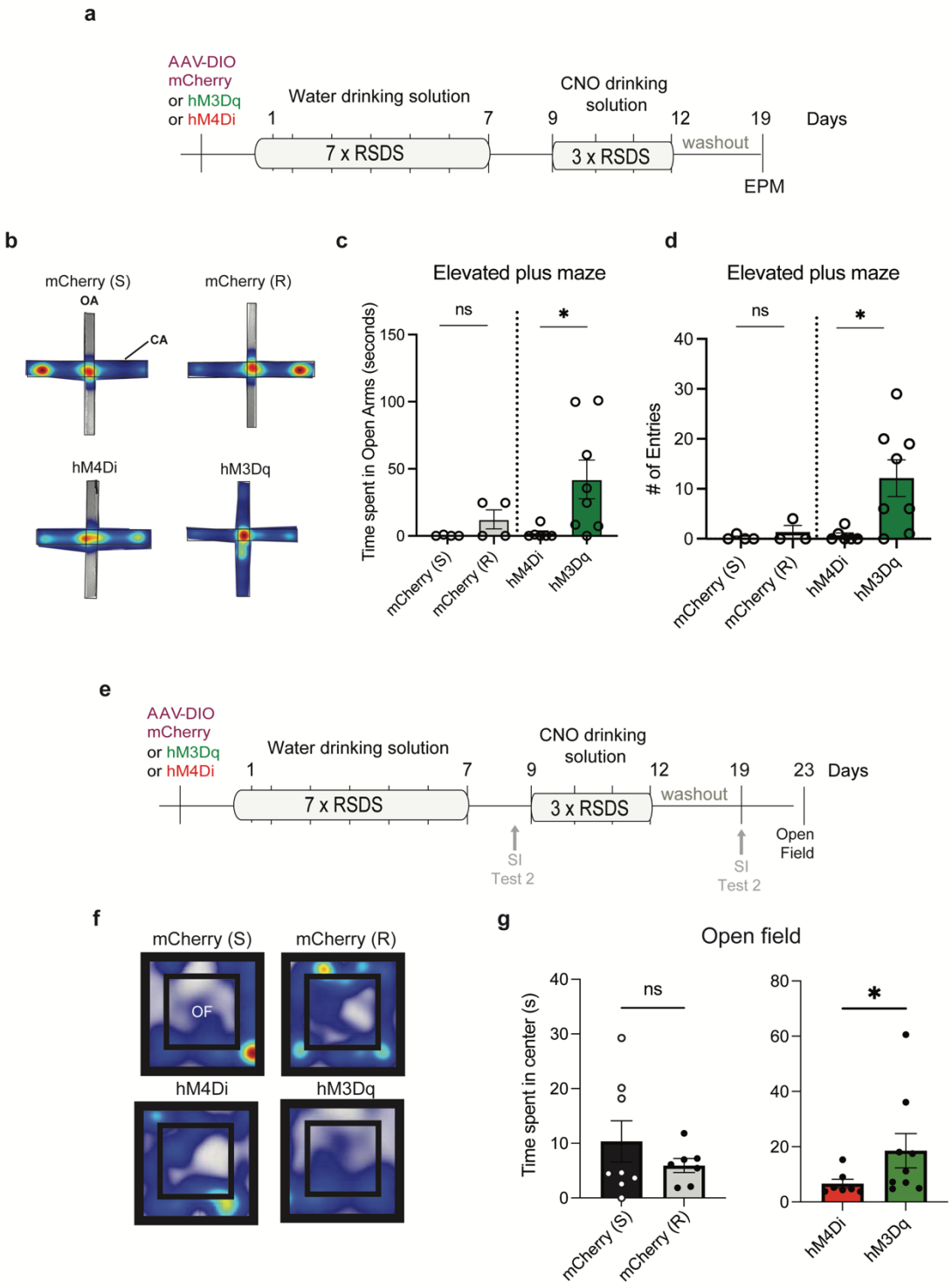

Figure 8: Chemogenetic manipulation of BNSTov^{CRF} neurons bidirectionally modulate anxiety states (Extended Data).

Figure 8: Chemogenetic manipulation of BNSTov^{CRF} neurons bidirectionally modulate anxiety states (Extended Data).

a, Experimental timeline. **b,** Representative heatmap of mice in EPM by treatment group. OA = open arm, CA = closed arm. **c,** Elevated plus maze analysis of time spent in open arm. mCherry (S), 0.2252+/-0.22522 s, n=4; mCherry (R), 12.32 +/- 7.1129 s, n=4; unpaired t-test, two-tailed, t=1.700, df=6, P=0.1401. hM3Dq, 42.1015+/-14.3932 s, n=8; hM4Di 1.95015+/-1.7760 s, n=6; unpaired t-test, two-tailed, t=2.381, df=12, P=0.0347. **c,** Representative heatmap of EPM behavior by treatment group. **d,** Elevated plus maze analysis of number of entries. mCherry (S), 0.2500+/-0.5000, n=4; mCherry (R), 1.333 +/- 2.3094, n=3; unpaired t-test, two-tailed, t=0.9387, df=5, P=0.3910. hM3Dq, 12.125+/-10.3845, n=8; hM4Di 0.6667+/-1.2110, n=6; unpaired t-test, two-tailed, t=2.662, df=12, P=0.0207. **e,** Experimental timeline, mice undergo RSDS with intervening SI tests and administered the open field test. SI test 1 and 2 depicted in gray denotes those findings are reported elsewhere in the report. **f,** Representative heatmap of open field behavior by treatment group. **g,** Time spent in the center of the open field arena. mCherry (S) vs mCherry (R), 10.35+/-3.766 s n=8, 5.926+/-1.284 s, n=7, Mann Whitney test, two-tailed, P=0.9551. hM3Dq 12.125+/-10.3845 s n=8, h4Di 0.6667+/-1.2110 n=7, P=0.0311.

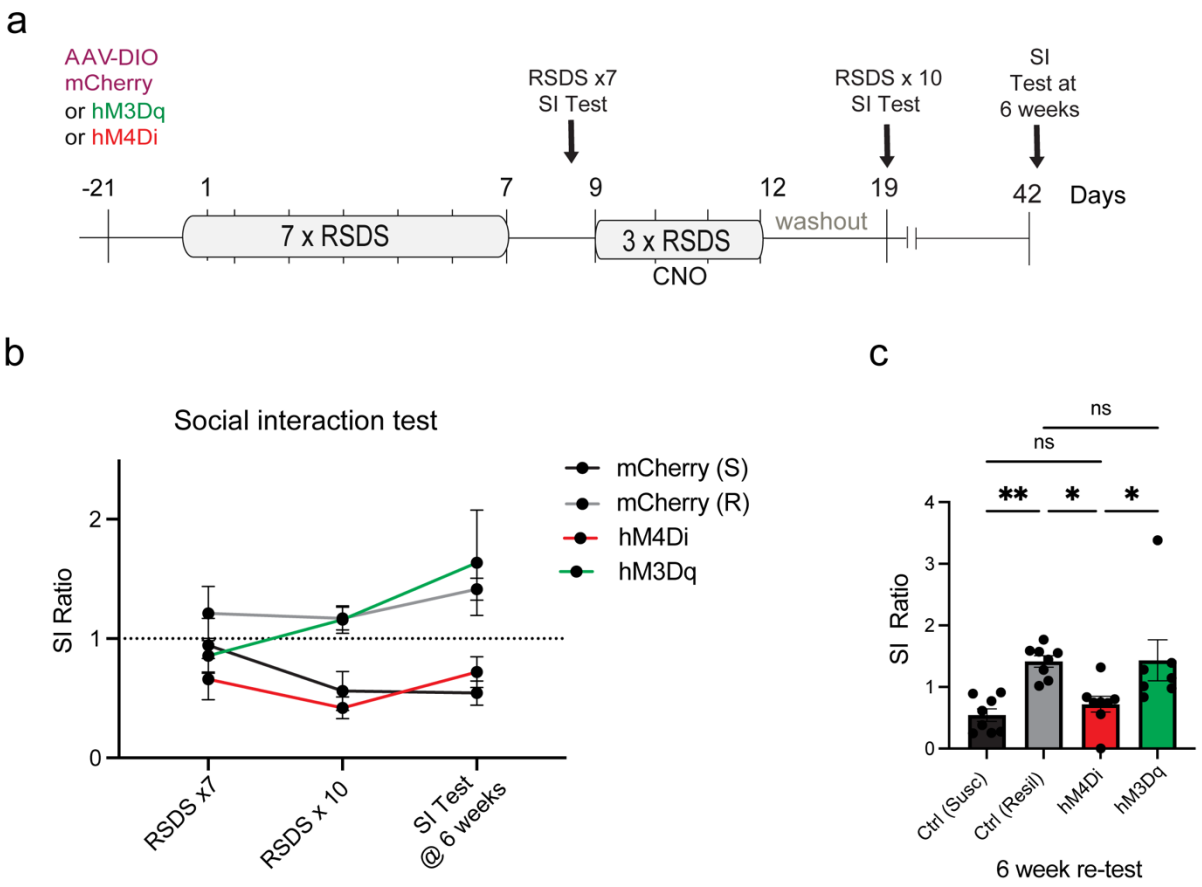

Figure 9: Social interaction testing at 6 weeks following CNO modulation (Extended Data).

Figure 9: Social interaction testing at 6 weeks following CNO modulation (Extended Data). **a,** Experimental timeline, mice are subjected to 7 and 10 SDEs, and administered an SI test after 7, 10, and six weeks from the start of the experiment. **b,** Display of animal behavior by treatment group over SI Testing. Dotting line at SI ratio = 1 demarcates the criteria for determining susceptible/resilient mice. SI ratio scores > 1 defines resilient, <1 defines susceptible phenotypes. **c,** Social interaction test mCherry (S), 0.5439+/-0.1019 n=8; mCherry (R), 1.415+/-0.09199, n=8; hM4Di, 0.7200+/-0.1286, n=8; hM3Dq 1.433+/-0.3323, n=7. One-Way ANOVA $F(3,27) = 6.761$, $P=0.0015$. Tukey's post hoc test mCherry (S) vs (R): **P=0.008; mCherry(S) vs hM3Dq: **P=0.009; mCherry(R) vs hM4Di: *P=0.0428; hM4Di vs hM3Dq: *P=0.0454.

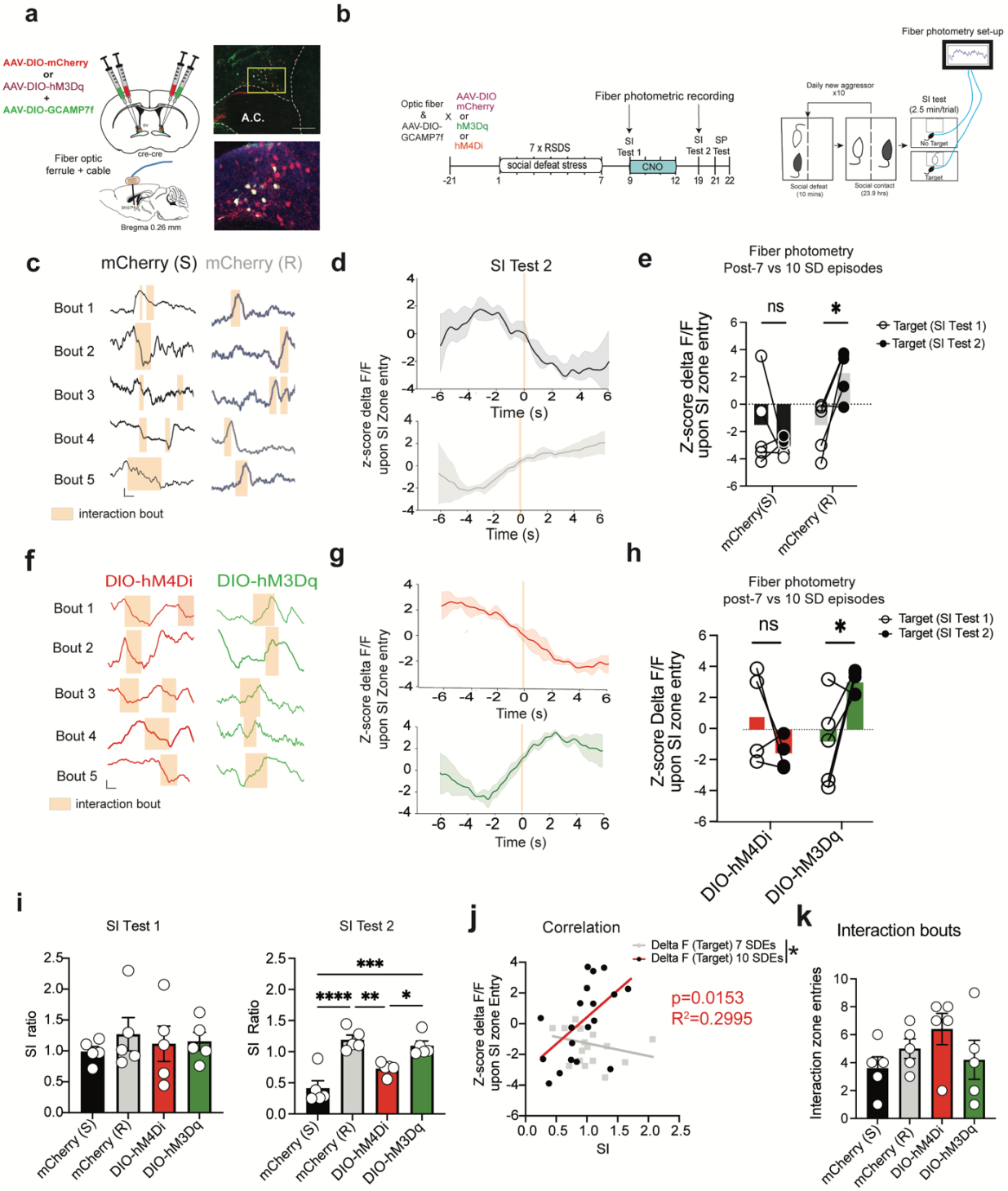

Figure 10. BNSTov^{CRF} calcium-dynamics encode stress effect on social interaction

Figure 10. BNSTov^{CRF} calcium-dynamics encode stress effect on social interaction

a, Viral targeting of the BNSTov. **b**, Experimental design of multiplexed chemogenetics with drinking water-CNO delivery and fiber photometry. **c,** representative calcium recordings of susceptible/resilient and hM3Dq/hM4Di respectively (**c, f,**). **d**, **g**, representative averaged trace centered around interaction bout. **e,** two-way RM ANOVA row factor F(3,14) = 1.401, pre vs post-CNO F(1,14) = 0.8179, subject (F 14, 14) = 1.195, Row x pre/post CNO F(3, 14) = 9.343, **p=0.0012. Sidak's post-hoc test susceptible vs resilient p=0.137 n.s. vs *p=0.0199 respectively (n=4 mice/group). **h,** hM4Di vs hM3Dq p=0.3069 vs *p=0.0236 respectively, n=4-5 mice/grp). **i**, pre-CNO social interaction test. One-way ANOVA F(3,16) = 0.291, p=0.8308, n=5 mice/group. Post-CNO social interaction test. One-Way ANOVA F(3,16) = 17.83, ****p<0.0001, Tukey's post-hoc test, susceptible vs resilient ****p<0.0001, susceptible vs hM3Dq ***p<0.0002, susceptible vs hM4Di p=0.0762, resilient vs hM3Dq p=0.8506, resilient vs HM4Di **p=0.0066, hM3Dq vs hM4Di *p=0.0335, n=5 mice/group. **j**, correlation of SI ratio and z-score delta F/F upon social entry, simple linear regression pre-CNO F(1,15)=0.7674, p=0.3948, post-CNO F(1,17)=7.268, *p=0.0153. Intersection of lines, F(1,32)=6.896, *p=0.0131, n=18 mice. **k**, Number of social interaction bouts, one-way ANOVA F(3,16)=1.346, p=0.2949, n=5 mice/group.

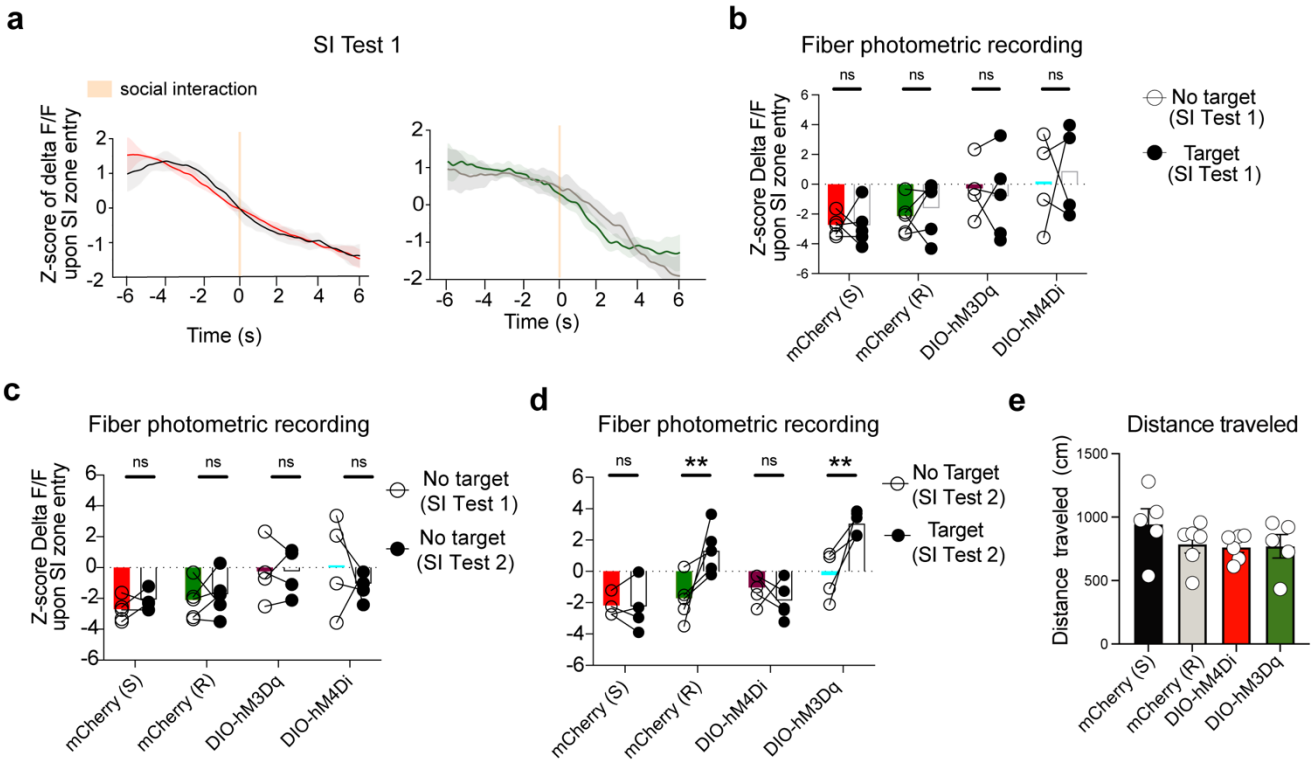

Figure 11: Prior to 10 SDEs BNSTov^{CRF} neurons are not activated in a novel social context (Extended Data).

Figure 11: Prior to 10 SDEs BNSTov^{CRF} neurons are not activated in a novel social context (Extended Data).

a, Representative fiber photometric tracings of mice engaging with a novel conspecific during the social interaction test. **b,** Fiber photometric analysis of mice surrounding (-6 to +6) of an interaction bout. Two-Way ANOVA interaction (treatment x social target) F(3,29)=0.14963 P=0.9291, treatment F(3,29)=4.175 *P=0.0142, social target F(1,29)=0.0611 P=0.8080, n=5,4,5,4 mice. **c,** Fiber photometric analysis of recording during trials where social target was absent in both SI test 1 and 2. Two-Way ANOVA treatment x SI test F(3,28)=0.6751 P=0.5746, treatment F(3,28)=4.146 *P=0.0150, social target F(1,28)=0.01632 P=0.8993, n=5,5,4,4 mice. **d,** Fiber photometric analysis of recording during trials when social target was absent vs present in SI Test 2. Two-Way ANOVA treatment (treatment x presence of social target) F(3,28)=6.000 **P=0.0027, treatment F(3,28) = 13.44, ****P<0.0001, social target F(1,28)=10.20, **P=0.0035. Tukey's post-hoc test: mCherry (S) vs mCherry (R) *P=0.0109, mCherry (S) vs hM3Dq ****P<0.0001, hM4Di vs hM3Dq ***P=0.0002, n=4,5,4,5 mice. **e,** Distance traveled. mCherry (S): 934.8633+/-96.1767 cm, n=8; mCherry (R): 1278.478+/-224.3500 cm, n=6; hM4Di: 1069.9941+/-73.7286 cm, n=8. hM3Dq: 999.5635+/-146.6165 cm, n=9, One-Way ANOVA treatment F(3,16)=1.028, P=0.4066.

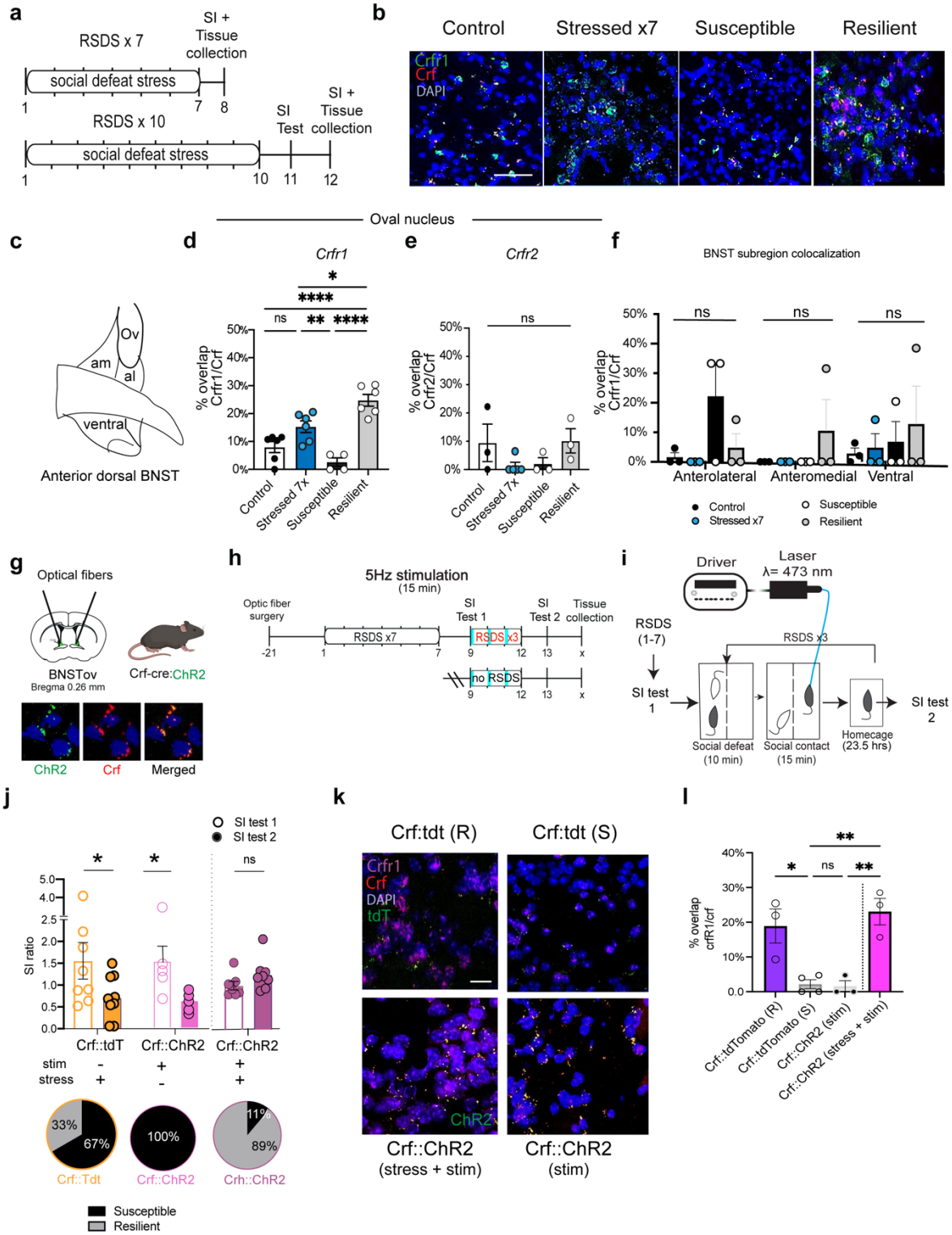

Figure 12. BNSTov Crfr1 is associated with the emergence of resiliency.

Figure 12. BNSTov Crfr1 is associated with the emergence of resiliency.
a, Experimental timeline of RNAScope ISH of mice that underwent social defeat stress. **b**, representative images of control, stressed x7, susceptible, and resilient. 20x magnification, scale bar (0.64 mm). **c**, schematic of anterior dorsal BNST. d, *Crfr1* mRNA colocalization, one-way ANOVA F(3,18)=20.91, ****p<0.0001, Tukey's posthoc test control vs stressed x7 p=0.0701, control vs susceptible p=0.3336, control vs resilient ****p<0.0001, stressed x7 vs susceptible **p=0.0033, stressed x7 vs resilient *p=0.0148, susceptible vs resilient ****p<0.0001 n=4-6 BNST brain samples. **e**, *Crfr2* mRNA colocalization, one-way ANOVA F(3,10)=1.790, p=0.2166, n=3 BNST brain samples. **f,** RNAscope BNST subregion comparison, two-way ANOVA interaction F(6,24)=1.057 p=0.4147, row factor F(2,24)=0.6092 p=0.5520, column factor F(3,24)=1.549, p=0.2275 n=3 BNST brain samples. **g**, Viral injection site. **h**, Experimental timeline. **i**, optogenetic and social behavioral setup, **j**, optogenetics social interaction two-way ANOVA interaction F(1,28)=5.059 *p=0.0325, row factor F(1,28)=1.061e-005, p=0.9974, column factor F(1,28)=1.419 p=0.2436. Sidak's post-hoc test *Crf*::tdT *p0.0357, *Crf*::ChR2 p=0.7233. n=7-9 mice/group. Optogenetic manipulation unpaired t-test, *Crf*::tdT t=2.556, df=40, *p=0.0425 (n=8-9 mice), *Crf*::ChR2 t=0.7758, df=40, p=0.442457 (n=8-9 mice), t=2.369, df=40, *p=0.045032 (n=6 mice). Holm-Sidak method for multiple comparisons. **k**, representative image, scale bar 0.64mm. **l**, optogenetics-RNAScope experiment. One-Way ANOVA F(3,9)=13.53, **p=0.0011. Tukey's post-hoc test *Crf*::ChR2 (stress+ stim) vs *Crf*::tdT (resilient) p=0.7872, *Crf*::chR2 (stress + stim) vs. *Crf*::tdTomato (s) **p=0.0032, *Crf*::chR2 (stress + stim) vs. *Crf*::chR2 (stim), **p=0.0042, *Crf:*:tdTomato (r) vs. *Crf:*:tdTomato (s) *p=0.0131, *Crf*::tdTomato (r) vs. *Crf:*:chR2 (stim) *p=0.0156, *Crf*::tdTomato (s) vs. *Crf*::chR2 (stim) p=0.9988.

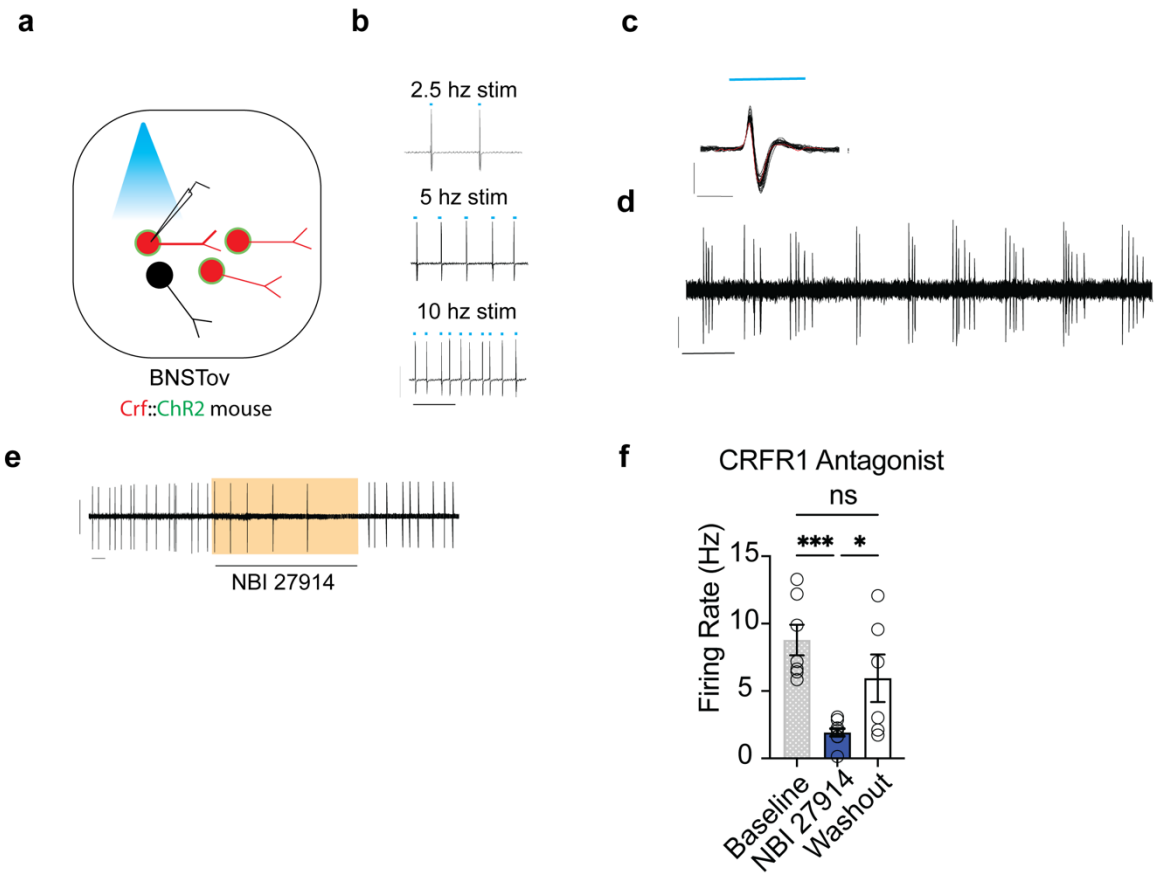

Figure 13. CRFR1-selective antagonist decreased spontaneous firing rate in CRF+ neurons of optogenetically-induced resilient mice (Extended Data).

Figure 13. CRFR1-selective antagonist decreased spontaneous firing rate in CRF+ neurons of optogenetically-induced resilient mice (Extended Data).

a, Schematic of slice configuration of CRF cells in Crf::ChR2 mice. **b,** Optogenetic activation of varying firing frequency of 2.5 Hz, 5 Hz, 10 Hz firing fidelity, scale bar = 0.5 sec. **c**, Optogenetic induced waveform, scale bar (0.25 ms, 0.5 mV), blue bar symbolizes length of light pulse (0.7 ms, 5 mW). **d,** Spontaneous burst firing observed following 5 Hz optogenetic stimulation. Scale bar = 1 sec, 0.7 mV. **e,** Sample trace of firing rate observed with bath application of NBI 27914 (CRFR1-specific antagonist). Scale bar is 1 sec, 0.5 mV. **f,** Firing rate of resilient mice (n= 3 mice) post-optical stimulation before and after NBI 27914 bath application. One-way ANOVA $F(2,19) = 11.73$ ***P=0=0.0005. Tukey's post-hoc test: Baseline vs NBI 27914 ***P=0.0004, NBI 27914 vs Washout *P=0.0374. Baseline vs Washout P=0.1985.

Chapter 4

CRF neurons of the BNST promote resilience by blunting the internal experience of aversion.

Introduction to Chapter 4

The BNST has been studied extensively for its role in coordinating what appears to be often opposing adaptive behaviors. However, what is missing in the literature is the link between internal affective states and the adaptive stress behaviors they motivate. Chapter 3 uncovered a stress window during which BNSTovCRF neuronal activity maintains resilient behavior through self-sustained activation. Here, we explore how BNSTov^{CRF} neurons achieve this through shifting the valence of stress contexts to represent less aversive experiences. Using cell-type-selective optogenetics and transgenic Crf-ChR2 mice, we show that BNSTov^{CRF} induces resiliency through dampening the deleterious effects of social defeat encoding, enhancing the positive salience of both appetitive and aversive stimuli, shifting socio-affective bias, and promoting tolerability of non-social physical stress. Adaptive responses to stress typically emanate as a response to negative internal states by external stimuli; here we show that in resilient mice, stressful environments are less aversive than susceptible mice, suggesting a different motivational capacity to endure stress in this group. Thus, we describe a novel role for BNSTov^{CRF} neurons in resisting the emotional effects of cumulative stress by reducing the internal experience of aversion.

Results

BNSTov^{CRF} neuronal stimulation in low- or no-stress conditions induces social avoidance.

Despite our findings that activation of Corticotropin-Releasing Factor (CRF)-expressing neurons contained within the oval nucleus of the Bed Nucleus of the Stria Terminalis (BNSTov) produces pro-resilient behavioral responses, several studies have reported that this activation induces negative emotional states (Jasnow et al. 2004; Stout et al. 2000; Engelhardt et al. 2021; Bagosi et al. 2017; Salimando et al. 2020; Dedic et al. 2018). In chapter 3, I show that BNSTov^{CRF} activation had a pro-social effect only after cumulative stress exposure, suggesting a role for BNSTov^{CRF} neurons in potentially promoting cooperative sociality under stressful conditions. This adaptive function confers an evolutionary advantage (Waraczynski 2016; Osório et al. 2017; Barthas et al. 2020). However, it is unknown what function these neurons serve in low or no stress conditions. While there are no published reports on the role of BNSTov^{CRF} neurons in social settings, we predicted that optical stimulation would produce avoidant responses to an otherwise pro-social appetitive experience in line with published work in non-social settings (Hu et al. 2020; Ramot et al. 2017; Tran et al. 2014; Hollon et al. 2015). To test this, transgenic mice expressing channelrhodopsin exclusively in Crf-expressing neurons (ChR2 mice) mice were implanted with fiber optic ferrules and received 5 Hz stimulation during the social interaction test (Fig 14a). Control mice showed no significant difference in time spent in the interaction zone with and without a social target; however, there was a trend toward more significant time spent with the target animal ($p=0.08$, t-test two-tailed, Fig 14b). In contrast, ChR2 mice had a significant decrease in time spent with a novel conspecific between the no target and target trials, suggesting that acute BNSTov^{CRF} stimulation induced negative valence onto an otherwise rewarding social context (Fig 14b). Social Interaction (SI) ratio is often used as an index for resilient/susceptible phenotypes based on genetic, electrophysiological, physiological, and behavioral measures (Krishnan and Nestler 2011; Walsh et al. 2014; Golden

et al. 2011; Krishnan et al. 2007; Wood et al. 2010; Berton et al. 2006; Matsuda et al. 1996). Mice typically prefer interacting with a novel mouse over an empty animal enclosure, as such mice scoring SI ratio>1 are classified as resilient (Golden et al. 2011). Relative to control mice, ChR2 mice showed a significant decrease in SI ratio (Fig 14c). Taken together, this data suggests that in conditions of low stress, BNSTov^{CRF} neurons blunt sociability. Given that in low-stress mice BNSTov^{CRF} neurons promote social avoidance, we then wondered if the stress window between 7 and 10 SDEs is where these neurons acquire the ability to switch from coordinating social avoidance to social approach behavior concomitant with resiliency.

Intra-defeat BNSTov^{CRF} neuronal stimulation increases engagement with threatening contexts

Resiliency is associated with the maintenance of spontaneous firing rates in BNSTov^{CRF} neurons between 7 and 10 SDEs. 5 Hz optogenetic stimulation during this stress-sensitive window was sufficient to recapitulate the naturally occurring stress-neuroadaptation that produces resilience. Moreover, cell-type-selective fiber photometry revealed that by the 10th social defeat episode (SDE) BNSTov^{CRF} neurons acquire the capacity to respond to social contexts. However, the neural activation does not provide insight into whether social interaction in resilient mice had maintained its expected rewarding properties. In particular, considering the data presented in Fig 14 suggests that BNSTov^{CRF} activation is aversive. Moreover, BNSTov^{CRF} neural activation was shown to promote resiliency, but only when paired with social defeat, suggesting that an essential component of its pro-resilient effect stems from exposure to the stressful context in which maladaptive behaviors could arise. The lines of converging data aforementioned led to answer several pertinent questions: (1) does stimulation during SDEs 7-10 induce the switch from social avoidance to social approach in resilient mice? (2) how does this intra-defeat stimulation affect social interaction with the familiar CD-1 aggressor present?

And (3) does the social behavior toward known aggressors correlate with post-defeat social behavior on the SI test? The following experiment seeks to answer these questions.

During deep brain stimulation (DBS) for treatment-resistant depression, clinicians probe the subject's emotional state after placing the stimulating electrode. Acute intraoperative stimulation during this placement procedure has been linked to durable DBS antidepressant efficacy (Sendi et al. 2021). The solicitation of negative emotions intraoperatively paired with DBS effectively mimics sensitization exposure therapy, where emotional rehabilitation occurs through re-experiencing negative events (Chen et al. 2018). $BNSTov^{CRF}$ stimulation in stress-naïve mice is aversive but produces resiliency in individuals with a history of chronic stress; however, the point at which this transition from aversive to appetitive responses occurs remains elusive. Our previous work revealed that BNST stress neuroadaptation between 7 and 10 SDEs is necessary and sufficient for resiliency. Therefore, we hypothesized that stimulation leverages this window of plasticity to promote resiliency by shifting the valence of $BNSTov^{CRF}$ activation from negative to positive, diminishing the impact of psychosocial stress during repeated social defeat stress (RSDS).

The sensory contact phase is a critical component of RSDS that is necessary to develop susceptibility (Challis et al. 2013). To test this, oval BNST ferrule implanted ChR2 received 5 Hz optogenetic stimulation during the sensory contact phase of the remaining 3 daily SDEs of a 10-day protocol as per previous studies (Fig 15a-b, Extended Data Fig 16a-b). We employed behavioral tracking software during optical stimulation to observe the effect of stimulation on social engagement with a familiar CD-1 aggressor (Fig 15b, Extended Data Fig 16b). CD-1 mice are larger and of a more aggressive strain (Golden et al. 2011). The behavioral assay spanned 8 bins (each bin was 2.5 min). The first bin consisted of non-stimulation-paired social interaction. Bins 2-7 consisted of stimulation, and bin 8 represented a post-stimulation period.

On day 1 of stimulation (day 8 of RSDS), there was no significant difference in time spent interacting with the CD-1 aggressor in control mice within, nor across all bins (Extended data Fig 16c). In contrast, ChR2 mice showed a significant increase in social interaction time across bins compared to control mice (Extended Data Fig 16c,f). On day 2 of stimulation (day 9 of RSDS), there were no significant differences in social investigation between or across bins among control and ChR2 mice (Extended Data Figure 16d,g). On day 3 of stimulation, there was an increase in social interaction of ChR2 relative to control mice when total time is averaged across bins (Extended Data Fig 16e,h). In examining the overall effect of stimulation across all 3 days, it was found that ChR2 mice spent more time on average interacting with CD-1 aggressors at bins 5 and 6 (~10-12.5 min post-defeat) (Fig 15c). Overall, 5 Hz photostimulation induced significantly higher social interaction times in ChR2 than control mice (Fig 15d). Interestingly, ChR2 mice whose fiber-optic ferrules were implanted off-target were shown to have significantly lower interaction times than both ChR2 and control mice (Fig 15d-f). The stimulation condition in ChR2 mice led to a significant increase in interaction time compared to controls which were not observed in pre- or post-stimulation trials (Fig 15d,e). Among ChR2 mice, interaction time increased during the stimulation phase and persisted post-stimulation (Fig 15e,f). In contrast, no significant differences were observed in the control mice across pre-, stim-and post-stimulation conditions (Fig 15d-f).

Per established protocols, c57bl/6j mice undergoing 10 days of RSDS will phenotypically display susceptibility or resiliency; therefore, the control group's mean masks the effects of these subgroups. Interestingly, when the control group is parsed into their respective phenotypes (based on SI ratio ((Golden et al. 2011; Krishnan et al. 2007)), *see methods*), susceptible mice were observed to have similar interaction times as the off-target ChR2 group (Fig 15g). Conversely, resilient mice displayed similar social interaction times as the ChR2 group (Fig 15h). The regression of intra-stimulation interaction time with CD-1 aggressor and time spent

with a novel conspecific at a later social interaction test revealed a positive and significant correlation in ChR2 but not control mice (Extended Data Fig 16i). Optogenetic stimulation appeared to prevent the eventual decline in of social interaction time with familiar aggressors in ChR2 that occurred in control mice amidst repeated attacks, thought this effect was not statistically significant (P=0.0524, Extended Data Fig 16j). In summary, these results reveal that neuromodulation during this stress window is crucial to the development of resiliency because it provokes desensitization exposure, which may neutralize the emotional valence of psychosocial aggression.

Optical real-time place preference reveals that BNSTov^{CRF} neuronal modulation biases social preference.

While BNSTov^{CRF} neurons robustly produce resilient phenotypes, it is unclear what motivates the observed increase in social interaction. On the one hand, increased pro-social behavior could be due to stress-related hypervigilance governed by a negative internal state because of cumulative stress exposure. Conversely, increased sociability could result from an enhancement in the rewarding properties of social contact. The distinction has clinical implications as many stress-related psychopathological states manifest as “functional” behaviors, despite distressing internal states such as in generalized anxiety disorder and post-traumatic stress disorder (Toth 2019; Osório et al. 2017; Rodríguez-Sierra et al. 2016). Whereas, clinically, resiliency represents an attenuation of negative affect, giving rise to experiencing the positive internal experience of rewarding social interactions. Therefore, we tested whether a positively motivated state drives the social behavior that characterizes resiliency. To answer this question, we used a modified social optical-real time place preference assay, or social o-RTPP, whereby a mouse was permitted to navigate between two compartments containing novel non-aggressive male CD-1s, with one paired with optical stimulation. Time spent in each chamber was used to determine the effect of stimulation on

preference. Control mice expressed no preference, as the percentage of time spent was similar across both chambers (Fig 17a). In contrast, ChR2 mice demonstrated a strong preference for the photostimulation paired chamber (Fig 17b), as evidenced by the increased percentage of time spent in the chamber, specifically when co-paired with stimulation (Fig 17c). Spending more time in a compartment demonstrates side preference but may not represent social preference, as spatial tracking does not consider specific actions undertaken in the chambers that may confound results such as distinguishing freezing versus interactions with the CD-1. Therefore, we analyzed posthoc the percentage of time ChR2 mice spent explicitly interacting with a novel conspecific both in the presence and absence of photostimulation. We uncovered that mice spent three-fold more time engaged in social interaction with the novel CD-1 while in the preferred chamber compared to the unpaired trial (19.80+/-9.096 vs. 59.40+/-4.167, no light vs. light, respectively, Fig 17d). These results suggest that BNSTov^{CRF} stress neuroadaptation coordinates resilient behavioral responses through generating appetitive, pro-affiliative social preference.

BNSTov^{CRF} stress neuromodulation enhances positive valence to appetitive and aversive socially-salient stimuli.

Resiliency involves gathering information about environments containing a variety of emotionally-valenced stimuli ranging from reward- to threat-related cues for surviva l(Friedman et al. 2014)(Han and Nestler 2017)(Osório et al. 2017). Rodents navigate using olfactory cues, and the BNST receives direct input from the vomeronasal accessory olfactory system (Chen et al. 2020; Hosokawa and Chiba 2007) . Stress modifies BNSTov^{CRF} neurons in resilient mice to maintain adaptive social behaviors in social defeat stress (Fig 15c-g), but we wondered whether this could generalize across contexts of varying valence. To test this, mice were placed in a three-chamber arena over several trials that contained distinct odorants of varying valence: water, male urine, female urine, and predator (Red fox) urine (Fig 18a, Extended Data Fig 19a)

and measured investigation times in trials lasting two-minute trials of 5 Hz stimulation (trial 1: “light off”, trial 2: “light on”). There was no significant difference in time investigating water between ChR2 and control mice (Fig 18b). Similarly, ChR2 and control mice expressed no difference in the investigation of male urine (Fig 18c). ChR2 compared to control mice spent significantly more time investigating female urine, suggesting that BNSTov^{CRF} enhances the valence of rewarding stimuli (Fig 18d). Indeed, resilient mice spent more time investigating female urine during the no stimulation trial (Extended data Fig 19b). To examine BNSTov^{CRF} neurons’ role in socially salient aversive stimuli, mice were subjected to predator urine. Predator urine odorant has been described as an innate fear stimulant (Asok et al. 2016; Giardino et al. 2018), and lesions of the dorsolateral BNST (a region that includes the oval nucleus) inhibit defensive/freezing responses in its presence. Interestingly, we observed that BNSTov^{CRF} activation promoted increased investigation and sniffing of predator urine compared to control mice (Fig 18e). This finding suggests that BNSTov^{CRF} neurons promote resiliency, in part, by shifting the valence of aversive contexts in response to stress. Notably, in the absence of optical stimulation (“no light” trials), there was no significant difference in sniffing time among all odorants between ChR2 and control mice (Fig 18f). Moreover, there was no significant difference between susceptible/resilient mice in investigation male urine during the no-light trials (Extended data Fig 19b). Predator urine solicited no significant differences between susceptible/resilient mice reflecting the innate fear potency of the odorant, as both groups investigated the stimulus for a very short period (Extended data Fig 19b). In summary, these findings suggest that resiliency induced by photostimulation between the 7th and 10th SDE promotes the investigation of a range of socially derived stimuli essential to survival.

BNSTov^{CRF} neuronal activation suppresses despair-like behavior on the tail suspension test

BNSTov^{CRF} neuronal activation promoted increased investigation of a familiar aggressor CD-1 (Fig 15d) and predator odorant (Fig 18e), suggesting that this increased activation may promote an increased tolerance for stressors. However, in both, mice had control over their proximity to the potentially threatening stimuli. Therefore, it challenges interpretations of whether activation of BNSTov^{CRF} neurons in an inescapable non-social physical stressor would promote resiliency. To test this, we utilized the tail-suspension test (TST) with optogenetic activation following RSDS and photostimulation during 8-10 SDEs (Fig 20a). Mice were initially suspended without stimulation for the first three minutes, and no significant differences between control and ChR2 mice were observed (Fig 20b). During the three-minute period of stimulation, ChR2 mice spent less time immobile than control mice (Fig 20b). Intriguingly, in the final three minutes following stimulation, ChR2 spent less time immobile, suggesting the internal state induced by stimulation persisted (Fig 20c). In summary, we show that BNSTov^{CRF} activation in a variety of stress-related contexts causes a positive shift in affective state, thereby motivating behaviors consistent with resiliency.

Discussion

By capturing direct social behavioral effects of 5 Hz optical stimulation, we observed increased sociability toward a familiar aggressor, an experience crucial to establishing resiliency. Photostimulation of stress-naïve and singly defeated mice induced social avoidance, reflecting the baseline role BNSTov^{CRF} neurons play in social contexts. Using social o-RTPP, we observed the effect of BNSTov^{CRF} activation on shifting socio-affective bias. This activation also modulated salience of odor-based, socially-valenced stimuli, as optogenetic stimulation-induced increased investigation of female urine and surprisingly predator urine, an innate stressor. Lastly, TST was used to assess whether the resiliency-inducing stimulation protocol had influenced adaptive responding to inescapable, non-social stressors. We uncovered that photoactivation induced a decrease in immobility that persisted after stimulation. The

experiments together provide important insight into how BNSTov^{CRF} neurons induce resilience by maintaining a positive internal state resistant to the insults of ongoing stress.

In this report, we observe that stress modulation of the BNSTov produces resilience by a positive shift in affective state. Unmitigated stress exposure has a deleterious effect on emotional state producing despair-like behavior and learned helplessness (Landgraf et al. 2015; Yao et al. 2019; Bougarel et al. 2011). We predicted that CRF activation would promote the internal states that produce despair-like behavior. Surprisingly, in a similar manner to our previous work on resiliency, we find that post-stress modifications to BNSTov^{CRF} neurons favor a positive internal state in the face of ongoing social stress. We observed that intra-defeat optogenetic stimulation during 8-10 SDEs, promoted more social interaction with a familiar aggressor. We show a significant positive correlation between interaction time with the aggressor and sociability to novel non-aggressive mice following 10 defeat episodes.

The sensory contact phase of RSDS is critical to the phenotypic display of resilience/susceptibility, as elimination of this component of RSDS failed to produce susceptible mice (Challis et al. 2014; Challis et al. 2013). Therefore, the 15 minutes of sensory stress on 8th-10th SDEs may represent a critical time during which emotional learning occurs. The development of resiliency may be shaped by emotional learning that occurs in the context of experiencing cumulative stress insults (Barthas et al. 2020; Strauman 2021). Indeed, mice implanted with fiber-optic ferules off-target failed to become resilient, suggesting that BNSTov^{CRF} engagement is protective during RSDS and the absence of which leads to susceptibility. Similarly, control mice (effectively serving as a sham group) did not display resiliency, further illustrating the importance of BNSTov^{CRF} activation for emotional learning. Male mice are innately territorial and engage in agonistic interactions with other mice, even in laboratory settings (Thurmond 1975; Kovalenko and Kudryavtseva 2015). Given the natural

tendency for mice to defend their territory, repeated attacks from a larger mouse of a more aggressive strain would constitute a form of social conditioning (Markham et al. 2009). During each SDE, mice acquire more information about their subordinate status where they assume behavioral changes, such as defensive posturing, consistent with susceptibility (Markham et al. 2009). This form of emotional learning is referred to as conditioned defeat (Cooper and Huhman 2007; Cooper and Huhman 2010; Markham et al. 2009; Jasnow et al. 1999) The BNST has been shown to be necessary for conditioned defeat status (Asok et al. 2016). Therefore, BNSTov^{CRF} stimulation during the period between 8 and 10 SDEs likely impaired the internal aversiveness of being defeated, impacting the way defeated mice would encode the experience. The stimulation-induced experience may dampen social defeat's aversiveness enough that conditioned defeat does not occur. In this study, optogenetic stimulation increased the time spent investigating CD-1, likely indicating the optical stimulation changed the subjective experience of stress, as male mice would typically avoid such a conspecific. Another plausible explanation is that stimulation increased vigilance, as BNST activation has been associated with increased arousal and anticipatory anxiety (Waddell et al. 2006; Clauss et al. 2019). However, the effect of stress on motivated social behavior could also be due to a blunting of circuits coordinated through the BNST in susceptible mice.

A possible explanation for why intra-defeat sociability predicts post-defeat resiliency is that the period comprising 8-10 SDEs represents a unique window by which mice assess their controllability, in order to maximize behavioral adaptation to this setting. Photostimulation may catalyze the continual promotion of behavioral flexibility and active coping by shifting internal states (Daniel and Rainnie 2016; Waraczynski 2016; Waters et al. 2015). Stimulation induces plasticity that allows incorporating a more optimistic context for a stressful environment. Cognitive tasks using instrumental conditioning, for instance, would be needed to assess this adequately. In fact, leveraging plasticity for therapeutic efficacy is shown in recent reports to

play a role in the success of deep brain stimulation (DBS) for treatment-resistant depression. A recent report showed that individualized tractography-guided implantation and intraoperative stimulation predicted early antidepressant effects (Sendi et al. 2021).

Previous work manipulated BNSTov^{CRF} neurons in the social defeat context, yet the behavioral effect was monitored in a separate novel context, only allowing inference of the direct stimulation on social behavior. Using social o-RTPP, we assessed the effects of neuronal stimulation on bivalently coordinating the internal emotional state. We observed that resiliency could effectuate both a state and trait, as 89% of the ChR2 mice were resilient and showed a preference for the side and social target in which they were stimulated, suggesting a state-dependent enhancement. In the context of socially-salient stimuli, such as female odor exposure, resilient mice displayed increased time investigating compared to susceptible mice, which was further enhanced during the “stimulation on” trials. This finding underlies how resilient mice may come to display higher social interaction times and hedonic-like consumption following BNSTov^{CRF} stimulation because it induces a positive internal state that enhances experiences that are generally positive. Notably, this effect is not simply relegated to all stimuli, as water or male urine did not solicit increased time sniffing during photostimulation. However, we cannot discount the modulatory role BNSTov^{CRF} neurons play in producing susceptibility. Indeed, in mice, we see the neuronal adaptation in both electrophysiological measurements and in calcium dynamics that support a state of decreased activation, suggesting that resiliency is the maintenance of activity in the face of threatening stimuli. This adaptation explains why photoactivation increased time spent sniffing predator urine, an innate stressor. Freezing to predator urine is thought to be BNST dependent, as lesions reduce defensive responses by way of the vomeronasal system. Interestingly, BNSTov^{CRF} activation would be predicted to increase freezing by synergizing accessory olfactory-BNST circuits (Kaouane et al. 2021); Hartley et al. 2019; Duvarci et al. 2009); Asok et al. 2016; Goode and Maren 2017; Fadok et al. 2017; Fendt et al. 2003), instead, we observed the opposite. This interpretation is reinforced by the effects

of BNSTov^{CRF} stimulation during TST in decreased immobility, suggesting that resiliency maintains positive internal states in the face of threats by neuronal activation.

A question that emerges from the data is, whether it is advantageous for an organism to frame aversive experiences more positively? After all, decreased exposure to known threats such as a familiar aggressor or predator urine has survival implications (Kaouane et al. 2021; Hartley et al. 2019). On the other hand, the role of BNSTov^{CRF} in valence switching promotes cognitive flexibility, decision-making, and social coordination, which can assist in foraging limited resources (Lemos et al. 2012; Kaul et al. 2021; Gold and Chrousos 2002; Backström and Winberg 2013; Heinrichs et al. 1995; Goode and Maren 2017; Marcinkiewcz et al. 2016). The BNST is important for integrating homeostatic needs with external input (Daniel and Rainnie 2016). Mice in the study were sated and had *ad libitum* access to water; it would be interesting to see how behavioral responses altered to meet homeostatic demands.

An important caveat to this study was that mice were subjected to intra-defeat optical stimulation, which produced resiliency, and later placed in a variety of behavioral tasks for which acute optogenetic activation occurred. A strength of this study design is that it enables the assessment of resiliency as a trait vs. state. Traits represent a stable and enduring pattern of behavior, whereas a state is a temporary mode of being relegated to acute circumstances. Chapter 3 focuses on resiliency as a trait, as mice displayed hedonic-like and pro-social behavior lasting up to 6 weeks. In this chapter, we uncover that acute optogenetic activation of (optically-induced) resilient mice enhances motivated exploratory behavior as a state. State-dependent resiliency is evident in the urine test, where no-light trials yielded no difference between control and ChR2 mice. In contrast, photostimulated ChR2 mice promoted increased female urine sniffing and social interaction with a novel conspecific, both of which are already elevated in resilient mice in the absence of manipulation.

Additionally, inhibitory optogenetics could explore the necessity and sufficiency of BNSTov^{CRF} neurons to state-dependent behaviors. Future studies could parse the contribution of state vs. trait by optogenetically activating during mice during behavioral tasks only after 10 SDEs. As neuromodulation becomes a more favored approach to treating mood disorders, an appreciation for stress-dependent changes in internal state may favor stimulation protocols (for DBS or transcranial magnetic stimulation) that may work in one context and not another. Thus, pioneering closed-loop or neurofeedback components into the stimulating device cannot be untethered from the patient's emotional reports, as they may serve as proxies for neurophysiological adaptations pertinent to antidepressant efficacy.

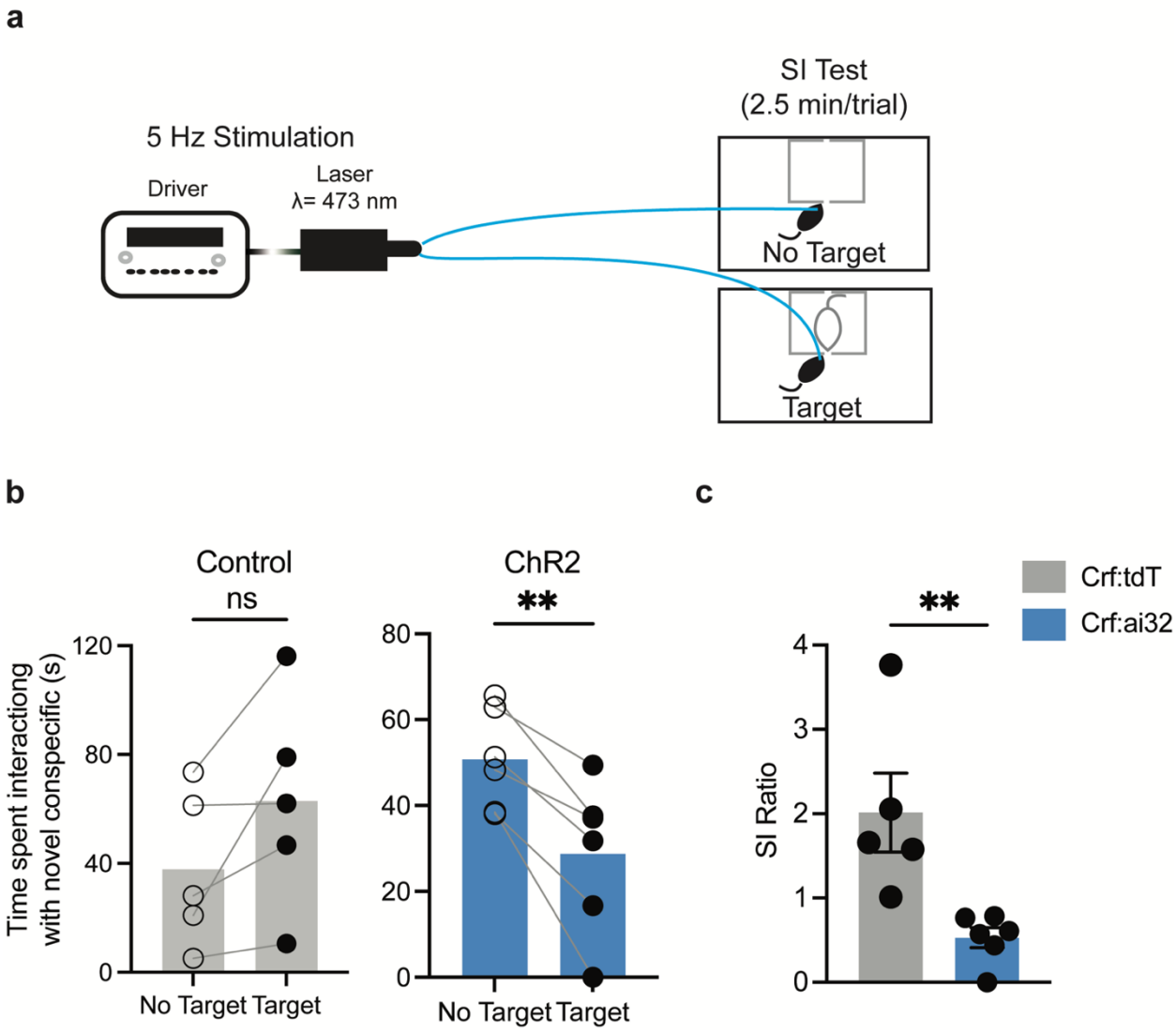

Figure 14. Acute BNSTov^{CRF} stimulation in low- or no-stress conditions induces social avoidance.

Figure 14. Acute BNSTov^{CRF} stimulation in low- or no-stress conditions induces social avoidance.

a, 5 Hz optogenetic 473 nm (blue light) photostimulation is induced with 2.5 minutes per trial with no target/target trials in tandem. **b**, Behavior of control mice during social interaction with novel conspecific within two (target vs no target) trials. Paired two-tailed t-test, t=2.282, df=4, P=0.0846, n=5. ChR2 mice receiving photostimulatoin during social interaction test. Paired two-tailed t-test, t=5.389, df=5, **P=0.0030, n=6. **c**, SI ratio of control and ChR2 mice during the social interaction test. Crf:tdT and crf:ai32, unpaired two-tailed t-test, t=3.352, df=9, **P=0.0085, n=5,6.

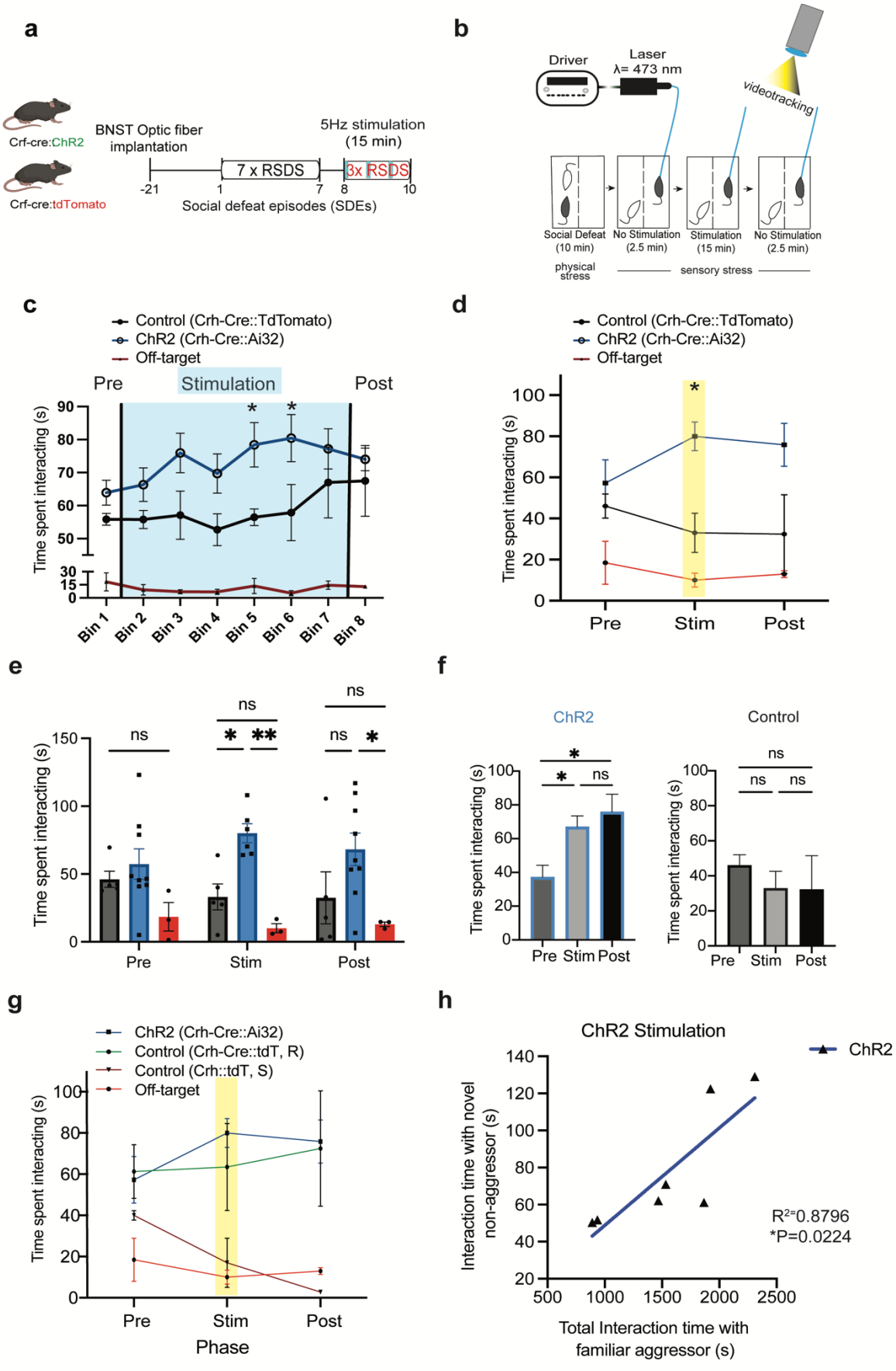
a
Crf-cre:ChR2
Crf-cre:tdTomato
BNST Optic fiber implantation
5Hz stimulation (15 min)
7 x RSDS
3x RSDS
-21
1
7
8
10
Social defeat episodes (SDEs)
b
Driver
Laser
λ= 473 nm
videotracking
Social Defeat (10 min)
No Stimulation (2.5 min)
Stimulation (15 min)
No Stimulation (2.5 min)
physical stress
sensory stress
c
Control (Crh-Cre::TdTomato)
ChR2 (Crh-Cre::Ai32)
Off-target
Pre
Stimulation
Post
Time spent interacting (s)
Bin 1
Bin 2
Bin 3
Bin 4
Bin 5
Bin 6
Bin 7
Bin 8
d
Control (Crh-Cre::TdTomato)
ChR2 (Crh-Cre::Ai32)
Off-target
Time spent interacting (s)
Pre
Stim
Post
e
Time spent interacting (s)
ns
Pre
Stim
Post
f
ChR2
Control
Time spent interacting (s)
Pre
Stim
Post
g
ChR2 (Crh-Cre::Ai32)
Control (Crh-Cre::tdT, R)
Control (Crh::tdT, S)
Off-target
Time spent interacting (s)
Pre
Stim
Post
Phase
h
ChR2 Stimulation
ChR2
Interaction time with novel non-aggressor (s)
R²=0.8796
*P=0.0224
Total Interaction time with familiar aggressor (s)

Figure 15. Intra-defeat BNSTov^{CRF} stimulation increases sociability toward familiar CD-1 aggressors and correlates with resiliency development.

a, Experimental schematic whereby Crf-cre::ChR2 mice are implanted with optical fibers in the BNSTov. **b,** Procedure during SDEs 8 through 10. Mice received optical blue light stimulation for 15 minutes during the sensory stress phase and social interaction is recorded using videotracking software. **c,** Interaction times pre-, intra-, and post-optical stimulation. Control (Crf-cre:tdTomato) n=6; ChR2 (Crf-cre::ChR2) n = 8; Off-target (Crf-cre::ChR2) n = 3. Two-way ANOVA (Bin x stimulation) interaction $F(14,47) = 0.6080$ $P=0.8447$, time (Bins) $F(7,47) = 0.9344$ $P=0.4892$, stimulation $F(2,47) = 208.4$ $P<0.0001$. Tukey's multiple comparisons post-hoc test, Control vs ChR2 ****$P<0.0001$, Control vs Off-target ****$P<0.0001$, ChR2 vs Off-target ****$P<0.0001$. Bin 5 and 6: Control vs ChR2 *$P=0.0438$ and *$P=0.0369$, respectively. Each bin corresponds to 2.5 minutes. **d,** Time spent interacting with all of the bins averaged according to phase. **e,** Time spent interacting across pre-, intra-, and post-stimulation phases. Two-Way ANOVA (Stimulation phase x genotype) $F(4,38) = 0.9630$, $P=0.4389$, Stimulation phase $F(2,38) = 0.002028$ $P=0.998$, genotype $F(2,38) = 16.76$, ****$P<0.0001$. Tukey's post-hoc test pre-stimulation: Control vs ChR2, Control vs Off-target, ChR2 vs Off-target = $P=0.7368$, $P=0.3446$, $P=0.0889$ respectively. Stimulation: Control vs ChR2, Control vs Off-target, ChR2 vs Off-target = *$P=0.017$, $P=0.475$, **$P=0.002$, respectively. Post-stimulation: Control vs ChR2, Control vs Off-target, ChR2 vs Off-target = *$P=0.0192$, $P=0.5844$, **$P=0.0037$, respectively. **f,** Time spent interacting across SDEs (8^{th}-10^{th}) according by group. ChR2 (n=8 mice) One-Way ANOVA $F(2,44) = 6.118$ **$P=0.0045$ Tukey's Post-hoc test: Pre vs Stim $P=0.0112$, Pre vs Post-stim *$P=0.0137$, Stim vs Post $P=0.7521$. Control (n=6) One-Way ANOVA Pre vs Stim $P=0.7573$, Pre vs Post $P=0.7362$, Stim vs Post $P=0.9993$. **g,** Retrospective analysis of stimulation during SDEs 8-10 effect on susceptible/resilient mice. ChR2 (n=8 mice), Control (R) (n= 2 mice), Control (S) (n = 4 mice), Off-target implanted ChR2 (n = 3 mice). Two-Way ANOVA Interaction (Stimulation phase x Condition) $F(6,38) = 0.6668$ $P=0.6768$, stimulation phase $F(2,38) = 0.03819$ $P=0.9626$, condition $F(3,38) =$

10.86 ****P<0.0001. Tukey's post-hoc test: stimulation ChR2 vs Off-target *P=0.0114. Post-stimulation: Control (R) vs Control (S) = P=0.0521, ChR2 vs Off-Target *P=0.019, ChR2 vs Control (S) *P=0.02. **h,** Correlation of intra-defeat stimulation (familiar aggressor) by social interaction time on the SI test (novel non-aggressor conspecific). ChR2 (n=9), linear regression goodness of fit test, ChR2 R^2=0.4979, F(1,7) = 6.941, *P=0.0337.

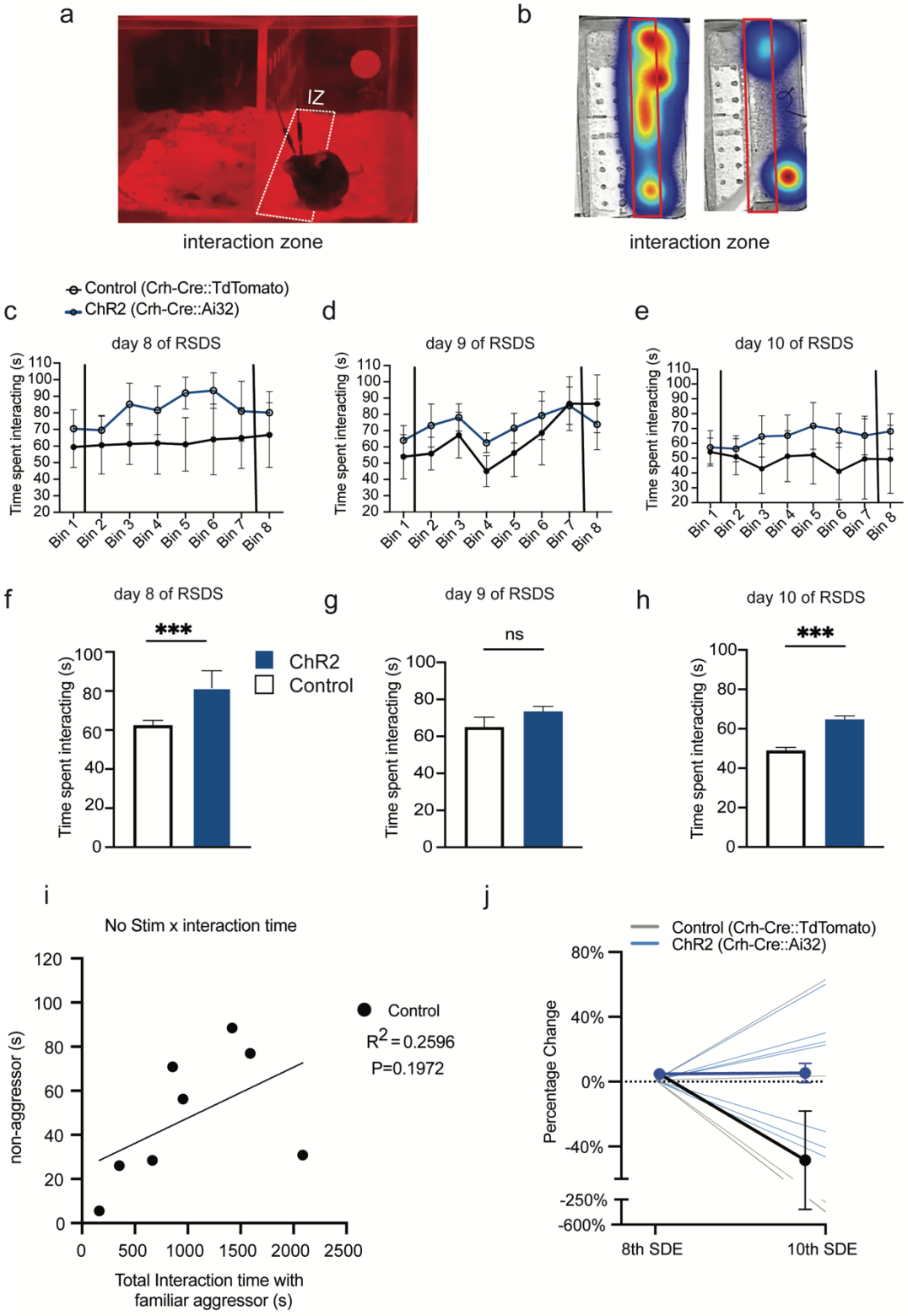

Figure 16: Intra-defeat stimulation increases interaction time with familiar CD-1 aggressors in ChR2 not control mice (Extended Data).

Figure 16: Intra-defeat stimulation increases interaction time with familiar CD-1 aggressors in ChR2 not control mice (Extended Data).

a, Day 8 of RSDS interaction times, vertical bar separate pre-, intra-, and post-optical stimulation phases, respectively. Control (Crf-cre:tdTomato) n=6; ChR2 (Crf-cre::ChR2) n = 8; Two-way ANOVA (Bin x stimulation) interaction $F(8,105) = 0.2587$ $P=0.9775$, time (Bins) $F(8,105) = 0.7179$ $P=0.6753$, stimulation $F(1,105) = 6.175$ $*P<0.0145$. Each bin corresponds to 2.5 minutes. **b,** Day 9 of RSDS interaction times, vertical bar separate pre-, intra-, and post-optical stimulation phases, respectively. Control (Crf-cre:tdTomato) n=6; ChR2 (Crf-cre::ChR2) n = 8; Two-way ANOVA (Bin x stimulation) interaction $F(7,103) = 0.3130$ $P=0.9467$, time (Bins) $F(7,103) = 1.356$ $P=0.2318$, stimulation $F(7,103) = 1.662$ $P=0.2003$. Each bin corresponds to 2.5 minutes. **c,** Day 10 of RSDS interaction times, vertical bar separate pre-, intra-, and post-optical stimulation phases, respectively. Control (Crf-cre:tdTomato) n=6; ChR2 (Crf-cre::ChR2) n = 8; Two-way ANOVA (Bin x stimulation) interaction $F(7,99) = 0.1448$ $P=0.9943$, time (Bins) $F(7,99) = 0.6926$ $P=0.9995$, stimulation $F(1,99) = 4.228$ $P=0.0424$. Each bin corresponds to 2.5 minutes. **d**, Interaction time with familiar aggressor during 15 minute stimulation averaged across bins on day 8 of RSDS. Two-tailed Mann-Whitney T-test $**P=0.0040$, (66.28 +/- 3.918, control) vs (83.06 +/- 3.068 ChR2), n=9,9. **e,** Interaction time with familiar aggressor during 15 minute stimulation averaged across bins on day 9 of RSDS. Two-tailed Mann-Whitney T-test $P=0.2345$, (65.00 +/- 5.380, control) vs (73.47 +/- 2.707 ChR2), n=8,8. **f,** Interaction time with familiar aggressor during 15 minute stimulation averaged across bins on day 10 of RSDS. Two-tailed Mann-Whitney T-test $***P=0.0002$, (48.93 +/- 1.615, control) vs (64.67 +/- 1.905 ChR2), n=8,8. **g,** percentage change of time spent interacting with familiar aggressor between the 8^{th} and 10^{th} SDE at Bin 1 of day 8 compared to bin 8 of day 10. Two-way ANOVA (Bin x stimulation) interaction $F(1,20) = 4.252$ $P=0.0524$, time (Bins) $F(1,20) = 4.038$ $P=0.0582$, stimulation $F(1,20) = 4.252$ $P=0.0524$. **h,** Correlation of intra-defeat stimulation (familiar aggressor) by social interaction time on the SI test (novel non-aggressor conspecific). Control (n=8), linear regression goodness of fit test, control

R^2=0.2596, F (1,6) = 2.103, P=0.1972. **l**, Effects of intra-defeat stimulation on ChR2 and Control mice toward familiar aggressor over time, as a percent change in social interaction time from baseline (bin 1, no stimulation of day 8) to post-stimulation (bin 8, no stimulation of day 9). Two-Way ANOVA Interaction F(1,20) = 4.252 P=0.0524, Time F(1,20) = 4.038, P=0.0582, Control vs ChR2 F(1,20) = 4.252, P=0.0524. **j,** Correlation of intra-defeat stimulation (familiar aggressor) by social interaction time on the SI time. F(1,6) = 2.103, P=0.1972.

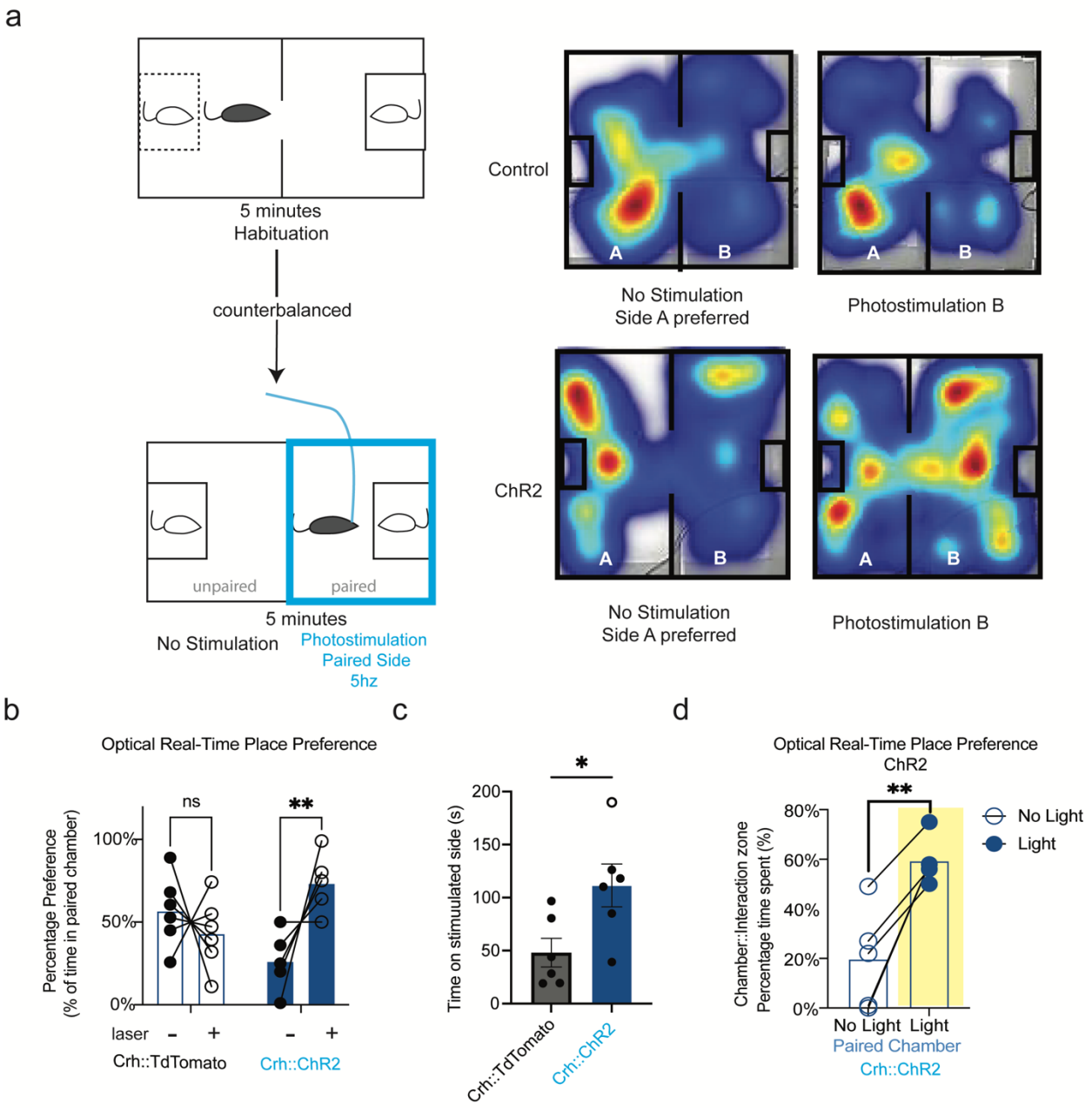

Figure 17. BNSTov^{CRF} neurons shift socio-affective bias on social optical real-time place preference assay.

Figure 17. BNSTov^{CRF} neurons shift socio-affective bias on social optical real-time place preference assay.

a, Schematic of social optical real-time place preference (o-RTPP), where mice have a 5 minute habituation followed by photostimulation paired to the side mice where spent the least amount of time during habituation. This is reflected in the heatmap of control and ChR2 mice. **b,** Social o-RTPP, where control crf:tdTomato and Crf::ChR2 mice spend more time on the laser paired side only in the ChR2 mice. Control = 5 mice, ChR2 = 6 mice. Two-way ANOVA Interaction ($laser_{on/off}$ x $genotype_{control/ChR2}$) F(1,18) = 0.0023 **P=0.0023. Genotype F(1,18) = 0.0000 P>0.9999. Laser F(1,18) = 3.792 P=0.0673. Sidak's post-hoc test Control P=0.4418, ChR2 **P=0.0032. **c,** Time spent on stimulated side between control and ChR2 mice. Unpaired t-test, two-wailed t=2.603, df=10, P=0.0263. **d,** Social o-RTPP of ChR2 mice as a percentage of time spent interacting when in stimulation paired chamber. Stimulation specially induces social interactivity when mice prefer a side (n=5 mice). Paired t-test, two-tiled, d=5.406, df=4, **P=0.0057.

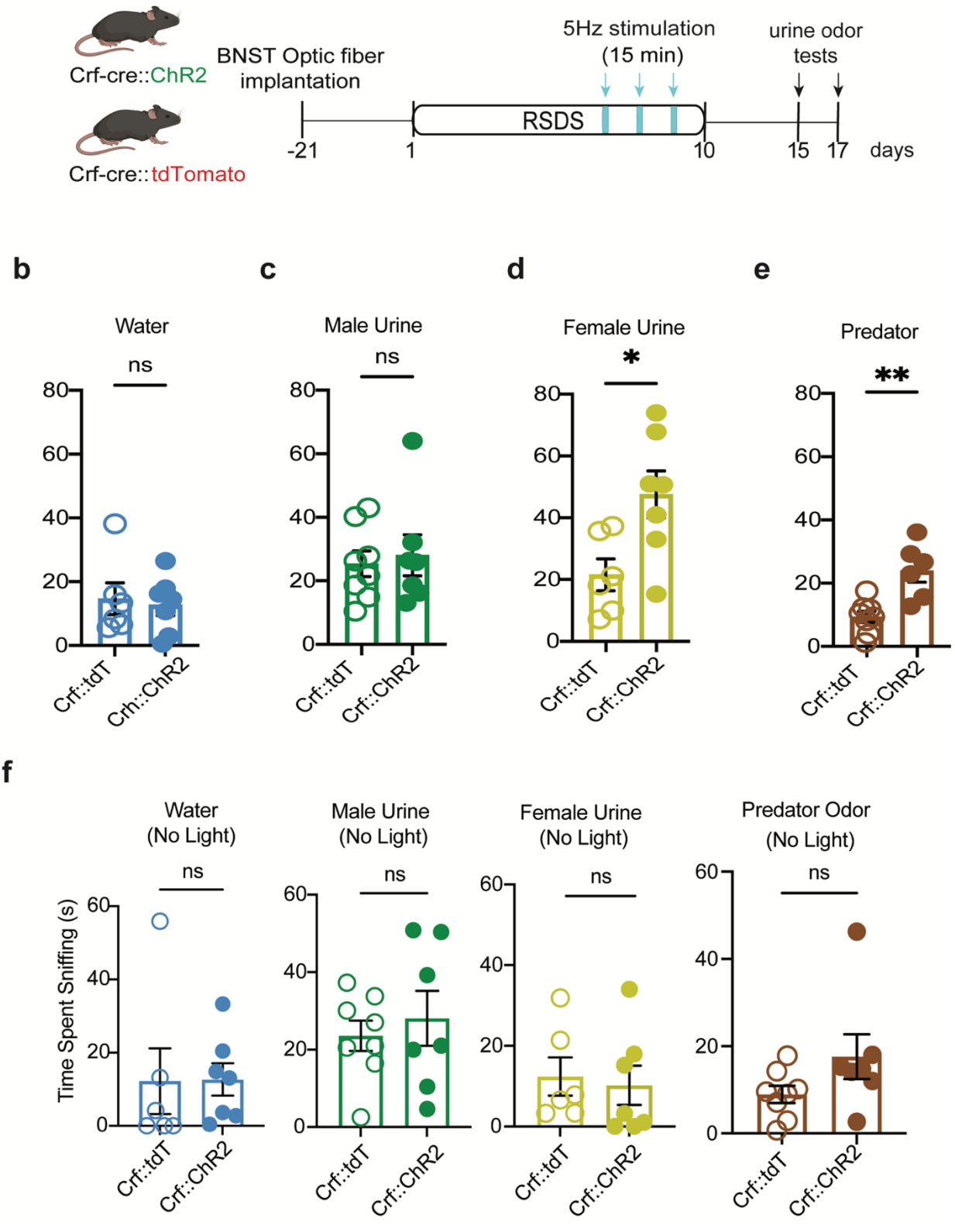

Figure 18. BNSTov^{CRF} stress modulation enhances positive valence to appetitive and aversive socially-salient stimuli.

Figure 18. BNSTov^{CRF} stress modulation enhances positive valence to appetitive and aversive socially-salient stimuli.

a, Experimental timeline, pending fiber optic implant mice are subjected to 10 SDEs with concomitant optogentic stimulation the final three episodes of RSDS and exposed to water, male-, female-, and predator urine over two days. **b,** The time spent sniffing water was recorded on behavioral recording software and quantified under direct effect of optical stimulation. Crf::tdt = 6 mice, Crf::ChR2 = 7 mice, unpaired two-tailed t-test, t=1.561, df=11 P=0.1469. **c,** The time spent sniffing male urine was recorded on behavioral recording software and quantified under direct effect of optical stimulation. Crf::tdt = 8 mice, Crf::ChR2 = 7 mice, unpaired two-tailed t-test, t=0.3592, df=13 P=0.7252. **d,** The time spent sniffing female urine was recorded on behavioral recording software and quantified under direct effect of optical stimulation. Crf::tdt = 6 mice, Crf::ChR2 = 7 mice, unpaired two-tailed t-test, t=2.726, df=11 *P=0.0197. **e,** The time spent sniffing predator urine was recorded on behavioral recording software and quantified. Crf::tdt = 8 mice, Crf::ChR2 = 6 mice, unpaired two-tailed t-test, t=3.943, df=12 **P=0.002. **f,** The time spent sniffing male urine was recorded on behavioral recording software and quantified in the absence of optical stimulation. Unpaired two-tailed t-test, water: t=1.561, df=11, P=0.1469; male urine: t=0.3592, df=13 P=0.7252; female urine: t=1.561, df=11 P=0.1469; predator urine: t=1.661, df=13 P=0.1207.

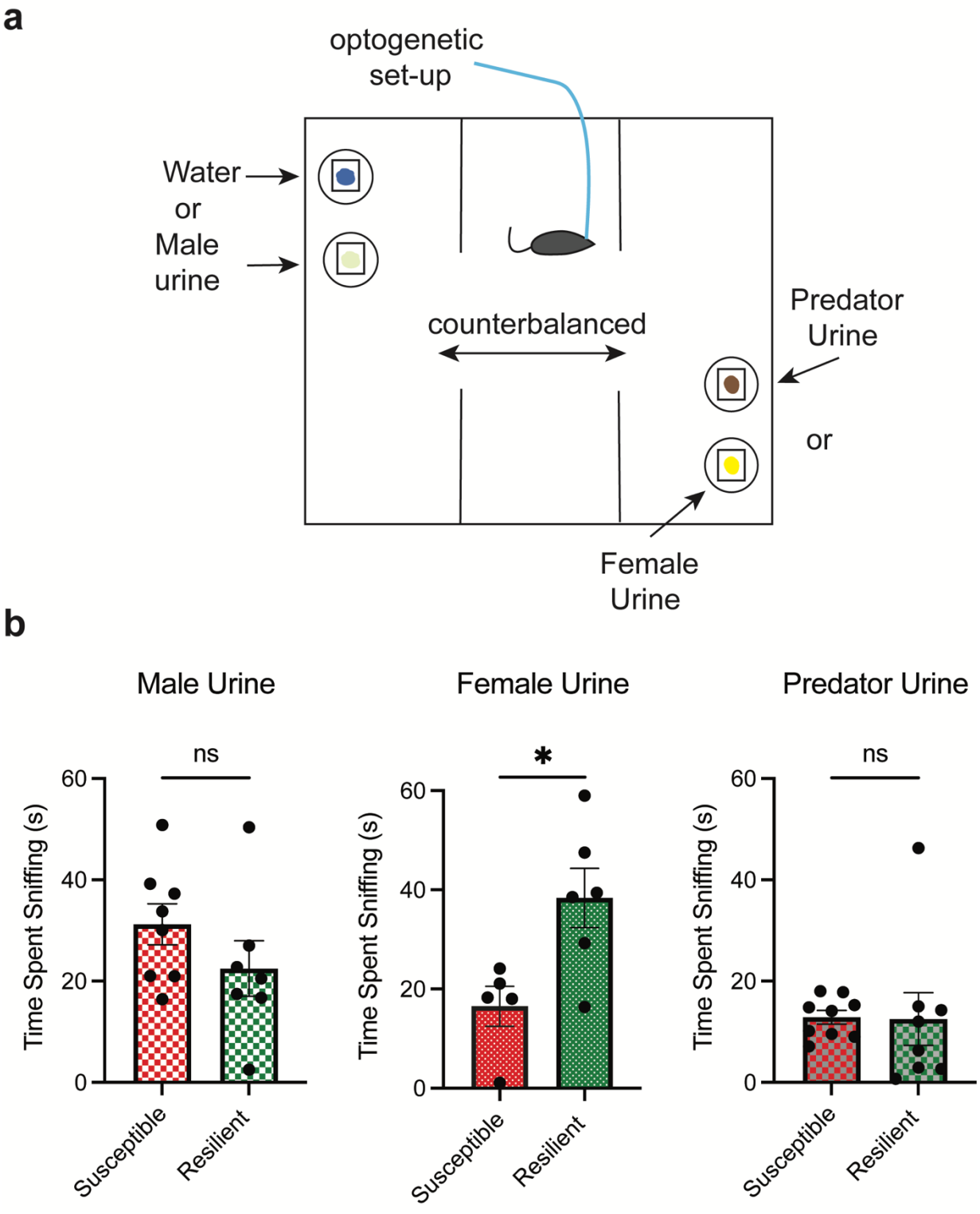

Figure 19: Distinct defeat-induced phenotypical differences convey individual preference for positively valenced odors (Extended Data).

Figure 19: Distinct defeat-induced phenotypical differences convey individual preference for positively valenced odors (Extended Data).

a, Schematic of placement of odorants in three-chamber setup where mice are subjected to three trials contained odorants. **b,** Susceptible and resilient mice during “no light” trial interaction with male urine. T-test, two-tailed, P=0.2156, n=8 susceptible, n=7 resilient. **c,** Susceptible and resilient mice during “no light” trial interaction with female urine. T-test, two-tailed, *P=0.0178, n=5 susceptible, n=6 resilient. **d,** Susceptible and resilient mice during “no light” trial interaction with predator urine. T-test, two-tailed, *P=0.9454, n=9 susceptible, n=8 resilient.

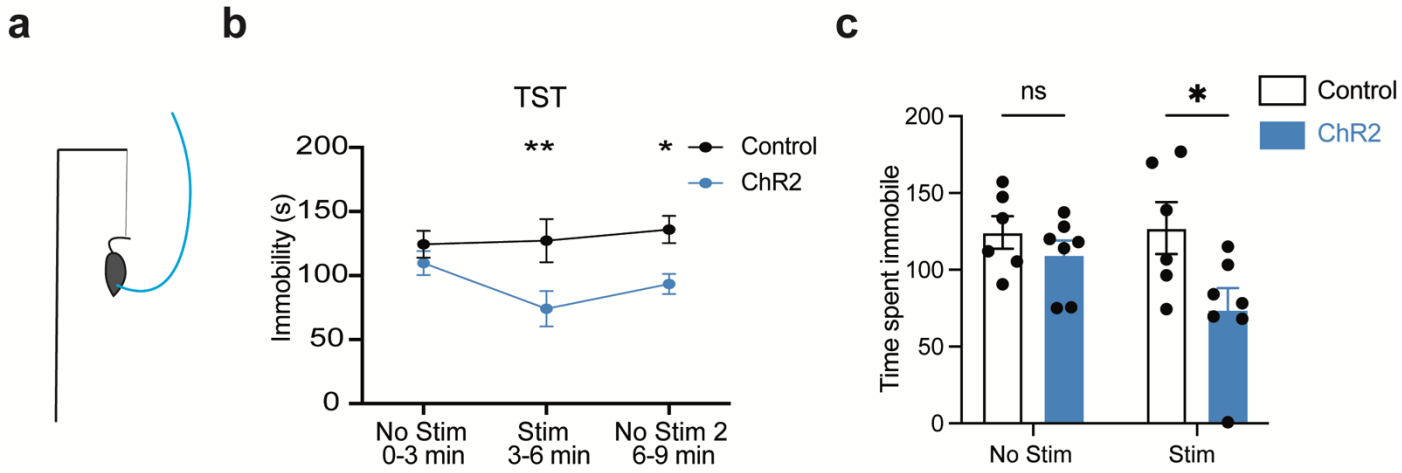

Figure 20. Optogenetic activation of BNSTov^{CRF} neurons suppresses despair-like behavior on TST that outlasts acute stimulation.

Figure 20. Optogenetic activation of BNSTov^{CRF} neurons suppresses despair-like behavior on TST that outlasts acute stimulation.

a, Tail suspension test scheme, whereby mice were suspended by tail and were tethered to an optogenetic fiber optic patch cord. **b,** Time spent immobile on the TST during no stimulation, stimulation, and post-stimulation phases, lasting 3 minutes each. Control = 6 mice, ChR2 = 7 mice. Two-Way ANOVA Interaction (Stimulation phase x Condition(genotype)) $F(2,33) = 1.410$ $P=0.2584$, Stimulation phase $F(2,33) = 1.128$ $P=0.3357$, Condition $F(1,33) = 14.53$ ***$P=0.0006$. Sidak's Post-hoc test: Control – ChR2 (no stim): $P=0.768$, (stim) **$P=0.0096$, (no stim 2) *$P=0.0467$. **c,** Time spent immobile on TST as a feature of control vs ChR2 conditions. Two-Way ANOVA Interaction (Stimulation phase x Condition(genotype)) $F(1,22) = 2.209$ $P=0.1514$, Stimulation phase $F(1,22) = 1.616$ $P=0.2169$, Condition $F(1,22) = 6.881$ *$P=0.0155$. Sidak's Post-hoc test: No Stim – Stim (control): $P=0.6752$, (ChR2) *$P=0.0163$

Chapter 5

Conclusion and Future Directions

Conclusion

Bruce McEwen's concept of allostasis (or adaptability to challenges) has been a central tenant to both stress and fields of resiliency (Karatsoreos and McEwen 2011). Allostasis or "maintaining stability or homeostasis, through change" has often been described in the literature as a see-saw-like process, where protective and detrimental factors on either end threaten the system's ability to return to a homeostatic set point. Stress and its accompanying molecular, genetic, and environmental factors can, over time, continually challenge a system beyond its capacity to return, termed allostatic load (Sterling 2012; McEwen 2004). In comparison, factors that support homeostasis (endogenously or exogenously) buffer against the ongoing challenge. A critique of allostasis is that it creates a binary for which a given substrate, such as cortisol, is either considered "bad" or "good." While many reports support a view that allostatic regulation occurs on a continuum, very few examine the point at which a "bad" substrate becomes "good." The work of this dissertation sought to provide a roadmap into a process in which a heavily studied stress modulator, CRF, undergoes such a change. In essence, providing a rationale that allostasis (or the capacity to adapt) inherently describes the development of resiliency and that allostatic load becomes the point at which healthy adaptation becomes pathological.

Recently, work by the Han lab and others has shown that resiliency exists as a separate process that occurs through an active mechanism (Franklin et al. 2012; Russo et al. 2012; Han and Nestler 2017; Friedman et al. 2016; Friedman et al. 2014). The work presented in this dissertation advances the field by putting forth work that resiliency is not only an active process but emanates from the neurophysiological adaptations that occur as a response to stress. In this way, *stress becomes instructive* in establishing resiliency, and chapter 2 (Fig 5), shows that stress is necessary for resiliency to occur. The BNST is a brain structure that receives input from interoceptive, sensory, homeostatic, and autonomic input to orchestrate divergent

behavioral outcomes and adapt to environmental challenges. The work of this dissertation ascribes a more nuanced role for this brain region as not only exerting influence over behavioral outcomes to promote resiliency but acts as a node for continuous emotional appraisal of one's capacity to handle future challenges according to stress history.

Throughout the dissertation, a question that has come up is "what constitutes 'adaptive' versus 'maladaptive' behavior?" By extension, this raises the question of the definition of resiliency. The original use of the SI ratio to determine resiliency was based on the observation that a C57BL/6J mouse subjected to RSDS would socially avoid a novel CD-1 and equivalently familiar C57BL/6J mice of both sexes, in an apparent deficit in behavior. Moreover, while much of the behavior measures focuses on sucrose preference and social interaction assays, other disturbances have been differentially observed in susceptible vs. resilient mice, such as weight change, circadian rhythm, cardiac hypertrophy, serum corticosterone levels, and white matter integrity (Friedman et al. 2014; Cathomas et al. 2019; Friedman et al. 2016; Koo et al. 2019; Krishnan et al. 2007; Han and Nestler 2017). Resiliency then would be defined by the changes that occur in response to ongoing challenges that support an organism's adaptive capacity. Conversely, the inability to develop or maintain those changes, as per this definition, would be considered maladaptive, such as the failure to maintain firing rates observed in susceptible mice.

One of the most debilitating aspects of MDD is the desire for social seclusion (Lynch et al. 2020; Yu et al. 2011; Hammen 2005; Gold 2013). Voluntary isolation detaches the individual from social support, prevents or severs the therapeutic relationship (if psychotherapy has been initiated), and is linked to poorer outcomes (Gold 2013; Kendler et al. 1999; Strauman 2021). The mechanism underlying the switch in social approach to social avoidance is intriguing in that prior study have shown CRF's ability to engage in valence switching (Lemos et al. 2012; Chen

et al. 2020). The dopaminergic VTA-NAcc circuit is essential for the rewarding aspects of social interaction (Heymann et al. 2020; Nestler and Carlezon 2006; Wanat et al. 2013). The VTA and NAcc receive efferent BNSTov^{CRF} projections (Takahashi et al. 2019; Dabrowska et al. 2016); moreover, the NAcc has local CRF neurons (Lemos et al. 2012; Walsh et al. 2014), leaving open the question of how CRF may regulate social behavior under conditions of social stress. In a previous study, under conditions of severe acute stress, CRF blunted the effect of dopamine in the NAcc and is thus attributed to the switch from appetitive to aversive nature that CRF acquires in the context of severe stress, which leads to avoidant behavior observed in stress psychopathology (Lemos et al. 2012). Similarly, another study revealed that a VTA CRF receptor antagonist blocked social avoidance induced by phasic VTA dopaminergic firing with a modified form of social defeat stress. Context also mattered because, in the absence of social stress, CRF receptor antagonists failed to blunt social avoidance, suggesting the stress-coincident detecting role of CRF (Walsh et al. 2014). In stark contrast, the work of my dissertation shows that persistent CRF activation not only contributes to but is necessary and sufficient for social approach. To understand this, one must explore the microcircuitry of the BNST that may govern BNSTov^{CRF} projections to the VTA and NAcc. Chronic stress leads to a reduction in input resistance and membrane time constant in BNSTov^{CRF} neurons (Daniel et al. 2019) that effectively means that a strong input would be needed to drive an action potential, thereby hampering the summation of eEPSCs would be difficult to drive activity. CRF neurons of the oval BNST primarily consist of local interneurons that form reciprocal inhibitory connections with few long-range GABAergic efferents (Daniel et al. 2019; Daniel and Rainnie 2016; Kim et al. 2013; Dabrowska, Hazra, Guo, Li, et al. 2013; Dabrowska, Hazra, Guo, Dewitt, et al. 2013; Dedic et al. 2018). Thus, under chronic stress, local interneurons inhibit each other and shape the response with the summation of local network activity of long-range BNSTov^{CRF} efferents (Partridge et al. 2016).

In chronic stress conditions (such as chronic pain), VTA-projecting BNST neurons contributed to condition place aversion and decreased dopaminergic neuronal activity (Takahashi et al. 2019). Extrapolating this to my study would suggest that susceptible mice with the decreased firing rate would reduce synaptic output to the mesolimbic VTA-BNST system, thereby promoting social avoidance (and anhedonic-like) responses. In contrast, resilient mice would maintain activating tone, thereby fostering social approach and hedonic-like behavior in an apparent resistance to the harmful effects of ongoing psychosocial stress. The relationship between $NAcc^{CRF}$ and VTA^{CRFR1} is less well understood, and to my knowledge, there is no evidence that these populations share a direct connection. This, however, does not account for the observed stress-history dependency under which $BNSTov^{CRF}$ regulation occurs. The ability to gate when neuroadaptation happens may be a specialized neuromodulating property of CRF. Indeed, chronic stress increases the proportion of CRF neurons receiving input from other CRF neurons, which boosts the signal-to-noise ratio in BNST (Partridge et al. 2016). Concomitantly, CRF neurons increase *Crf* gene regulation in CRF neurons, making them resistant to the strong regulatory effects of glucocorticoids (Konishi et al. 2003). Glucocorticoids have been shown to act on histones to cause methylation of the *Crh* promoter, thereby serving as a regulator of CRF signaling (Elliott et al. 2010). In the absence of this negative feedback, CRF neurons can maintain a high degree of CRF output, which has been shown *in vitro* to cause upregulation in CRFR1 in hypothalamic cell culture (Konishi et al. 2003). Typically, in conditions of high CRF concentration, CRFR1 is internalized (Dos Santos Claro et al. 2019; Broccoli et al. 2018; McClard et al. 2018; Hu et al. 2020; Hillhouse and Grammatopoulos 2006; Gold and Chrousos 2002), but the studies put forth in this dissertation provide evidence to a previously undescribed mechanism by which CRFR1 behaves in an auto-receptor-like fashion that is not subject to the same glucocorticoid regulation observed in HPA axis regulation. Indeed, corticosteroid levels are not significantly different in mice with long-term conditional overexpression of CRF in the dorsal lateral BNST (Sink et al. 2013; Regev et al. 2011).

Limitations of the study include the lack of direct manipulations *of CRF in vivo* and independent investigations of the contributory role of GABA aside from CRF, observed in susceptible/resilient development. Additionally, *Crfr1* gene regulation is assumed to contribute to CRFR1 protein levels, but formal studies should be carried out to assert this. Further, pharmacologic CRFR1 agonist/antagonist studies should be considered to further describe the receptor's functional role in behavior. Studies interrogating the internal state of resiliency (chapter 4) notably did not include inhibitory optical stimulation. Bidirectional optical studies would be used to test whether internal state valence changes are required to shape behavioral responses associated with resilience.

Under low- or no-stress conditions, we observed that CRF stimulation provoked avoidant actions. During an immediate perturbation of basal conditions (such as acute stress), avoidance may be required, suggesting that CRF may play a modulatory in reducing stress most efficiently. However, prolonged stress requires more active forms of coping, which relies upon increased tolerability and potential interaction with the aversive stimulus/stimuli. This increased exposure to the stimulus, while it may seem maladaptive in the short term, becomes adaptive in the long term. It would facilitate better stress coping, coordination of resources and close enough assessment of the issue to better construct a tenable long-term solution of dealing with the stressor (Jasnow et al. 2004; Engelhardt et al. 2021; Hostetler and Ryabinin 2013). In this way, *stress becomes instructive* to the organism by way of the BNST's computational and neuroadaptive capacity. In a clinical context, CRF antagonists given during this period would normalize the stress-induced acute response, but perhaps, may place the individual at a lesser advantage by removing his adaptive capacity. Basic science experiments involving inhibitory optical stimulation and pharmacology, for instance, would test this hypothesis directly. Similarly, stress inoculation studies have shown that soldiers with pre-exposure combat training displayed

a lower incidence of PTSD and depression than those who had not, suggesting its importance in promoting future stress adaptability and, in turn, resilience (Jackson et al. 2019).

The dynamic modulatory role of BNSTov^{CRF} neurons provides a challenging road ahead for the clinical treatment of MDD. It may underscore the need for novel antidepressants that consider the dynamic relationship between ongoing environmental stressors and neuronal contributors to maladaptive behaviors. Indeed, ignoring the contributory role of stress-history-dependent CRF transmission would lead to one-size-fits-all models upon which novel therapeutics would be developed. This has been the case with CRFR1 antagonists such as Astressin, which performed well in preclinical models of acute stress and failed subsequent clinical trials (Spierling and Zorrilla 2017). The findings of this dissertation make a case for more electrophysiology- and anatomy-based neuromodulation therapies such as DBS or transcranial magnetic stimulation (TMS). Modern pharmacology using static receptor agonist/antagonist motifs is limiting in contexts when receptors respond not only to intracellular/molecular milieu (such as CRF concentration) but also to neural network changes brought about by stress-history that influences epigenetic, molecular, and circuit substrates. DBS or TMS has practical challenges in scalability, but perhaps part of the challenge is in patient selection (Woodham et al. 2021; Razza et al. 2021; Tan et al. 2020; Riva-Posse et al. 2014). As traditional SSRIs are effective in 50-60% of patients, more invasive approaches may be considered, particularly in treatment-resistant subpopulations (Riva-Posse et al. 2014). It is my hope that these findings place more nuance around the context of affective disturbances, particularly that substrates, like CRF, thought to contribute to pathological states, may have self-regulating features that promote endogenous resiliency. The concept of critical periods may not only pertain to developmental biology but can extrapolate to the development of adult-onset mood disorders. Within an individual's stress history, there may be points at which strategic intervention could shift affective trajectories that lead to enduring resiliency. For people at high risk for developing

stress-related psychopathology, such an intervention would obviate the daunting life-long treatment course that awaits many of those who develop full-blown mood disorders.

Summary

Stress adaptation by its very nature requires substrates that can serve as coincident detectors as a proxy of stress severity and chronicity. CRF has been hypothesized to serve in this role in various studies (Ichiyama et al. 2022; Vom Berg-Maurer et al. 2016), yet how it does this remains elusive. Our study developed a modified version of RSDS wherein we uncovered a "tipping point" by which susceptibility or resiliency is established. We observed a neuroadaptive increase in firing rates using electrophysiology, which had previously been found to generate depressive- and anxiety-like responses, which paradoxically was maintained solely in resilient mice. We tested the causal link between BNSTov^{CRF} firing adaptation and the development of resiliency using chemo- and optogenetics. We discovered that not only was neuronal activation necessary and sufficient for resiliency but there was another dimension to the modulation that was dependent on stress history. *In vivo* circuit dynamics were observed using fiber photometry where social contexts solicited more BNSTov^{CRF} neural activity after 10, but not 7 SDEs, supporting its role in resiliency establishment. RNAScope in situ hybridization provided the cellular link of *Crfr1* gene expression being enhanced and maintained exclusively in BNSTov^{CRF} neurons of resilient mice. Both neuroadaptation and social stress were critical components to bolstering resiliency. In chapter 4, the resiliency-promoting neuroadaptation of BNSTov^{CRF} neurons was taken further to explore contributions on internal motivation state. We uncovered that BNSTov^{CRF} activation emboldens sociality in the face of social threat and biases social preference. Interestingly, BNSTov^{CRF} activation promotes social avoidance in low-stress conditions, suggesting that the stress-history-dependent modulation does so by shifting the valence of external stimuli. Although not the focus of this thesis work, the negative valence shift in a context typically regarded as positive may explain the decrease in pro-social and hedonic-

like behavior observed in susceptible mice. This valence-shifting hypothesis was verified in experiments where BNSTov^{CRF} chemogenetic inhibition produced a decrease in SI ratio, sucrose-preference test, and susceptible mice spent less time investigating female urine compared to resilient mice. Conversely, BNSTov^{CRF} neuronal activation promoted increased time spent investigating an innate stressor (red fox urine) and enhanced mobility time on the tail-suspension test. Overall, the dissertation examines the biological substrate determining individual psychological "breaking points." I present a collection of experiments that provide strong evidence that neuroadaptation in BNSTov^{CRF} neurons (likely a key node of several networks) determines the timing and behavioral response to cumulative psychosocial stress, thereby playing a critical role in the development of stress resiliency (Fig. 21 & 22).

Future Directions

Stress neuroadaptation led to increased firing rates maintained solely in resilient mice, which raises questions surrounding circuit mechanisms that underlie this phenomenon. The BNSTov receives inputs from the infralimbic cortex, VTA, and notably the Paraventricular Thalamus (PVT).

Similar to the BNSTov, the paraventricular thalamus (PVT) is reported to play a role in the etiology of stress-related depression (Hsu et al. 2014). Functional neuroimaging studies reveal aberrant functional connectivity between PVT and limbic areas involved in emotional regulation in depressed patients (Kirouac 2015). Notably, the PVT encodes information about stress duration and regulates adaptive behavioral responses via connectivity with downstream targets such as the BNST (Vertes et al. 2012). PVT-mediated behavioral changes in response to stress require an incubation period (Hsu et al. 2014; Sousa 2016; Serra-Blasco et al. 2016). However, mechanisms underlying the latency between stressor-onset and maladaptive changes in

behavior remain a mystery. I hypothesize the temporal profile and emergence of stress susceptibility in the face of persistent psychosocial stress through PVT synaptic influence on CRF BNSTov neurons (PVT-BNSTov^{CRF}).

The PVT and BNST as Regions Correlated with Susceptible/Resilient Phenotypes

The sensory contact phase of RSDS is relevant to assessing brain activation involved in the acquisition of susceptibility (Challis et al. 2013). Therefore, after either subthreshold (7 days) or 10 days of social defeat, I subjected Crf-tdTomato transgenic mice to a 30-minute sensory exposure with a novel male aggressive CD-1 through a Plexiglas barrier and conducted c-Fos immunohistochemistry. I observed that indeed BNSTov^{CRF} neurons exhibited a greater pattern of activation [indicated by the overlap of c-Fos (GFP) with CRF^{+} neurons (tdTomato)] in susceptible versus resilient and control animals (not shown**)**. PVT neurons, however, revealed an opposite pattern whereby the # of c-Fos (GFP) cells were greater in resilient relative to susceptible and control animals (Fig 23a). Overall, c-Fos levels were similar between PVT and BNSTov regions. In the PVT # of c-Fos cells peaked in the RSDS x 7 conditions (mice subjected to 7 SDEs) when c-Fos/tdTomato overlap lowest in the BNSTov. Because the RSDS x 7 condition (mice subjected to 7 SDEs) reflects neural changes occurring just preceding susceptibility, the heightened activation in the PVT may represent a "last-ditch" effort in buffering stress-related changes in interoceptive state. Interestingly, resilient animals maintain enhanced c-Fos activity, whereas susceptible exhibit a significant decrease. Additionally, a sparse PVT^{CRF} neuronal population showed a similar trend of c-Fos activation that may play a role in susceptibility (not shown). Given the dearth of knowledge regarding how PVT regulates behavior and the complex cell types in this area, in the future, I would focus exclusively on BNST-input-defined PVT neuronal populations (which contain CRF^{+} PVT neurons, among many others). Injections of a retrograding cre-dependent (rAAV-DIO-mCherry) retrograde virus into the BNSTov^{CRF} neurons revealed dense cell bodies in the PVT, some of which were also CRF^{+}

(not shown) indicating a PVT-BNSTov^{CRF} circuit (Fig. 23b). In future studies, I plan to pursue a circuit-level dissection of the PVT-BNSTov^{CRF} circuit and its involvement in the maintenance of resiliency using cell-type and pathway-specific optogenetics.

This dissertation shows the correlation between firing rates and the maintenance of resilient responding between mice subjected to 7 and 10 SDEs; however, we did not explore neurophysiological mechanisms that may underlie this. Stress has been shown to affect synaptic plasticity. For instance, acute versus chronic stress was led to switching from LTP to LTD of EPSCs in the BNST (Daniel and Rainnie 2016). In another study, vSUB-BNST versus ILCx-BNST circuits contributed to LTP and LTD and their respective anxiolytic and anxiogenic responses. The overall behavioral state of the animal was shown to be the combination of both inputs, with net synaptic influence determining the expressed basal state of the animal. Despite being characterized by the categorical cut-off of SI ratio < or > 1, I hypothesize that susceptibility/resiliency exists in the continuum with the overall behavior shaped by inputs. I hypothesize that PVT-BNST circuit changes may regulate BNSTov^{CRF} excitability that I show is necessary for the persistence of resiliency. Interestingly, there exists a Central Amygdala (CeA) CeA^{CRF}→BNSTov^{CRF} circuit that synapses onto the same cells innervated by PVT^{CRF} neurons, the sum of which may be responsible for (1) the window of plasticity about which resiliency is established and (2) the determination of susceptible/resiliency as a result of glutamatergic PVT^{CRF}-BNSTov^{CRF} vs. GABAergic CeAL^{CRF}→BNSTov^{CRF} neuronal activity.

Moreover, we have shown the correlation between changes in neuronal excitability and *Crfr1* gene expression. To demonstrate a causal link, perturbations involving CRISPR-CAS9 where *Crfr1* expression is blocked from epigenetic regulation during 8-10 SDEs could provide insight. Indeed, dCas9 has been developed precisely for applications of making promoter regions

resistant to repression or transcription, thereby highlighting the functional contributions of the gene in question (Ren et al. 2022; Villegas Kcam et al. 2022; Carullo et al. 2021). The underlying hypothesis is that *Crfr1* gene expression is upregulated as an adaptation to stress but is maintained in resilience. Therefore, mice with CRISPR-dCas9 should develop resiliency, whereas mice expressing CRISPR-Cas9 (*Crfr1* deletion) would develop susceptibility. The increase in *Crfr1* may increase CRFR1 on CRF neurons, which maintains the relatively high firing rates observed in resilient mice. It is equally possible that increased presynaptic drive (for instance, from the PVT) may serve as a catalyst to drive epigenetic changes about *Crfr1* gene regulation in the setting of stress. Interestingly, these findings suggest that the interplay between cell-type, circuit-, and stress-history specific adaptation converge on this PVT^{CRF}-$BNSTov^{CRF}$ to orchestrate the dynamic coordination of socioemotional behaviors that reflect outcomes of RSDS.

$BNSTov^{CRF}$ neurons send projections to areas important for social motivation, such as the VTA, PVN, and Dorsal Raphe. Future studies could also probe for downstream changes that may underlie the behavioral repertoire of resiliency/susceptibility.

Lastly, many of the studies conducted in this dissertation relied heavily on behavioral readouts to infer something about an animal's internal and emotional state under stress. The ability to engage in the cognitive appraisal of one's external circumstances according to one's internal state is crucial to stress reactivity and resiliency. Therefore, in future studies, I would like to incorporate instrumental conditioning paradigms wherein mice are made to engage in selection strategies based on prior consequences. My prediction is that mice subjected to 7 SDEs would maintain more optimistic-like decision-making in the face of ambiguous choice determination. Moreover, they would favor decisions linked to prior reward even if the choice is yoked to a higher probability of punishment.

Conversely, in susceptible mice, the action selection strategy would switch whereby mice would favor choices more closely linked to avoiding aversive stimuli, even if the statistically the probability favors reward retrieval. I hypothesize that optogenetic activation of BNSTov^{CRF} neurons during SDEs 8-10 would bias mice toward the latter, and inhibition would bias toward the former. Together, these results would suggest that resiliency coordinated by the BNSTov^{CRF} neuronal population is associated with a more positive internal state (as observed in chapter 4) and a more optimistic cognitive style, enabling the assortment of pro-social, hedonic-like, anxiolytic-like responses observed (in chapter 3).

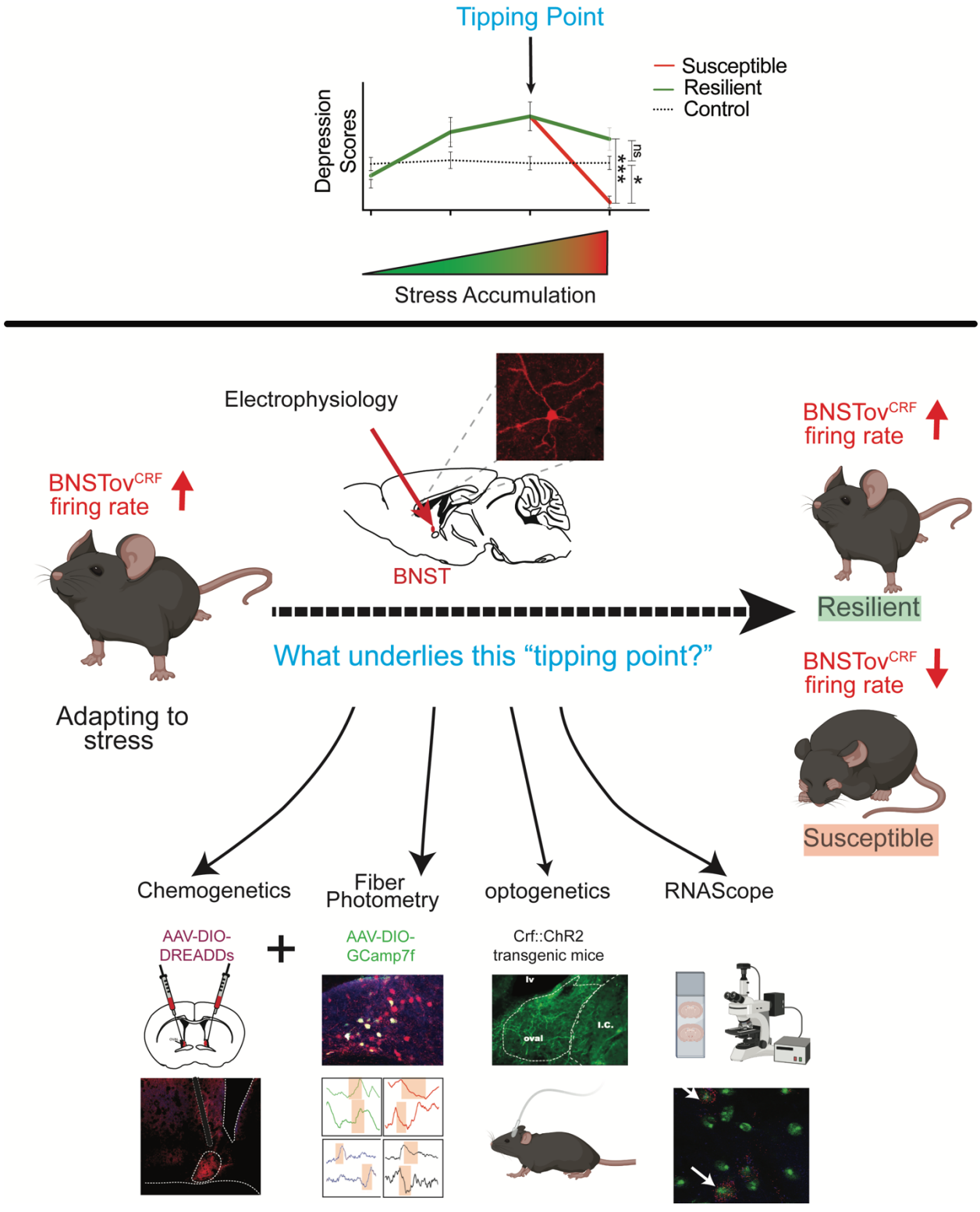

Figure 21. Visual summary of Chapter 3

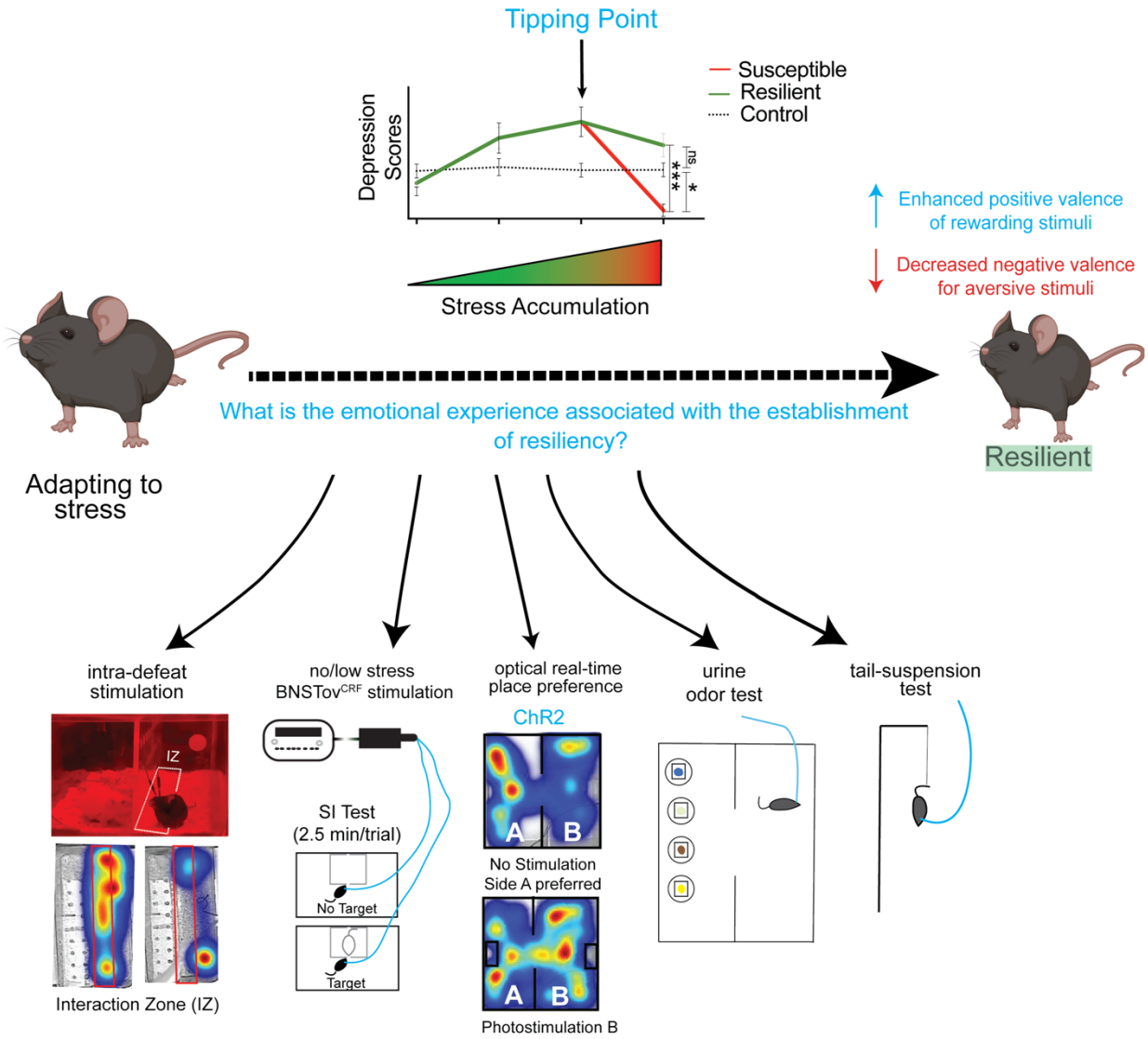

Figure 22. Visual summary of chapter 4

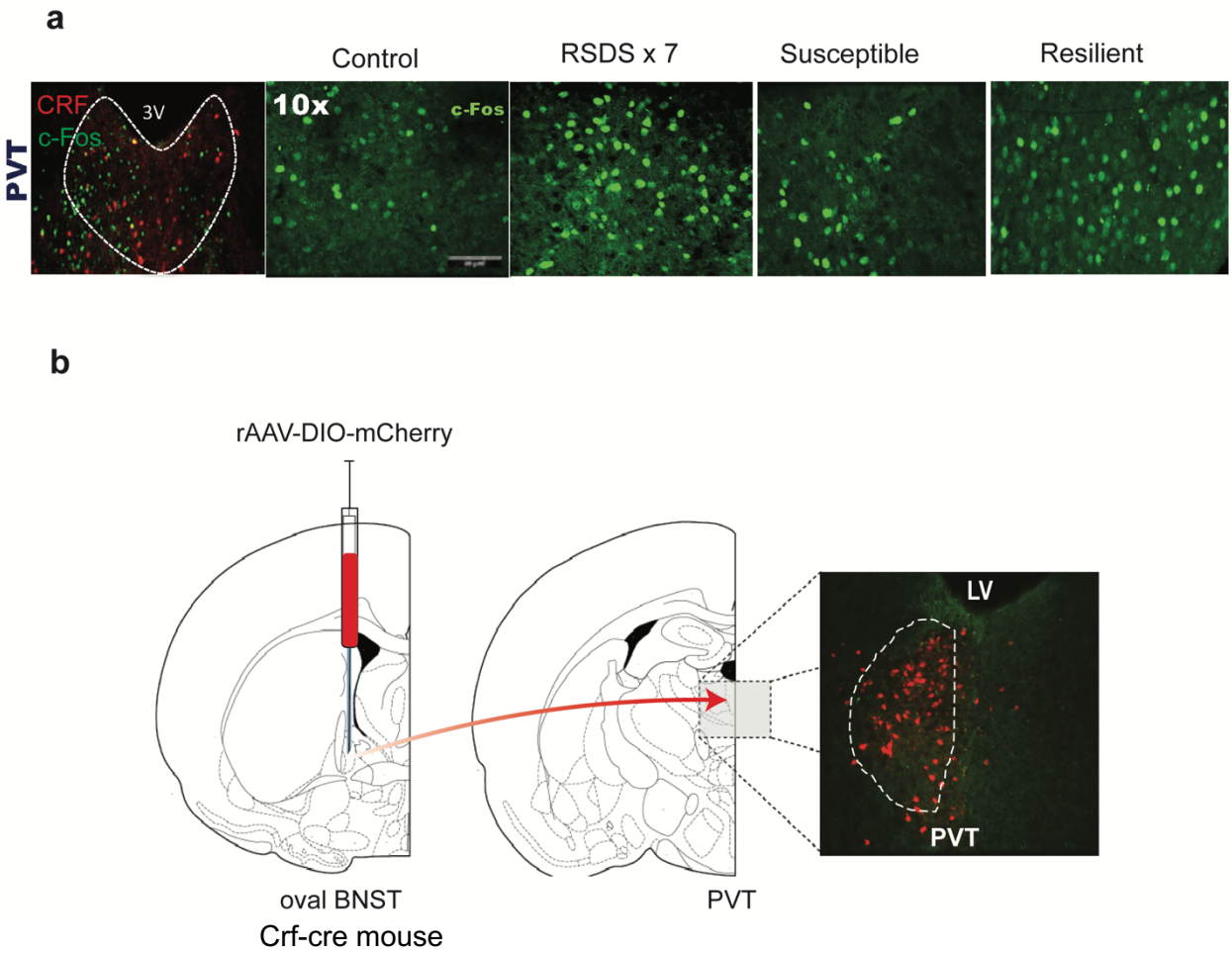

Figure 23. Future directions preliminary data revealing differential patterns of activation with c-Fos in PVT neurons in a non-socially threatening context and evidence of a PVT-BNSTov^{CRF} circuit.

Figure 23. Future directions preliminary data revealing differential patterns of activation with c-Fos in PVT neurons in a non-socially threatening context and evidence of a PVT-BNSTov^{CRF} circuit.

a, The pattern of activation suggests a role of these cells being engaged in adaptive responding. While susceptible mice appear to have decreased PVT activity, this appears to be correlated to BNST c-fos activation (Fig 23a, 4d,e). Conversely, in resilient mice, PVT activation appears to be elevated and is sustained in the BNST (Fig 23a, 4d,e). In the RSDS x7 condition, there appears to be a greater degree of activation in the PVT, suggesting its involvement in stress adaptation. **b,** Viral tracing involving cre-dependent, mCherry-tagged, retrograding AAV virus in Crf-cre transgenic mice targeting BNSTov^{CRF} afferent neurons. The PVT displayed mCherry fluorescence thereby labeling PVT cells that directly project to the oval BNST.

Chapter 6

References

Bibliography

Ago, Y., Tanaka, T., Ota, Y., Kitamoto, M., Imoto, E., Takuma, K., and Matsuda, T. (2014). Social crowding in the night-time reduces an anxiety-like behavior and increases social interaction in adolescent mice. Behav. Brain Res. *270*, 37–46.

American Psychiatric Association (2013). Diagnostic and Statistical Manual of Mental Disorders.

Asok, A., Schulkin, J., and Rosen, J.B. (2016). Corticotropin releasing factor type-1 receptor antagonism in the dorsolateral bed nucleus of the stria terminalis disrupts contextually conditioned fear, but not unconditioned fear to a predator odor. Psychoneuroendocrinology *70*, 17–24.

Avery, S.N., Clauss, J.A., and Blackford, J.U. (2016). The human BNST: functional role in anxiety and addiction. Neuropsychopharmacology *41*, 126–141.

Backström, T., and Winberg, S. (2013). Central corticotropin releasing factor and social stress. Front. Neurosci. *7*, 117.

Bagosi, Z., Karasz, G., Czébely-Lénárt, A., Csabafi, K., Jászberényi, M., and Telegdy, G. (2017). The effects of CRF and urocortins on the sociability of mice. Brain Res. *1663*, 114–122.

Barthas, F., Hu, M.Y., Siniscalchi, M.J., Ali, F., Mineur, Y.S., Picciotto, M.R., and Kwan, A.C. (2020). Cumulative Effects of Social Stress on Reward-Guided Actions and Prefrontal Cortical Activity. Biol. Psychiatry *88*, 541–553.

Behan, D.P., De Souza, E.B., Lowry, P.J., Potter, E., Sawchenko, P., and Vale, W.W. (1995). Corticotropin releasing factor (CRF) binding protein: a novel regulator of CRF and related peptides. Front. Neuroendocrinol. *16*, 362–382.

Belmaker, R.H., and Agam, G. (2008). Major depressive disorder. N. Engl. J. Med. *358*, 55–68.

Berton, O., McClung, C.A., Dileone, R.J., Krishnan, V., Renthal, W., Russo, S.J., Graham, D., Tsankova, N.M., Bolanos, C.A., Rios, M., et al. (2006). Essential role of BDNF in the mesolimbic dopamine pathway in social defeat stress. Science *311*, 864–868.

Bougarel, L., Guitton, J., Zimmer, L., Vaugeois, J.-M., and El Yacoubi, M. (2011). Behaviour of a genetic mouse model of depression in the learned helplessness paradigm. Psychopharmacology (Berl) *215*, 595–605.

Bowerman, M. (2020). Recent advances and future perspectives in the development of therapeutic approaches for neurodegenerative diseases. Brain Sci. *10*.

Broccoli, L., Uhrig, S., von Jonquieres, G., Schönig, K., Bartsch, D., Justice, N.J., Spanagel, R., Sommer, W.H., Klugmann, M., and Hansson, A.C. (2018). Targeted overexpression of CRH receptor subtype 1 in central amygdala neurons: effect on alcohol-seeking behavior. Psychopharmacology (Berl) *235*, 1821–1833.

Caillé, S., Guillem, K., Cador, M., Manzoni, O., and Georges, F. (2009). Voluntary nicotine consumption triggers in vivo potentiation of cortical excitatory drives to midbrain dopaminergic neurons. J. Neurosci. *29*, 10410–10415.

Cao, J.-L., Covington, H.E., Friedman, A.K., Wilkinson, M.B., Walsh, J.J., Cooper, D.C., Nestler, E.J., and Han, M.-H. (2010). Mesolimbic dopamine neurons in the brain reward circuit mediate susceptibility to social defeat and antidepressant action. J. Neurosci. *30*, 16453–16458.

Carullo, N.V.N., Hinds, J.E., Revanna, J.S., Tuscher, J.J., Bauman, A.J., and Day, J.J. (2021). A Cre-Dependent CRISPR/dCas9 System for Gene Expression Regulation in Neurons. ENeuro *8*.

Cassimjee, N., van Coller, R., Slabbert, P., Fletcher, L., and Vaidyanathan, J. (2018). Longitudinal neuropsychological outcomes in treatment-resistant depression following bed nucleus of the stria terminalis-area deep brain stimulation: a case review. Neurocase *24*, 231–237.

Cathomas, F., Murrough, J.W., Nestler, E.J., Han, M.-H., and Russo, S.J. (2019). Neurobiology of resilience: interface between mind and body. Biol. Psychiatry *86*, 410–420.

Challis, C., Boulden, J., Veerakumar, A., Espallergues, J., Vassoler, F.M., Pierce, R.C., Beck, S.G., and Berton, O. (2013). Raphe GABAergic neurons mediate the acquisition of avoidance after social defeat. J. Neurosci. *33*, 13978–13988, 13988a.

Challis, C., Beck, S.G., and Berton, O. (2014). Optogenetic modulation of descending prefrontocortical inputs to the dorsal raphe bidirectionally bias socioaffective choices after social defeat. Front. Behav. Neurosci. *8*, 43.

Chaudhury, D., Walsh, J.J., Friedman, A.K., Juarez, B., Ku, S.M., Koo, J.W., Ferguson, D., Tsai, H.-C., Pomeranz, L., Christoffel, D.J., et al. (2013). Rapid regulation of depression-related behaviours by control of midbrain dopamine neurons. Nature *493*, 532–536.

Chen, A.-X., Yan, J.-J., Zhang, W., Wang, L., Yu, Z.-X., Ding, X.-J., Wang, D.-Y., Zhang, M., Zhang, Y.-L., Song, N., et al. (2020a). Specific Hypothalamic Neurons Required for Sensing Conspecific Male Cues Relevant to Inter-male Aggression. Neuron *108*, 763-774.e6.

Chen, D., Wu, J., Yao, Z., Lei, K., Luo, Y., and Li, Z. (2018). Negative association between resilience and event-related potentials evoked by negative emotion. Sci. Rep. *8*, 7149.

Chen, P., Lou, S., Huang, Z.-H., Wang, Z., Shan, Q.-H., Wang, Y., Yang, Y., Li, X., Gong, H., Jin, Y., et al. (2020b). Prefrontal Cortex Corticotropin-Releasing Factor Neurons Control Behavioral Style Selection under Challenging Situations. Neuron *106*, 301-315.e7.

Chen, Y., Molet, J., Gunn, B.G., Ressler, K., and Baram, T.Z. (2015). Diversity of Reporter Expression Patterns in Transgenic Mouse Lines Targeting Corticotropin-Releasing Hormone-Expressing Neurons. Endocrinology *156*, 4769–4780.

Clauss, J.A., Avery, S.N., Benningfield, M.M., and Blackford, J.U. (2019). Social anxiety is associated with BNST response to unpredictability. Depress. Anxiety *36*, 666–675.

Cooper, M.A., and Huhman, K.L. (2007). Corticotropin-releasing factor receptors in the dorsal raphe nucleus modulate social behavior in Syrian hamsters. Psychopharmacology (Berl) *194*, 297–307.

Cooper, M.A., and Huhman, K.L. (2010). Blocking corticotropin-releasing factor-2 receptors, but not corticotropin-releasing factor-1 receptors or glucocorticoid feedback, disrupts the development of conditioned defeat. Physiol. Behav. *101*, 527–532.

Costi, S., Han, M.-H., and Murrough, J.W. (2022). The potential of KCNQ potassium channel openers as novel antidepressants. CNS Drugs.

Cramer, A.O.J., van Borkulo, C.D., Giltay, E.J., van der Maas, H.L.J., Kendler, K.S., Scheffer, M., and Borsboom, D. (2016). Major depression as a complex dynamic system. PLoS ONE *11*, e0167490.

Crestani, C.C., Alves, F.H.F., Correa, F.M.A., Guimarães, F.S., and Joca, S.R.L. (2010). Acute reversible inactivation of the bed nucleus of stria terminalis induces antidepressant-like effect in the rat forced swimming test. Behav. Brain Funct. *6*, 30.

Cummings, S., Elde, R., Ells, J., and Lindall, A. (1983). Corticotropin-releasing factor immunoreactivity is widely distributed within the central nervous system of the rat: an immunohistochemical study. J. Neurosci. *3*, 1355–1368.

Dabrowska, J., Hazra, R., Guo, J.-D., Dewitt, S., and Rainnie, D.G. (2013a). Central CRF neurons are not created equal: phenotypic differences in CRF-containing neurons of the rat paraventricular hypothalamus and the bed nucleus of the stria terminalis. Front. Neurosci. *7*, 156.

Dabrowska, J., Hazra, R., Guo, J.-D., Li, C., Dewitt, S., Xu, J., Lombroso, P.J., and Rainnie, D.G. (2013b). Striatal-enriched protein tyrosine phosphatase-STEPs toward understanding chronic stress-induced activation of corticotrophin releasing factor neurons in the rat bed nucleus of the stria terminalis. Biol. Psychiatry *74*, 817–826.

Dabrowska, J., Martinon, D., Moaddab, M., and Rainnie, D.G. (2016). Targeting Corticotropin-Releasing Factor Projections from the Oval Nucleus of the Bed Nucleus of the Stria Terminalis Using Cell-Type Specific Neuronal Tracing Studies in Mouse and Rat Brain. J. Neuroendocrinol. *28*.

Daniel, S.E., and Rainnie, D.G. (2016). Stress modulation of opposing circuits in the bed nucleus of the stria terminalis. Neuropsychopharmacology *41*, 103–125.

Daniel, S.E., Menigoz, A., Guo, J., Ryan, S.J., Seth, S., and Rainnie, D.G. (2019). Chronic stress induces cell type-selective transcriptomic and electrophysiological changes in the bed nucleus of the stria terminalis. Neuropharmacology *150*, 80–90.

Dedic, N., Kühne, C., Jakovcevski, M., Hartmann, J., Genewsky, A.J., Gomes, K.S., Anderzhanova, E., Pöhlmann, M.L., Chang, S., Kolarz, A., et al. (2018). Chronic CRH depletion from GABAergic, long-range projection neurons in the extended amygdala reduces dopamine release and increases anxiety. Nat. Neurosci. *21*, 803–807.

Dedic, N., Kühne, C., Gomes, K.S., Hartmann, J., Ressler, K.J., Schmidt, M.V., and Deussing, J.M. (2019). Deletion of CRH From GABAergic Forebrain Neurons Promotes Stress Resilience and Dampens Stress-Induced Changes in Neuronal Activity. Front. Neurosci. *13*, 986.

Dias-Ferreira, E., Sousa, J.C., Melo, I., Morgado, P., Mesquita, A.R., Cerqueira, J.J., Costa, R.M., and Sousa, N. (2009). Chronic stress causes frontostriatal reorganization and affects decision-making. Science *325*, 621–625.

Dong, H.W., Petrovich, G.D., Watts, A.G., and Swanson, L.W. (2001). Basic organization of projections from the oval and fusiform nuclei of the bed nuclei of the stria terminalis in adult rat brain. J. Comp. Neurol. *436*, 430–455.

Dos Santos Claro, P.A., Inda, C., Armando, N.G., Piazza, V.G., Attorresi, A., and Silberstein, S. (2019). Assessing real-time signaling and agonist-induced CRHR1 internalization by optical methods. Methods Cell Biol. *149*, 239–257.

Drysdale, A.T., Grosenick, L., Downar, J., Dunlop, K., Mansouri, F., Meng, Y., Fetcho, R.N., Zebley, B., Oathes, D.J., Etkin, A., et al. (2017). Resting-state connectivity biomarkers define neurophysiological subtypes of depression. Nat. Med. *23*, 28–38.

Duque-Wilckens, N., Torres, L.Y., Yokoyama, S., Minie, V.A., Tran, A.M., Petkova, S.P., Hao, R., Ramos-Maciel, S., Rios, R.A., Jackson, K., et al. (2020). Extrahypothalamic oxytocin neurons drive stress-induced social vigilance and avoidance. Proc Natl Acad Sci USA *117*, 26406–26413.

Duvarci, S., Bauer, E.P., and Paré, D. (2009). The bed nucleus of the stria terminalis mediates inter-individual variations in anxiety and fear. J. Neurosci. *29*, 10357–10361.

Eggart, M., Lange, A., Binser, M.J., Queri, S., and Müller-Oerlinghausen, B. (2019). Major Depressive Disorder Is Associated with Impaired Interoceptive Accuracy: A Systematic Review. Brain Sci. *9*.

Elliott, E., Ezra-Nevo, G., Regev, L., Neufeld-Cohen, A., and Chen, A. (2010). Resilience to social stress coincides with functional DNA methylation of the Crf gene in adult mice. Nat. Neurosci. *13*, 1351–1353.

Engelhardt, C., Tang, F., Elkhateib, R., Bordes, J., Brix, L.M., van Doeselaar, L., Häusl, A.S., Pöhlmann, M.L., Schraut, K., Yang, H., et al. (2021). FKBP51 in the Oval Bed Nucleus of the Stria Terminalis Regulates Anxiety-Like Behavior. ENeuro *8*.

Feder, A., Nestler, E.J., and Charney, D.S. (2009). Psychobiology and molecular genetics of resilience. Nat. Rev. Neurosci. *10*, 446–457.

Fendt, M., Endres, T., and Apfelbach, R. (2003). Temporary inactivation of the bed nucleus of the stria terminalis but not of the amygdala blocks freezing induced by trimethylthiazoline, a component of fox feces. J. Neurosci. *23*, 23–28.

Fiedler, D., Sasi, M., Blum, R., Klinke, C.M., Andreatta, M., Pape, H.-C., and Lange, M.D. (2021). Brain-Derived Neurotrophic Factor/Tropomyosin Receptor Kinase B Signaling Controls Excitability and Long-Term Depression in Oval Nucleus of the BNST. J. Neurosci. *41*, 435–445.

Fitzgerald, P.B., Segrave, R., Richardson, K.E., Knox, L.A., Herring, S., Daskalakis, Z.J., and Bittar, R.G. (2018). A pilot study of bed nucleus of the stria terminalis deep brain stimulation in treatment-resistant depression. Brain Stimulat. *11*, 921–928.

Flanigan, M.E., and Kash, T.L. (2020). Coordination of social behaviors by the bed nucleus of the stria terminalis. Eur. J. Neurosci.

Franklin, T.B., Saab, B.J., and Mansuy, I.M. (2012). Neural mechanisms of stress resilience and vulnerability. Neuron *75*, 747–761.

Friedman, A.K., Walsh, J.J., Juarez, B., Ku, S.M., Chaudhury, D., Wang, J., Li, X., Dietz, D.M., Pan, N., Vialou, V.F., et al. (2014). Enhancing depression mechanisms in midbrain dopamine neurons achieves homeostatic resilience. Science *344*, 313–319.

Friedman, A.K., Juarez, B., Ku, S.M., Zhang, H., Calizo, R.C., Walsh, J.J., Chaudhury, D., Zhang, S., Hawkins, A., Dietz, D.M., et al. (2016). KCNQ channel openers reverse depressive symptoms via an active resilience mechanism. Nat. Commun. *7*, 11671.

Gafford, G.M., Guo, J.-D., Flandreau, E.I., Hazra, R., Rainnie, D.G., and Ressler, K.J. (2012). Cell-type specific deletion of GABA(A)α1 in corticotropin-releasing factor-containing neurons enhances anxiety and disrupts fear extinction. Proc Natl Acad Sci USA *109*, 16330–16335.

Galvão, A.C. de M., Almeida, R.N., de Sousa Júnior, G.M., Leocadio-Miguel, M.A., Palhano-Fontes, F., de Araujo, D.B., Lobão-Soares, B., Maia-de-Oliveira, J.P., Nunes, E.A., Hallak, J.E.C., et al. (2021). Potential biomarkers of major depression diagnosis and chronicity. PLoS ONE *16*, e0257251.

Garcia-Garcia, A.L., Canetta, S., Stujenske, J.M., Burghardt, N.S., Ansorge, M.S., Dranovsky, A., and Leonardo, E.D. (2018). Serotonin inputs to the dorsal BNST modulate anxiety in a 5-HT1A receptor-dependent manner. Mol. Psychiatry *23*, 1990–1997.

Giardino, W.J., Eban-Rothschild, A., Christoffel, D.J., Li, S.-B., Malenka, R.C., and de Lecea, L. (2018). Parallel circuits from the bed nuclei of stria terminalis to the lateral hypothalamus drive opposing emotional states. Nat. Neurosci. *21*, 1084–1095.

Glangetas, C., Massi, L., Fois, G.R., Jalabert, M., Girard, D., Diana, M., Yonehara, K., Roska, B., Xu, C., Lüthi, A., et al. (2017). NMDA-receptor-dependent plasticity in the bed nucleus of the stria terminalis triggers long-term anxiolysis. Nat. Commun. *8*, 14456.

Golden, S.A., Covington, H.E., Berton, O., and Russo, S.J. (2011). A standardized protocol for repeated social defeat stress in mice. Nat. Protoc. *6*, 1183–1191.

Gold, P.W. (2013). Evidence that stress per se has a role in the precipitation and natural history of depressive illness. Mol. Psychiatry *18*, 954–956.

Gold, P.W., and Chrousos, G.P. (2002). Organization of the stress system and its dysregulation in melancholic and atypical depression: high vs low CRH/NE states. Mol. Psychiatry *7*, 254–275.

Goode, T.D., and Maren, S. (2017). Role of the bed nucleus of the stria terminalis in aversive learning and memory. Learn. Mem. *24*, 480–491.

Gungor, N.Z., and Paré, D. (2016). Functional heterogeneity in the bed nucleus of the stria terminalis. J. Neurosci. *36*, 8038–8049.

Gururajan, A., Bastiaanssen, T.F.S., Ventura Silva, A.P., Moloney, G.M., and Cryan, J.F. (2021). The impact of psychosocial defeat stress on the BNST transcriptome in adult male mice. Eur. J. Neurosci.

Hammen, C. (2005). Stress and depression. Annu. Rev. Clin. Psychol. *1*, 293–319.

Han, M.-H., and Nestler, E.J. (2017). Neural substrates of depression and resilience. Neurotherapeutics *14*, 677–686.

Harshaw, C. (2015). Interoceptive dysfunction: toward an integrated framework for understanding somatic and affective disturbance in depression. Psychol. Bull. *141*, 311–363.

Hartley, N.D., Gaulden, A.D., Báldi, R., Winters, N.D., Salimando, G.J., Rosas-Vidal, L.E., Jameson, A., Winder, D.G., and Patel, S. (2019). Dynamic remodeling of a basolateral-to-central amygdala glutamatergic circuit across fear states. Nat. Neurosci. *22*, 2000–2012.

Hayes, A.M., Yasinski, C., Ben Barnes, J., and Bockting, C.L.H. (2015). Network destabilization and transition in depression: New methods for studying the dynamics of therapeutic change. Clin. Psychol. Rev. *41*, 27–39.

Heinrichs, S.C., Menzaghi, F., Merlo Pich, E., Britton, K.T., and Koob, G.F. (1995). The role of CRF in behavioral aspects of stress. Ann. N. Y. Acad. Sci. *771*, 92–104.

Heo, M., Murphy, C.F., Fontaine, K.R., Bruce, M.L., and Alexopoulos, G.S. (2008). Population projection of US adults with lifetime experience of depressive disorder by age and sex from year 2005 to 2050. Int. J. Geriatr. Psychiatry *23*, 1266–1270.

Heymann, G., Jo, Y.S., Reichard, K.L., McFarland, N., Chavkin, C., Palmiter, R.D., Soden, M.E., and Zweifel, L.S. (2020). Synergy of distinct dopamine projection populations in behavioral reinforcement. Neuron *105*, 909-920.e5.

Hillhouse, E.W., and Grammatopoulos, D.K. (2006). The molecular mechanisms underlying the regulation of the biological activity of corticotropin-releasing hormone receptors: implications for physiology and pathophysiology. Endocr. Rev. *27*, 260–286.

Hollon, N.G., Burgeno, L.M., and Phillips, P.E.M. (2015). Stress effects on the neural substrates of motivated behavior. Nat. Neurosci. *18*, 1405–1412.

Hosokawa, N., and Chiba, A. (2007). Effects of sexual experience on conspecific odor preference and male odor-induced activation of the vomeronasal projection pathway and the nucleus accumbens in female rats. Brain Res. *1175*, 66–75.

Hostetler, C.M., and Ryabinin, A.E. (2013). The CRF system and social behavior: a review. Front. Neurosci. *7*, 92.

Hsu, D.T., Kirouac, G.J., Zubieta, J.-K., and Bhatnagar, S. (2014). Contributions of the paraventricular thalamic nucleus in the regulation of stress, motivation, and mood. Front. Behav. Neurosci. *8*, 73.

Hultman, R., Ulrich, K., Sachs, B.D., Blount, C., Carlson, D.E., Ndubuizu, N., Bagot, R.C., Parise, E.M., Vu, M.-A.T., Gallagher, N.M., et al. (2018). Brain-wide Electrical Spatiotemporal Dynamics Encode Depression Vulnerability. Cell *173*, 166-180.e14.

Hu, P., Liu, J., Maita, I., Kwok, C., Gu, E., Gergues, M.M., Kelada, F., Phan, M., Zhou, J.-N., Swaab, D.F., et al. (2020). Chronic Stress Induces Maladaptive Behaviors by Activating Corticotropin-Releasing Hormone Signaling in the Mouse Oval Bed Nucleus of the Stria Terminalis. J. Neurosci. *40*, 2519–2537.

Ichiyama, A., Mestern, S., Benigno, G.B., Scott, K., Allman, B.L., Muller, L., and Inoue, W. (2022). State-dependent activity dynamics of hypothalamic stress effector neurons. BioRxiv.

Imaki, T., Shibasaki, T., Hotta, M., and Demura, H. (1993). Intracerebroventricular administration of corticotropin-releasing factor induces c-fos mRNA expression in brain regions related to stress responses: comparison with pattern of c-fos mRNA induction after stress. Brain Res. *616*, 114–125.

Ismaylova, E., Di Sante, J., Szyf, M., Nemoda, Z., Yu, W.-J., Pomares, F.B., Turecki, G., Gobbi, G., Vitaro, F., Tremblay, R.E., et al. (2017). Serotonin transporter gene promoter methylation in peripheral cells in healthy adults: Neural correlates and tissue specificity. Eur. Neuropsychopharmacol. *27*, 1032–1041.

Jackson, S., Baity, M.R., Bobb, K., Swick, D., and Giorgio, J. (2019). Stress inoculation training outcomes among veterans with PTSD and TBI. Psychol. Trauma *11*, 842–850.

Jasnow, A.M., Banks, M.C., Owens, E.C., and Huhman, K.L. (1999). Differential effects of two corticotropin-releasing factor antagonists on conditioned defeat in male Syrian hamsters (Mesocricetus auratus). Brain Res. *846*, 122–128.

Jasnow, A.M., Davis, M., and Huhman, K.L. (2004). Involvement of central amygdalar and bed nucleus of the stria terminalis corticotropin-releasing factor in behavioral responses to social defeat. Behav. Neurosci. *118*, 1052–1061.

Jennings, J.H., Sparta, D.R., Stamatakis, A.M., Ung, R.L., Pleil, K.E., Kash, T.L., and Stuber, G.D. (2013). Distinct extended amygdala circuits for divergent motivational states. Nature *496*, 224–228.

Johnson, S.B., Emmons, E.B., Anderson, R.M., Glanz, R.M., Romig-Martin, S.A., Narayanan, N.S., LaLumiere, R.T., and Radley, J.J. (2016). A basal forebrain site coordinates the modulation of endocrine and behavioral stress responses via divergent neural pathways. J. Neurosci. *36*, 8687–8699.

Justice, N.J., Yuan, Z.F., Sawchenko, P.E., and Vale, W. (2008). Type 1 corticotropin-releasing factor receptor expression reported in BAC transgenic mice: implications for reconciling ligand-receptor mismatch in the central corticotropin-releasing factor system. J. Comp. Neurol. *511*, 479–496.

Kaouane, N., Ada, S., Hausleitner, M., and Haubensak, W. (2021). Dorsal Bed Nucleus of the Stria Terminalis-Subcortical Output Circuits Encode Positive Bias in Pavlovian Fear and Reward. Front. Neural Circuits *15*, 772512.

Karatsoreos, I.N., and McEwen, B.S. (2011). Psychobiological allostasis: resistance, resilience and vulnerability. Trends Cogn Sci (Regul Ed) *15*, 576–584.

Kash, T.L., Pleil, K.E., Marcinkiewcz, C.A., Lowery-Gionta, E.G., Crowley, N., Mazzone, C., Sugam, J., Hardaway, J.A., and McElligott, Z.A. (2015). Neuropeptide regulation of signaling and behavior in the BNST. Mol. Cells *38*, 1–13.

Kaul, D., Schwab, S.G., Mechawar, N., and Matosin, N. (2021). How stress physically re-shapes the brain: Impact on brain cell shapes, numbers and connections in psychiatric disorders. Neurosci. Biobehav. Rev. *124*, 193–215.

Kendler, K.S., Karkowski, L.M., and Prescott, C.A. (1999). Causal relationship between stressful life events and the onset of major depression. Am. J. Psychiatry *156*, 837–841.

Kennis, M., Gerritsen, L., van Dalen, M., Williams, A., Cuijpers, P., and Bockting, C. (2020). Prospective biomarkers of major depressive disorder: a systematic review and meta-analysis. Mol. Psychiatry *25*, 321–338.

Kim, S.-Y., Adhikari, A., Lee, S.Y., Marshel, J.H., Kim, C.K., Mallory, C.S., Lo, M., Pak, S., Mattis, J., Lim, B.K., et al. (2013). Diverging neural pathways assemble a behavioural state from separable features in anxiety. Nature *496*, 219–223.

Kirouac, G.J. (2015). Placing the paraventricular nucleus of the thalamus within the brain circuits that control behavior. Neurosci. Biobehav. Rev. *56*, 315–329.

Konishi, S., Kasagi, Y., Katsumata, H., Minami, S., and Imaki, T. (2003). Regulation of corticotropin-releasing factor (CRF) type-1 receptor gene expression by CRF in the hypothalamus. Endocr. J. *50*, 21–36.

Koob, G.F., and Zorrilla, E.P. (2012). Update on corticotropin-releasing factor pharmacotherapy for psychiatric disorders: a revisionist view. Neuropsychopharmacology *37*, 308–309.

Koo, J.W., Chaudhury, D., Han, M.-H., and Nestler, E.J. (2019). Role of Mesolimbic Brain-Derived Neurotrophic Factor in Depression. Biol. Psychiatry *86*, 738–748.

Kovalenko, I.L., and Kudryavtseva, N.N. (2015). [Alteration of Social Behaviors in Male Mice of CBA/Lac Strain under Agonistic Interactions]. Zh. Vyssh. Nerv. Deiat. Im. I P Pavlova *65*, 486–497.

Krishnan, V., and Nestler, E.J. (2011). Animal models of depression: molecular perspectives. Curr. Top. Behav. Neurosci. *7*, 121–147.

Krishnan, V., Han, M.-H., Graham, D.L., Berton, O., Renthal, W., Russo, S.J., Laplant, Q., Graham, A., Lutter, M., Lagace, D.C., et al. (2007). Molecular adaptations underlying susceptibility and resistance to social defeat in brain reward regions. Cell *131*, 391–404.

Kudryavtseva, N.N., Bakshtanovskaya, I.V., and Koryakina, L.A. (1991). Social model of depression in mice of C57BL/6J strain. Pharmacol. Biochem. Behav. *38*, 315–320.

Kumar, S., Hultman, R., Hughes, D., Michel, N., Katz, B.M., and Dzirasa, K. (2014). Prefrontal cortex reactivity underlies trait vulnerability to chronic social defeat stress. Nat. Commun. *5*, 4537.

Kundakovic, M., Lim, S., Gudsnuk, K., and Champagne, F.A. (2013). Sex-specific and strain-dependent effects of early life adversity on behavioral and epigenetic outcomes. Front. Psychiatry *4*, 78.

Ku, S.M., and Han, M.-H. (2017). HCN channel targets for novel antidepressant treatment. Neurotherapeutics *14*, 698–715.

Laine, M.A., Sokolowska, E., Dudek, M., Callan, S.-A., Hyytiä, P., and Hovatta, I. (2017). Brain activation induced by chronic psychosocial stress in mice. Sci. Rep. *7*, 15061.

Laine, M.A., Trontti, K., Misiewicz, Z., Sokolowska, E., Kulesskaya, N., Heikkinen, A., Saarnio, S., Balcells, I., Ameslon, P., Greco, D., et al. (2018). Genetic Control of Myelin Plasticity after Chronic Psychosocial Stress. ENeuro *5*.

Landgraf, D., Long, J., Der-Avakian, A., Streets, M., and Welsh, D.K. (2015). Dissociation of learned helplessness and fear conditioning in mice: a mouse model of depression. PLoS ONE *10*, e0125892.

Lebow, M.A., and Chen, A. (2016). Overshadowed by the amygdala: the bed nucleus of the stria terminalis emerges as key to psychiatric disorders. Mol. Psychiatry *21*, 450–463.

van de Leemput, I.A., Wichers, M., Cramer, A.O.J., Borsboom, D., Tuerlinckx, F., Kuppens, P., van Nes, E.H., Viechtbauer, W., Giltay, E.J., Aggen, S.H., et al. (2014). Critical slowing down as early warning for the onset and termination of depression. Proc Natl Acad Sci USA *111*, 87–92.

Lee, Y., Fitz, S., Johnson, P.L., and Shekhar, A. (2008). Repeated stimulation of CRF receptors in the BNST of rats selectively induces social but not panic-like anxiety. Neuropsychopharmacology *33*, 2586–2594.

Lemos, J.C., Wanat, M.J., Smith, J.S., Reyes, B.A.S., Hollon, N.G., Van Bockstaele, E.J., Chavkin, C., and Phillips, P.E.M. (2012). Severe stress switches CRF action in the nucleus accumbens from appetitive to aversive. Nature *490*, 402–406.

Levey, D.F., Stein, M.B., Wendt, F.R., Pathak, G.A., Zhou, H., Aslan, M., Quaden, R., Harrington, K.M., Nuñez, Y.Z., Overstreet, C., et al. (2021). Bi-ancestral depression GWAS in the Million Veteran Program and meta-analysis in >1.2 million individuals highlight new therapeutic directions. Nat. Neurosci. *24*, 954–963.

Liu, C.-H., Ma, X., Yuan, Z., Song, L.-P., Jing, B., Lu, H.-Y., Tang, L.-R., Fan, J., Walter, M., Liu, C.-Z., et al. (2017). Decreased Resting-State Activity in the Precuneus Is Associated With Depressive Episodes in Recurrent Depression. J. Clin. Psychiatry *78*, e372–e382.

Liu, P.-H., Li, Y., Zhang, A.-X., Sun, N., Li, G.-Z., Chen, X., Bai, T.-J., Bo, Q.-J., Chen, G.-M., Chen, N.-X., et al. (2021). Brain structural alterations in MDD patients with gastrointestinal symptoms: Evidence from the REST-meta-MDD project. Prog Neuropsychopharmacol Biol Psychiatry *111*, 110386.

Long, Y., Cao, H., Yan, C., Chen, X., Li, L., Castellanos, F.X., Bai, T., Bo, Q., Chen, G., Chen, N., et al. (2020). Altered resting-state dynamic functional brain networks in major depressive disorder: Findings from the REST-meta-MDD consortium. Neuroimage Clin. *26*, 102163.

Lutz, P.-E., Tanti, A., Gasecka, A., Barnett-Burns, S., Kim, J.J., Zhou, Y., Chen, G.G., Wakid, M., Shaw, M., Almeida, D., et al. (2017). Association of a history of child abuse with impaired myelination in the anterior cingulate cortex: convergent epigenetic, transcriptional, and morphological evidence. Am. J. Psychiatry *174*, 1185–1194.

Lv, H., Wang, Z., Tong, E., Williams, L.M., Zaharchuk, G., Zeineh, M., Goldstein-Piekarski, A.N., Ball, T.M., Liao, C., and Wintermark, M. (2018). Resting-State Functional MRI: Everything That Nonexperts Have Always Wanted to Know. AJNR Am J Neuroradiol *39*, 1390–1399.

Lynch, C.J., Gunning, F.M., and Liston, C. (2020). Causes and consequences of diagnostic heterogeneity in depression: paths to discovering novel biological depression subtypes. Biol. Psychiatry *88*, 83–94.

Maita, I., Bazer, A., Blackford, J.U., and Samuels, B.A. (2021). Functional anatomy of the bed nucleus of the stria terminalis-hypothalamus neural circuitry: Implications for valence surveillance, addiction, feeding, and social behaviors. Handb. Clin. Neurol. *179*, 403–418.

Mansbach, R.S., Brooks, E.N., and Chen, Y.L. (1997). Antidepressant-like effects of CP-154,526, a selective CRF1 receptor antagonist. Eur. J. Pharmacol. *323*, 21–26.

Marcinkiewcz, C.A., Mazzone, C.M., D'Agostino, G., Halladay, L.R., Hardaway, J.A., DiBerto, J.F., Navarro, M., Burnham, N., Cristiano, C., Dorrier, C.E., et al. (2016). Serotonin engages an anxiety and fear-promoting circuit in the extended amygdala. Nature *537*, 97–101.

Mariani, N., Cattane, N., Pariante, C., and Cattaneo, A. (2021). Gene expression studies in Depression development and treatment: an overview of the underlying molecular mechanisms and biological processes to identify biomarkers. Transl. Psychiatry *11*, 354.

Markham, C.M., Norvelle, A., and Huhman, K.L. (2009). Role of the bed nucleus of the stria terminalis in the acquisition and expression of conditioned defeat in Syrian hamsters. Behav. Brain Res. *198*, 69–73.

Martinez, M., Phillips, P.J., and Herbert, J. (1998). Adaptation in patterns of*c-fos* expression in the brain associated with exposure to either single or repeated social stress in male rats. European Journal of Neuroscience *10*, 20–33.

Matsuda, S., Peng, H., Yoshimura, H., Wen, T.C., Fukuda, T., and Sakanaka, M. (1996). Persistent c-fos expression in the brains of mice with chronic social stress. Neurosci. Res. *26*, 157–170.

Matthews, G.A., Nieh, E.H., Vander Weele, C.M., Halbert, S.A., Pradhan, R.V., Yosafat, A.S., Glober, G.F., Izadmehr, E.M., Thomas, R.E., Lacy, G.D., et al. (2016). Dorsal raphe dopamine neurons represent the experience of social isolation. Cell *164*, 617–631.

Mazzone, C.M., Pati, D., Michaelides, M., DiBerto, J., Fox, J.H., Tipton, G., Anderson, C., Duffy, K., McKlveen, J.M., Hardaway, J.A., et al. (2018). Acute engagement of Gq-mediated signaling in the bed nucleus of the stria terminalis induces anxiety-like behavior. Mol. Psychiatry *23*, 143–153.

McClard, C.K., Kochukov, M.Y., Herman, I., Liu, Z., Eblimit, A., Moayedi, Y., Ortiz-Guzman, J., Colchado, D., Pekarek, B., Panneerselvam, S., et al. (2018). POU6f1 Mediates Neuropeptide-Dependent Plasticity in the Adult Brain. J. Neurosci. *38*, 1443–1461.

McEwen, B.S. (2004). Protection and damage from acute and chronic stress: allostasis and allostatic overload and relevance to the pathophysiology of psychiatric disorders. Ann. N. Y. Acad. Sci. *1032*, 1–7.

Nestler, E.J., and Carlezon, W.A. (2006). The mesolimbic dopamine reward circuit in depression. Biol. Psychiatry *59*, 1151–1159.

Nestler, E.J., Peña, C.J., Kundakovic, M., Mitchell, A., and Akbarian, S. (2016). Epigenetic basis of mental illness. Neuroscientist *22*, 447–463.

Neumann, W.J., Huebl, J., Brücke, C., Gabriëls, L., Bajbouj, M., Merkl, A., Schneider, G.H., Nuttin, B., Brown, P., and Kühn, A.A. (2014). Different patterns of local field potentials from limbic DBS targets in patients with major depressive and obsessive compulsive disorder. Mol. Psychiatry *19*, 1186–1192.

Osório, C., Probert, T., Jones, E., Young, A.H., and Robbins, I. (2017). Adapting to stress: understanding the neurobiology of resilience. Behav. Med. *43*, 307–322.

Partridge, J.G., Forcelli, P.A., Luo, R., Cashdan, J.M., Schulkin, J., Valentino, R.J., and Vicini, S. (2016). Stress increases GABAergic neurotransmission in CRF neurons of the central amygdala and bed nucleus stria terminalis. Neuropharmacology *107*, 239–250.

Paulus, M.P., and Stein, M.B. (2010). Interoception in anxiety and depression. Brain Struct. Funct. *214*, 451–463.

Post, R.M. (1992a). Transduction of psychosocial stress into the neurobiology of recurrent affective disorder. Am. J. Psychiatry *149*, 999–1010.

Post, R.M. (1992b). Transduction of psychosocial stress into the neurobiology of recurrent affective disorder. Am. J. Psychiatry *149*, 999–1010.

Ramot, A., Jiang, Z., Tian, J.-B., Nahum, T., Kuperman, Y., Justice, N., and Chen, A. (2017). Hypothalamic CRFR1 is essential for HPA axis regulation following chronic stress. Nat. Neurosci. *20*, 385–388.

Razza, L.B., De Smet, S., Moffa, A., Sudbrack-Oliveira, P., Vanderhasselt, M.-A., and Brunoni, A.R. (2021). Follow-up effects of transcranial direct current stimulation (tDCS) for the major depressive episode: A systematic review and meta-analysis. Psychiatry Res. *302*, 114024.

Regev, L., Neufeld-Cohen, A., Tsoory, M., Kuperman, Y., Getselter, D., Gil, S., and Chen, A. (2011). Prolonged and site-specific over-expression of corticotropin-releasing factor reveals differential roles for extended amygdala nuclei in emotional regulation. Mol. Psychiatry *16*, 714–728.

Ren, C., Li, H., Liu, Y., Li, S., and Liang, Z. (2022). Highly efficient activation of endogenous gene in grape using CRISPR/dCas9-based transcriptional activators. Hortic. Res.

Reul, J. (2002). Corticotropin-releasing factor receptors 1 and 2 in anxiety and depression. Curr. Opin. Pharmacol. *2*, 23–33.

Riga, D., Schmitz, L.J.M., Hoogendijk, W.J.G., Smit, A.B., and Spijker, S. (2017). Temporal profiling of depression vulnerability in a preclinical model of sustained depression. Sci. Rep. *7*, 8570.

Riva-Posse, P., Choi, K.S., Holtzheimer, P.E., McIntyre, C.C., Gross, R.E., Chaturvedi, A., Crowell, A.L., Garlow, S.J., Rajendra, J.K., and Mayberg, H.S. (2014). Defining critical white matter pathways mediating successful subcallosal cingulate deep brain stimulation for treatment-resistant depression. Biol. Psychiatry *76*, 963–969.

Rodaros, D., Caruana, D.A., Amir, S., and Stewart, J. (2007). Corticotropin-releasing factor projections from limbic forebrain and paraventricular nucleus of the hypothalamus to the region of the ventral tegmental area. Neuroscience *150*, 8–13.

Rodríguez-Sierra, O.E., Turesson, H.K., and Pare, D. (2013). Contrasting distribution of physiological cell types in different regions of the bed nucleus of the stria terminalis. J. Neurophysiol. *110*, 2037–2049.

Rodríguez-Sierra, O.E., Goswami, S., Turesson, H.K., and Pare, D. (2016). Altered responsiveness of BNST and amygdala neurons in trauma-induced anxiety. Transl. Psychiatry *6*, e857.

Roeckner, A.R., Oliver, K.I., Lebois, L.A.M., van Rooij, S.J.H., and Stevens, J.S. (2021). Neural contributors to trauma resilience: a review of longitudinal neuroimaging studies. Transl. Psychiatry *11*, 508.

Ruiz, N.A.L., Del Ángel, D.S., Olguín, H.J., and Silva, M.L. (2018). Neuroprogression: the hidden mechanism of depression. Neuropsychiatr. Dis. Treat. *14*, 2837–2845.

Russo, S.J., Murrough, J.W., Han, M.-H., Charney, D.S., and Nestler, E.J. (2012). Neurobiology of resilience. Nat. Neurosci. *15*, 1475–1484.

Salimando, G.J., Hyun, M., Boyt, K.M., and Winder, D.G. (2020). BNST GluN2D-Containing NMDA Receptors Influence Anxiety- and Depressive-like Behaviors and ModulateCell-Specific Excitatory/Inhibitory Synaptic Balance. J. Neurosci. *40*, 3949–3968.

Samuels, B.A., Leonardo, E.D., Gadient, R., Williams, A., Zhou, J., David, D.J., Gardier, A.M., Wong, E.H.F., and Hen, R. (2011). Modeling treatment-resistant depression. Neuropharmacology *61*, 408–413.

Sanford, C.A., Soden, M.E., Baird, M.A., Miller, S.M., Schulkin, J., Palmiter, R.D., Clark, M., and Zweifel, L.S. (2017). A Central Amygdala CRF Circuit Facilitates Learning about Weak Threats. Neuron *93*, 164–178.

Schalbetter, S.M., Mueller, F.S., Scarborough, J., Richetto, J., Weber-Stadlbauer, U., Meyer, U., and Notter, T. (2021). Oral application of clozapine-N-oxide using the micropipette-guided drug administration (MDA) method in mouse DREADD systems. Lab Anim (NY) *50*, 69–75.

Schmaal, L., Pozzi, E., C Ho, T., van Velzen, L.S., Veer, I.M., Opel, N., Van Someren, E.J.W., Han, L.K.M., Aftanas, L., Aleman, A., et al. (2020). ENIGMA MDD: seven years of global neuroimaging studies of major depression through worldwide data sharing. Transl. Psychiatry *10*, 172.

Sendi, M.S.E., Waters, A.C., Tiruvadi, V., Riva-Posse, P., Crowell, A., Isbaine, F., Gale, J.T., Choi, K.S., Gross, R.E., S Mayberg, H., et al. (2021). Intraoperative neural signals predict rapid antidepressant effects of deep brain stimulation. Transl. Psychiatry *11*, 551.

Serra-Blasco, M., de Diego-Adeliño, J., Vives-Gilabert, Y., Trujols, J., Puigdemont, D., Carceller-Sindreu, M., Pérez, V., Álvarez, E., and Portella, M.J. (2016). Naturalistic course of major depressive disorder predicted by clinical and structural neuroimaging data: a 5-year follow-up. Depress. Anxiety *33*, 1055–1064.

Shelton, R.C. (1999). Treatment options for refractory depression. J. Clin. Psychiatry *60 Suppl 4*, 57–61; discussion 62.

Silberman, Y., Matthews, R.T., and Winder, D.G. (2013). A corticotropin releasing factor pathway for ethanol regulation of the ventral tegmental area in the bed nucleus of the stria terminalis. J. Neurosci. *33*, 950–960.

Singh, J.B., Fedgchin, M., Daly, E.J., and Drevets, W.C. (2020). Relapse prevention in treatment-resistant major depressive disorder with rapid-acting antidepressants. Adv. Pharmacol. *89*, 237–259.

Sink, K.S., Walker, D.L., Freeman, S.M., Flandreau, E.I., Ressler, K.J., and Davis, M. (2013). Effects of continuously enhanced corticotropin releasing factor expression within the bed

nucleus of the stria terminalis on conditioned and unconditioned anxiety. Mol. Psychiatry *18*, 308–319.

Solomon, D.A., Keller, M.B., Leon, A.C., Mueller, T.I., Lavori, P.W., Shea, M.T., Coryell, W., Warshaw, M., Turvey, C., Maser, J.D., et al. (2000). Multiple recurrences of major depressive disorder. Am. J. Psychiatry *157*, 229–233.

Sousa, N. (2016). The dynamics of the stress neuromatrix. Mol. Psychiatry *21*, 302–312.

Spierling, S.R., and Zorrilla, E.P. (2017). Don't stress about CRF: assessing the translational failures of CRF1antagonists. Psychopharmacology (Berl) *234*, 1467–1481.

Stahl, S.M. (1998). Basic psychopharmacology of antidepressants, part 1: Antidepressants have seven distinct mechanisms of action. J. Clin. Psychiatry *59 Suppl 4*, 5–14.

Sterling, P. (2012). Allostasis: a model of predictive regulation. Physiol. Behav. *106*, 5–15.

Stout, S.C., Mortas, P., Owens, M.J., Nemeroff, C.B., and Moreau, J. (2000). Increased corticotropin-releasing factor concentrations in the bed nucleus of the stria terminalis of anhedonic rats. Eur. J. Pharmacol. *401*, 39–46.

Strauman, T.J. (2021). Modeling the onset of a depressive episode: A self-regulation perspective. Curr. Opin. Psychol. *41*, 100–106.

Swanson, L.W., Sawchenko, P.E., Rivier, J., and Vale, W.W. (1983). Organization of ovine corticotropin-releasing factor immunoreactive cells and fibers in the rat brain: an immunohistochemical study. Neuroendocrinology *36*, 165–186.

Tahmasian, M., Knight, D.C., Manoliu, A., Schwerthöffer, D., Scherr, M., Meng, C., Shao, J., Peters, H., Doll, A., Khazaie, H., et al. (2013). Aberrant intrinsic connectivity of hippocampus and amygdala overlap in the fronto-insular and dorsomedial-prefrontal cortex in major depressive disorder. Front. Hum. Neurosci. *7*, 639.

Takahashi, D., Asaoka, Y., Kimura, K., Hara, R., Arakaki, S., Sakasai, K., Suzuki, H., Yamauchi, N., Nomura, H., Amano, T., et al. (2019). Tonic Suppression of the Mesolimbic Dopaminergic System by Enhanced Corticotropin-Releasing Factor Signaling Within the Bed Nucleus of the Stria Terminalis in Chronic Pain Model Rats. J. Neurosci. *39*, 8376–8385.

Tan, A., Costi, S., Morris, L.S., Van Dam, N.T., Kautz, M., Whitton, A.E., Friedman, A.K., Collins, K.A., Ahle, G., Chadha, N., et al. (2020). Effects of the KCNQ channel opener ezogabine on functional connectivity of the ventral striatum and clinical symptoms in patients with major depressive disorder. Mol. Psychiatry *25*, 1323–1333.

Thase, M.E. (2019). Current and emerging treatments to address unmet needs in MDD. J. Clin. Psychiatry *80*.

Thurmond, J.B. (1975). Technique for producing and measuring territorial aggression using laboratory mice. Physiol. Behav. *14*, 879–881.

Tinaz, S., Kamel, S., Aravala, S.S., Sezgin, M., Elfil, M., and Sinha, R. (2021). Distinct neural circuits are associated with subclinical neuropsychiatric symptoms in Parkinson's disease. J. Neurol. Sci. *423*, 117365.

Toth, M. (2019). The other side of the coin: Hypersociability. Genes Brain Behav. *18*, e12512.

Tran, L., Schulkin, J., and Greenwood-Van Meerveld, B. (2014). Importance of CRF receptor-mediated mechanisms of the bed nucleus of the stria terminalis in the processing of anxiety and pain. Neuropsychopharmacology *39*, 2633–2645.

Treadway, M.T., Grant, M.M., Ding, Z., Hollon, S.D., Gore, J.C., and Shelton, R.C. (2009). Early adverse events, HPA activity and rostral anterior cingulate volume in MDD. PLoS ONE *4*, e4887.

Turnbull, A.V., and Rivier, C. (1997). Corticotropin-Releasing Factor (CRF) and Endocrine Responses to Stress: CRF Receptors, Binding Protein, and Related Peptides. Exp. Biol. Med. *215*, 1–10.

Tu, Z., Jia, Y.Y., Wang, T., Qu, H., Pan, J.X., Jie, J., Xu, X.Y., Wang, H.Y., and Xie, P. (2018). Modulatory interactions of resting-state brain functional connectivity in major depressive disorder. Neuropsychiatr. Dis. Treat. *14*, 2461–2472.

Vasconcelos, M., Stein, D.J., Albrechet-Souza, L., Miczek, K.A., and de Almeida, R.M.M. (2019). Recovery of stress-impaired social behavior by an antagonist of the CRF binding protein, CRF6-33, in the bed nucleus of the stria terminalis of male rats. Behav. Brain Res. *357–358*, 104–110.

Veer, I.M., Riepenhausen, A., Zerban, M., Wackerhagen, C., Puhlmann, L.M.C., Engen, H., Köber, G., Bögemann, S.A., Weermeijer, J., Uściłko, A., et al. (2021). Psycho-social factors associated with mental resilience in the Corona lockdown. Transl. Psychiatry *11*, 67.

Ventura-Silva, A.P., Pêgo, J.M., Sousa, J.C., Marques, A.R., Rodrigues, A.J., Marques, F., Cerqueira, J.J., Almeida, O.F.X., and Sousa, N. (2012). Stress shifts the response of the bed nucleus of the stria terminalis to an anxiogenic mode. Eur. J. Neurosci. *36*, 3396–3406.

Vertes, R.P., Hoover, W.B., and Rodriguez, J.J. (2012). Projections of the central medial nucleus of the thalamus in the rat: node in cortical, striatal and limbic forebrain circuitry. Neuroscience *219*, 120–136.

Villegas Kcam, M.C., Tsong, A.J., and Chappell, J. (2022). Uncovering the Distinct Properties of a Bacterial Type I-E CRISPR Activation System. ACS Synth. Biol. *11*, 1000–1003.

Vom Berg-Maurer, C.M., Trivedi, C.A., Bollmann, J.H., De Marco, R.J., and Ryu, S. (2016). The severity of acute stress is represented by increased synchronous activity and recruitment of hypothalamic CRH neurons. J. Neurosci. *36*, 3350–3362.

Waddell, J., Morris, R.W., and Bouton, M.E. (2006). Effects of bed nucleus of the stria terminalis lesions on conditioned anxiety: aversive conditioning with long-duration conditional stimuli and reinstatement of extinguished fear. Behav. Neurosci. *120*, 324–336.

Walker, D.L., Toufexis, D.J., and Davis, M. (2003). Role of the bed nucleus of the stria terminalis versus the amygdala in fear, stress, and anxiety. Eur. J. Pharmacol. *463*, 199–216.

Walker, D.L., Miles, L.A., and Davis, M. (2009). Selective participation of the bed nucleus of the stria terminalis and CRF in sustained anxiety-like versus phasic fear-like responses. Prog Neuropsychopharmacol Biol Psychiatry *33*, 1291–1308.

Walsh, J.J., Friedman, A.K., Sun, H., Heller, E.A., Ku, S.M., Juarez, B., Burnham, V.L., Mazei-Robison, M.S., Ferguson, D., Golden, S.A., et al. (2014). Stress and CRF gate neural activation of BDNF in the mesolimbic reward pathway. Nat. Neurosci. *17*, 27–29.

Wanat, M.J., Bonci, A., and Phillips, P.E.M. (2013). CRF acts in the midbrain to attenuate accumbens dopamine release to rewards but not their predictors. Nat. Neurosci. *16*, 383–385.

Wang, Q., Timberlake, M.A., Prall, K., and Dwivedi, Y. (2017). The recent progress in animal models of depression. Prog Neuropsychopharmacol Biol Psychiatry *77*, 99–109.

Wang, Y., Hu, P., Shan, Q., Huang, C., Huang, Z., Chen, P., Li, A., Gong, H., and Zhou, J.-N. (2021). Single-cell morphological characterization of CRH neurons throughout the whole mouse brain. BMC Biol. *19*, 47.

Waraczynski, M. (2016). Toward a systems-oriented approach to the role of the extended amygdala in adaptive responding. Neurosci. Biobehav. Rev. *68*, 177–194.

Waters, R.P., Rivalan, M., Bangasser, D.A., Deussing, J.M., Ising, M., Wood, S.K., Holsboer, F., and Summers, C.H. (2015). Evidence for the role of corticotropin-releasing factor in major depressive disorder. Neurosci. Biobehav. Rev. *58*, 63–78.

Wess, J., Nakajima, K., and Jain, S. (2013). Novel designer receptors to probe GPCR signaling and physiology. Trends Pharmacol. Sci. *34*, 385–392.

Woodham, R., Rimmer, R.M., Mutz, J., and Fu, C.H.Y. (2021). Is tDCS a potential first line treatment for major depression? Int. Rev. Psychiatry *33*, 250–265.

Wood, S.K., Walker, H.E., Valentino, R.J., and Bhatnagar, S. (2010). Individual differences in reactivity to social stress predict susceptibility and resilience to a depressive phenotype: role of corticotropin-releasing factor. Endocrinology *151*, 1795–1805.

Wook Koo, J., Labonté, B., Engmann, O., Calipari, E.S., Juarez, B., Lorsch, Z., Walsh, J.J., Friedman, A.K., Yorgason, J.T., Han, M.-H., et al. (2016). Essential Role of Mesolimbic Brain-Derived Neurotrophic Factor in Chronic Social Stress-Induced Depressive Behaviors. Biol. Psychiatry *80*, 469–478.

Wu, H., Sun, H., Xu, J., Wu, Y., Wang, C., Xiao, J., She, S., Huang, J., Zou, W., Peng, H., et al. (2016). Changed hub and corresponding functional connectivity of subgenual anterior cingulate cortex in major depressive disorder. Front. Neuroanat. *10*, 120.

Yao, L., Li, Y., Qian, Z., Wu, M., Yang, H., Chen, N., Qiao, Y., Wei, C., Zheng, Q., Han, J., et al. (2019). Loss of control over mild aversive events produces significant helplessness in mice. Behav. Brain Res. *376*, 112173.

Yu, T., Guo, M., Garza, J., Rendon, S., Sun, X.-L., Zhang, W., and Lu, X.-Y. (2011). Cognitive and neural correlates of depression-like behaviour in socially defeated mice: an animal model of depression with cognitive dysfunction. Int. J. Neuropsychopharmacol. *14*, 303–317.

Zhang, H., Chaudhury, D., Nectow, A.R., Friedman, A.K., Zhang, S., Juarez, B., Liu, H., Pfau, M.L., Aleyasin, H., Jiang, C., et al. (2019). α1- and β3-Adrenergic Receptor-Mediated Mesolimbic Homeostatic Plasticity Confers Resilience to Social Stress in Susceptible Mice. Biol. Psychiatry *85*, 226–236.

Zhan, J., Komal, R., Keenan, W.T., Hattar, S., and Fernandez, D.C. (2019). Non-invasive Strategies for Chronic Manipulation of DREADD-controlled Neuronal Activity. J. Vis. Exp.

Zheng, Z., Guo, C., Li, M., Yang, L., Liu, P., Zhang, X., Liu, Y., Guo, X., Cao, S., Dong, Y., et al. (2022). Hypothalamus-habenula potentiation encodes chronic stress experience and drives depression onset. Neuron.